United States Department of Commerce
Technology Administration
National Institute of Standards and Technology

NIST Technical Note 1500-1
Materials Reliability Series

Tensile Testing of Thin Films: Techniques and Results

D.T. Read

NIST Technical Note 1500-1
Materials Reliability Series

Tensile Testing of Thin Films: Techniques and Results

D.T. Read

Materials Reliability Division
Materials Science and Engineering Laboratory
National Institute of Standards and Technology
325 Broadway
Boulder, Colorado 80303-3328

December 1997

U.S. DEPARTMENT OF COMMERCE, William M. Daley, Secretary
TECHNOLOGY ADMINISTRATION, Gary R. Bachula, Acting Under Secretary for Technology
NATIONAL INSTITUTE OF STANDARDS AND TECHNOLOGY, Raymond G. Kammer, Director

National Institute of Standards and Technology Technical Note
Natl. Inst. Stand. Technol., Tech. Note 1500-1, 92 pages (December 1997)
CODEN:NTNOEF

U.S. GOVERNMENT PRINTING OFFICE
WASHINGTON: 1997

For sale by the Superintendent of Documents, U.S. Government Printing Office, Washington, DC 20402-9325

Contents

Foreword

The Materials Reliability Series of NIST Technical Notes are reports covering significant research accomplishments of the Materials Reliability Division. The Division develops measurement technologies which enable the producers and users of materials to improve the quality and reliability of their products. Measurement technologies are developed for process control to improve the quality and consistency of materials, nondestructive evaluation to assure quality of finished materials and products, and for materials evaluation to assure reliable performance. Within these broad areas of measurement technology, the Division has focused its resources on three research themes:

- Intelligent Processing of Materials — To develop on-line sensors for measuring the materials characteristics and/or processing conditions needed for real-time process control.

- Ultrasonic Characterization of Materials — To develop ultrasonic measurements for characterizing internal geometries of materials, such as defects, microstructures and lattice distortions.

- Micrometer-Scale Measurements for Materials Evaluation — To develop measurement techniques for evaluating the mechanical, thermal and magnetic behavior of thin films and coatings at the appropriate size scale.

This report is the first in the series. It covers research on mechanical testing of thin films, one of the projects in our research on Micrometer-Scale Measurements.

Tensile Testing of Thin Films: Techniques and Results

D.T. Read
Materials Reliability Division
National Institute of Standards and Technology
Boulder, Colorado 80303

Five technical papers covering the development of a set of techniques for measuring the tensile properties of thin films are gathered here. Also included are drawings of the mechanical components of the apparatus and listings of two computer programs. Additional necessary parts include a computer, instrumentation, two piezoelectric stacks, and an appropriate platform equipped with a microscope. Piezoelectric stacks are used as actuators. Noncontacting eddy-current displacement sensors measure both the tensile displacement and the force. Closed-loop feedback control allows a variety of test programs. The maximum available displacement is about 50 μm, and the maximum available force is about 0.3 N. The resolution of displacement is about 25 nm, and the resolution of force is about 100 μN. Cyclic loading has been demonstrated for cycles as short as 20 s.

Key words: Displacement, force, mechanical property, microtensile, piezoelectric, strain, strength, stress, thin film.

1. Introduction

Five technical papers [1-5] covering the development of a set of techniques for measuring the tensile properties of thin films are gathered here. Also included are drawings of the mechanical parts of the current apparatus and of the specimen. Additional necessary parts include a computer, instrumentation, two piezoelectric stacks, and an appropriate platform equipped with a microscope. The National Institute of Standards and Technology has not patented this tester, but rather placed it in the public domain. One institution has already cloned it, and another is doing the same. The author is interested in working with other parties who are considering building and using this microtensile tester.

"Thin film" here means metal layers produced by physical vapor deposition or electrodeposition, with thicknesses around 1 μm. Traditional mechanical test techniques, including specimen designs, specimen fabrication routes, and test equipment, are not suitable for these thin films. The apparatus described here tests specimens whose gauge section is typically 0.8 mm long and 50 to 200 μm wide. Specimens with thicknesses ranging from 0.3 to 15 μm have been tested. The silicon substrate is removed from beneath the gauge section, so that the behavior of the free-standing film is studied.

Piezoelectric stacks are used as actuators. The current microtensile tester uses noncontacting eddy-current displacement sensors to measure both the tensile displacement and the force. Closed-loop feedback control allows a variety of test programs. The maximum available displacement is about 50 μm, and the maximum available force is about 0.3 N. The displacement resolution is about 25 nm, and the force resolution is about 100 μN. Cyclic loading has been demonstrated for cycles as short as 20 s.

The measurement techniques and results described here were developed to serve the advanced microelectronics industry. All microchips include thin films. Thin films are beginning to appear in advanced electronic interconnection structures that link microchips to the external world. Their function is principally electrical. However, their mechanical properties are relevant to the manufacturability and reliability of advanced devices, because mechanical failure of the films themselves and at their interfaces to other materials can cause failure of the electrical function of such devices. As the devices are miniaturized, elements which once had only an electrical function must now also take on a mechanical function. The specimens described here can be produced in semiconductor fabrication facilities using normal microlithographic techniques.

As results on the mechanical behavior of thin films accumulate, certain differences between their characteristics and those of bulk specimens of similar chemical composition are becoming clear. These differences result mainly from microstructure. Effects produced by the constraint of the substrate are treated in the literature, but are not measured by the present experimental technique.

2. Overviews of the Individual Technical Publications

1993: A New Method for Measuring the Strength and Ductility of Thin Films [1]

This paper, included as Appendix A, introduced the use of the silicon-framed tensile specimen for testing metal thin films. It was shown that the silicon could be etched out from underneath the gauge section of the tensile specimen, and that the silicon frame could be cut manually just before testing, without damaging the thin film tensile specimen. The sensors described here are still used. This version of the tester was actuated by a manual differential micrometer, and the load was measured by a flat meander spring. Both of these two characteristics of the tester have been changed in later versions, described below.

Electron-beam evaporated aluminum was used as the specimen material. The specimens consisted of up to four parallel tensile strips, so that the measured values of strength and elongation reflected the average behavior. The reason for including four narrow strips instead of one wide one was that previous attempts had shown that wider strips tore themselves during preparation, because the stresses in the film caused it to curl at the edges. Narrower strips curled less severely. This version of the technique produced evidence for the two major differences between thin film and bulk behavior: the films have higher strengths, because of their small grain sizes; and the films have very low tensile elongation to failure, for reasons still not completely understood.

1994: Mechanical Behavior of Aluminum and Copper Thin Films [2]

The previous work provided convincing evidence that the tester could be redesigned with a much smaller stroke capacity, because elongation to failure of the films was quite low. The shorter stroke opened up some advantageous possibilities: more restraint of the specimen motion could be provided, to make it easier to cut the specimen without damage; the tension could be actuated by thermal expansion of aluminum columns, so that the load could be ramped smoothly and reproducibly; and the moving grip could be cantilevered, so that friction could be eliminated. A second eddy-current sensor for specimen displacement was added, and the two sensors were mounted in the same horizontal plane as the specimen, to avoid possible spurious indications of displacement.

This paper clarified and confirmed the differences indicated above between thin-film and bulk behavior for electron-beam-evaporated aluminum and copper films. The widths of the individual tensile strips in the specimens were varied to look for size effects. The limited data were scattered, but no effects of specimen width on measured properties were found. This paper did not address the issue of specimen thickness. A decrease in elongation to failure with decreasing thickness in the range of 1 to 10 μm of thickness is suspected.

1995: Fatigue of Microlithographically-Patterned Free-Standing Aluminum Thin Film under Axial Stresses [3]

This paper used the original tester [1] to study the effect of repeated loading on electron-beam-

evaporated aluminum films. The paper includes details of specimen preparation not previously shown. The reproducibility of the fatigue life among the specimens was surprisingly good. The stress-stress fatigue resistance, normalized against ultimate tensile strength, seemed poorer than that of bulk sheet-metal specimens as described in the literature. Geometrical defects produced in specimen fabrication and metallurgical effects related to the high strength of the films, relative to that of typical pure, bulk polycrystalline aluminum, were the suspected causes of the observed behavior.

1997: Tension-Tension Fatigue of Copper Thin Films [4]

This paper introduced a significant redesign of the tester to include piezoelectric stacks as actuators to replace the heated columns and the application of closed-loop feedback control. The sensitivity and reproducibility of the tester were good enough that specimens with only one tensile strip, instead of four, could be used routinely. A dental drill was used to cut the silicon specimen frame, instead of simply chipping it away with a sharp stylus.

On the previous version of the tester [2], the force signal drifted whenever the tester was actuated by heating the columns. This was attributed to twisting and bending of the reference and force-sensing beams caused by temperature variations. The temperature could not be kept constant because heat was needed to produce the tensile displacement. The force could be measured only by interpolating the zero-force signal between the beginning of loading and the failure of the specimen, and taking the difference between the estimated zero-force signal and the actual signal. This was a laborious and error-prone process. In addition, while the extension rate could be controlled by the electrical current in the heaters, the cooling rate was much harder to control. Cooling fluid could not be applied to the columns with acceptable control.

The replacement of the heated columns by piezoelectric stacks was a great improvement. The drift of the force signal with extension of the tester was reduced to a small fraction of its previous level. The moving grip could be extended and retracted smoothly at controlled rates.

More specimens were used in this study than had been used in the previous study of fatigue in aluminum films, and the apparent scatter in the data was higher. However, relative to its ultimate tensile strength, the fatigue resistance of the copper was superior to that of the aluminum previously tested. The fatigue resistance of the copper appeared to reach normal levels for typical bulk materials. Fatigue lives of over 100 000 cycles were demonstrated, as opposed to the maximum of 78 reached in the previous study.

An attempt was made to study the mechanism of the fatigue process using optical and transmission electron microscopy. Small cracks that developed in the titanium passivation layer on the copper films were shown to be arrested at the copper surface. Few individual dislocations and no sign of dislocation cells were found.

1997: Piezo-Actuated Microtensile Test Apparatus [5]

This paper, to be published in the ASTM *Journal of Testing and Evaluation* and reprinted in Appendix E, documents the tester in its present state. Detailed mechanical drawings are given in Appendix F.

3. Discussion

3.1 Instrumentation

The drawings in Appendix F include all the mechanical parts of the tester itself. Several additional components are needed in order to conduct tensile tests. These are obtainable commercially as standard products. They include mainly a probing station to serve as a base for the tester, the sensors, a computer equipped with an analog-to-digital converter card, the piezoelectric stacks, and a power supply to drive them. A dental drill to cut the silicon frame on the specimen chip is also needed. The traveling microscope built in to the probing station used as a platform for the microtensile tester has proved very useful. The three displacement sensors used have a full-scale range of 50 μm, and a corresponding output voltage that ranges from −1 to 1 V . These eddy-current sensors apply negligible force on the moving grip of the tester. Alternative noncontacting sensor types could be used. For instance, capacitive and optical displacement sensors with similar sensitivities and ranges are commercially available.

The piezoelectric stacks used have a stroke of about 50 μm. This was sufficient for most specimens, but one set of very ductile electrodeposited copper films challenged the extension capacity of the tester. Therefore, actuators with this stroke or higher are recommended. Alternatives such as magnetostrictive actuators could be considered; however, the perturbations and instabilities introduced by the dissipation of energy associated with the necessary electric current would have to be considered carefully. A power supply is needed to drive the piezos, and it must be controllable by the computer to enable closed-loop feedback.

3.2 Computer Programs

Source listings of the computer programs used with this tester are included on floppy disk as Appendix G. There are two programs: test and data analysis. PC-compatible computers are used for both testing and data analysis. These programs operate satisfactorily with the present tester and its data. However, they have not been tested on other computers or by other users. Therefore, caution is in order regarding the use of these programs and any calculated results.

The test program is menu-driven and provides displacement, load, and piezo-voltage-controlled ramps, and sinusoidal displacements and loads. It controls the motion of the moving grip of the tester in closed-loop feedback. It also stores raw instrument readings five times per second. This program is written for a commercially available Basic compiler.

The data-analysis program accepts a raw data file and a parameter file as input, and displays the force-displacement or stress-strain curve in metric units. The parameter file includes specimen dimensions and instrument calibration factors that can vary from test to test. It is usually generated by modifying the parameter file for a previous specimen, though it could be created from scratch. The yield and ultimate strengths can be calculated, and a line can be fitted to the loading slope. Results can be stored as text files. This program is written for a commercially available C++ compiler.

3.3 Plans

The present tester works well for specimens from 0.3 to 15 μm thick, in widths down to about 20 μm for specimens 1 μm thick and greater. The very small specimens introduce problems in two areas: accuracy of the force measurement, and damage to the specimen in the wet etch that removes the silicon from beneath the tensile gauge section. The very small specimens also seem to be more susceptible to damage during the cutting of the silicon, from fragments and exhaust air from the dental drill, for example.

The thinking at present is that the tester described in this technical note is a valuable intermediate between full-scale conventional testers and a future, truly submicrometer-scale, test technique. The submicrometer scale is clearly important, because metal lines on present-day integrated circuit chips have widths well within the submicron range. The author is not currently pursuing incremental steps to modify the present tester to test smaller specimens, primarily because the key step in the present procedure for specimen preparation, that is, etching all the way through the silicon wafer, seems out of scale with submicrometer-width specimens. Instead, alternative concepts for measuring tensile properties measurements on specimens with widths of 1 μm and less are under consideration.

4. References

[1] Read, D.T.; Dally, J.W.; A new method for measuring the strength and ductility of thin films. *Journal of Materials Research* **8**(7): 1542-1549; 1993.

[2] Read, D.T.; Dally, J.W.; Mechanical Behavior of Aluminum and Copper Thin Films. *Mechanics and Materials for Electronic Packaging: Volume 2 Thermal and Mechanical Behavior and Modeling*, edited by M. A. Schen, H. Abe, and E. Suhir, American Society of Mechanical Engineers. pp. 41-49; 1994.

[3] Read, D.T.; Dally, J.W.; Fatigue of Microlithographically-Patterned Free-Standing Aluminum Thin Film Under Axial Stresses. *Journal of Electronic Packaging, Transactions of the ASME* **117**(1): 1-6; 1995.

[4] Read, D.T.; Tension-Tension Fatigue of Copper Thin Films. *International Journal of Fatigue*, to be published.

[5] Read, D.T.; Piezo-Actuated Microtensile Tester. *ASTM Journal of Testing and Evaluation,* to be published.

Appendix A. 1993: A New Method for Measuring the Strength and Ductility of Thin Films

A new method for measuring the strength and ductility of thin films

David T. Read
Materials Reliability Division, National Institute of Standards and Technology, Boulder, Colorado 80303-3328

James W. Dally
Mechanical Engineering Department, University of Maryland, College Park, Maryland 20742

(Received 1 June 1992; accepted 10 February 1993)

A new method of measuring the mechanical strength of thin films is described. We prepare miniature arrays of four tensile specimens, each 0.25 mm wide, 1 mm long, and 2.2 μm thick, using deposition, patterning, and etching processes common to the semiconductor industry. Each array of four specimens is carried on and protected by a rectangular silicon frame. Thirty-six such specimens are produced on a single wafer. After a specimen frame is mounted, its vertical sides are severed without damaging the specimens. The load is applied by micrometers through a special tension spring. Tensile properties of a 2.2 μm thick Ti–Al–Ti film were determined.

I. INTRODUCTION

A. Background

In spite of the widespread application of thin films, we know very little about their constitutive properties. Considering the vapor deposition process used in preparing thin films, we anticipate that some of the mechanical properties of the thin films may differ significantly from those of bulk materials of the same chemical composition. Measurements of the constitutive properties of thin films, including elastic modulus, yield strength, ultimate strength, ductility, strain-hardening coefficient, creep and stress relaxation constants, fatigue strength, and crack initiation toughness, are necessary to develop models that predict the behavior of films when subjected to mechanical and thermal stresses. The experimental challenges encountered in measuring the constitutive properties are due to difficulties in fabricating the thin film tensile specimens, in handling these thin and fragile specimens with cross-sectional areas of the order of 10^{-3} mm^2, and in measuring small forces and displacements.

Experimental techniques applied to thin-film testing[1–9] can be divided into four different categories. In the first approach,[1] a thin film is deposited on a suitable substrate, and then the specimen array is patterned in the film. The specimens are then stripped from the substrate and manually mounted in the grips of a miniature tensile testing device. The second approach is identical to the first, except that the grips are attached to the film specimen before it is stripped from the substrate.[2–4] Mounting the grips on the specimen before stripping facilitates handling and improves alignment in the tensile loading device.

A third group of investigators[5,6] uses nano-indentation to measure yield strength and elastic modulus. In nano-indentation, the force on the indenter is determined as a function of the penetration depth, with the film bonded to the substrate.

The fourth approach[7,8] involves tensile testing of small thin-film specimens, where the substrate is removed from under the specimen by etching. The advantage of separating the film and the substrate by etching is the relief of the residual stress produced in the vapor deposition process.

B. Features of the new method

In this paper, we describe a new method to measure the mechanical strength of thin films. The method involves: (1) The production of damage-free thin-film tensile specimens with controlled geometry, using microlithography and substrate etching. (2) The use of a miniature rectangular silicon frame suspension for the specimens; the frame maintains alignment and protects the specimens. The frame also provides a test element large enough to handle efficiently. (3) The production of many (36) identical frame-supported specimen arrays on a single 51 mm diameter wafer of silicon. (4) Mounting a specimen frame in the microtensile tester and severing the vertical members of the frame to free the specimen, while maintaining the alignment required for testing. (5) The use of a microloading system with an optical microscope, video recording system, and an x-y table to permit the controlled application of axial tensile loads up to 1 N (100 gram-force) with the capability to observe the specimens at magnifications up to 2500×. (6) The use of an instrumentation system to measure and record the applied loads and the resulting specimen elongation.

Many elements of this method are borrowed from previous investigations, as detailed above. The most

novel aspect is the ability to produce a freely suspended thin-film specimen that has never been handled or deformed. The process of stripping a thin film from a substrate and handling it during mounting admits the possibility of mechanical damage to the specimen. Use of water-soluble substrates such as sodium chloride is an option, but sodium chloride is a deleterious contaminant in semiconductor fabrication, while the silicon substrate used here is compatible with semiconductor fabrication processes. An additional novel benefit of the present method is that it lends itself conveniently to replicate testing. Because several specimens are fabricated with the same geometry, results of multiple tests can be treated statistically.

II. SPECIMEN FABRICATION METHODS

The tensile specimens are produced by employing photolithographic techniques common to the semiconductor industry. The process begins with a 51 mm (2 in.) diameter by 0.25 mm (0.010 in.) thick silicon wafer. The silicon is *n*-type, and the wafer is cut in the ⟨100⟩ orientation. The wafers are procured with both sides polished. The first step in specimen fabrication is to heat the wafers in a steam environment to obtain an oxide layer about 0.5 μm thick. The wafers are patterned by photolithography and etched to remove the oxide layer from the locations of the gage sections of the tensile specimens. Next, the metal films are deposited over the entire surface of the wafer using electron beam evaporation. In this investigation, the metallization was not sintered. A multilayer film was deposited, consisting of titanium-aluminum-titanium with thicknesses of 0.1, 1.98, and 0.1 μm. Other materials and other thicknesses can be deposited as well.

The metallized side of the wafer was then coated with negative photoresist, and the pattern of the specimen illustrated in Fig. 1 was contact printed in the photoresist. The glass master used in this printing operation had 36 specimen patterns geometrically arranged to fit on the 51 mm diameter wafer. The specimen geometry was produced subtractively using a series of etching treatments. The titanium layers are etched with a dilute mixture of hydrofluoric and nitric acids buffered with ammonium nitrate. The aluminum layer is etched in a phosphoric-acetic acid mixture at 40 °C.

After the specimen geometries were produced at each site on the wafer surface, both sides of the wafer were coated with a positive photoresist. Two additional glass masters were then used to contact print the lattice representing the rectangular frames: one on the front side of the wafer and the other on the back. Both masters were aligned to the specimen pattern in a manual mask aligner. The pattern on the back side of the wafer was aligned by viewing the wafer and master with infrared

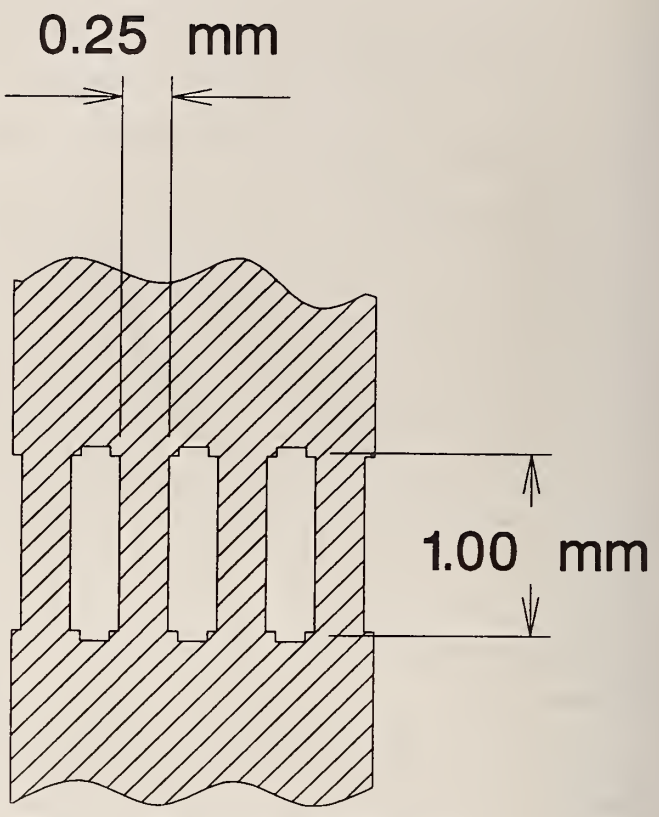

FIG. 1. Array of four thin-film tensile specimens.

light transmitted through the wafer. After developing the photoresist, the wafers were etched in buffered hydrofluoric acid to remove the SiO_2 layer over areas not incorporated in the frame lattice. The SiO_2 remaining served as a mask for the silicon etch.

A water solution of hydrazine[9,10] at 110 °C was employed to etch the silicon wafer in the areas not protected by the SiO_2 patterns. The hydrazine etches the silicon at a relatively rapid rate, about 2 μm/min. The etch is highly anisotropic in that it etches the ⟨111⟩ faces much more slowly than the others. The hydrazine etchant also does not attack either Al or Ti, although it may attack the grain boundaries to some degree. It has several disadvantages. Most important, it is quite hazardous and requires effective precautions in venting and disposal during and after use. It also causes the metallic films to peel if they are not well bonded to the substrate during vapor deposition.

This method of specimen fabrication produces a very large number of specimens with uniform properties. For example, the 51 mm wafer shown in Fig. 2 has a total of 36 specimens. Each specimen is supported by a rectangular frame 6 by 8 mm, which is essentially a die. Scribe lines are etched in the wafer to facilitate separation of the dies by controlled fracture. A photograph showing several frames is presented in Fig. 3(a). An enlargement of the specimen array is shown in Fig. 3(b).

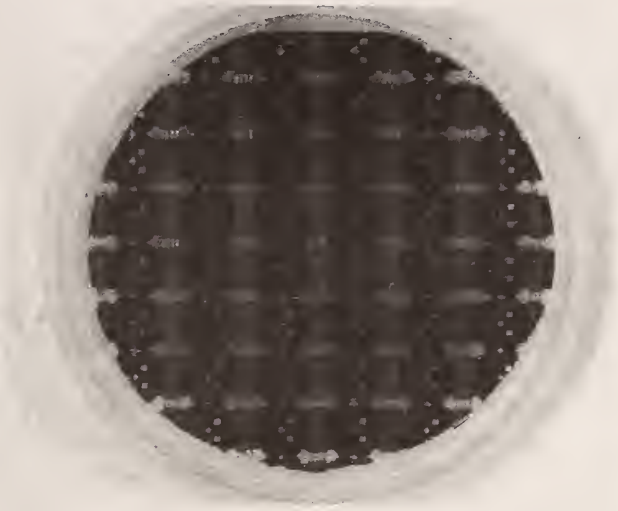

FIG. 2. Picture frame supported tensile specimens are produced on a single 50-mm-diameter wafer.

III. MICROTENSILE LOADING SYSTEM

A microtensile loading system was developed to accommodate the thin-film specimens with the frame suspension. The system is capable of applying uniaxial static loads in excess of 1 N (100 gf). Both the load and the resulting elongations are measured using eddy current sensors.

The mechanical features of the loading system, illustrated in Figs. 4 and 5, include a fixed and a sliding platen with a pair of specimen-mounting plates, a calibrated spring, and a series connected pair of micrometers. The mounting plates are fixed to the two platens with small screws, so that they can be removed and recycled. The specimen frame, after alignment, is bonded to the mounting plates with a quick-setting methyl-2-cyanoacrylate adhesive. The load is applied by displacing one end of the spring with one or the other of the two micrometers. One micrometer is a differential type with graduations of 1 μm, and the other is a conventional type with graduations of 10 μm. The other end of the spring is fastened to the sliding platen. As the spring is extended, the spring force is transmitted through the sliding platen to the specimen array. With the spring stiffness of 0.667 N/mm, a minimum load increment of 0.667 mN can be applied with the differential micrometer. Since the loads to failure usually range from 0 to 0.49 N (50 gf), the minimum increment is sufficiently small for controlled application of the load.

The primary disadvantage of this loading technique is the frictional constraint developed on the sliding platen. The frictional effects are minimized by applying the axial load in small increments (3 to 6 mN) and then tapping the support structure of the loading system with a light striker. The resulting vibrations unlock the asperities and relieve the frictional forces that impede the motion of the sliding platen.

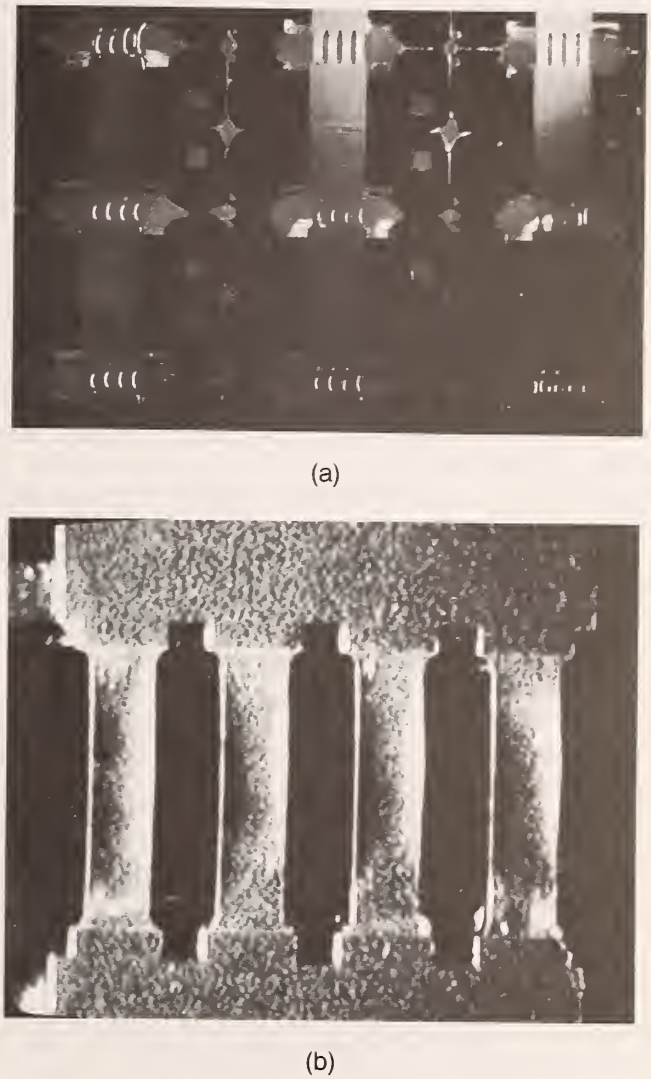

(a)

(b)

FIG. 3. (a) Picture frame supported array of specimens. (b) Enlargement showing the specimen array.

The instruments used to measure the load and specimen elongation employ noncontacting eddy current sensors. The load is measured by sensing the displacement of the spring. This measurement is made by mounting the coil side of a conventional eddy current displacement transducer in the support block for the spring. The transducer senses the position of an aluminum flag that is attached to the sliding platen. The operating principles of the eddy current sensor are illustrated in Fig. 6(a), where the flag on the sliding platen is represented by the "target" that is being tracked.

The voltage output from this sensor is linear over a range of spring extension from 0 to 1 mm. A calibrated output is possible for spring extensions as large as 5 mm, but the voltage output is nonlinear. The sensitivity of the sensor in the linear range is 0.4 V/mm with the gain

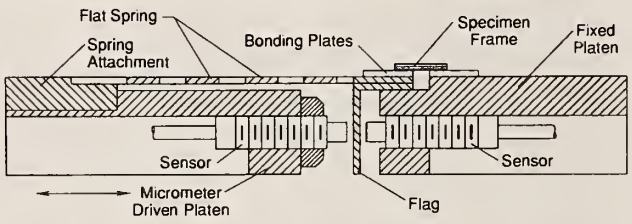

FIG. 4. Illustration of the microtensile loading system with sensors for measuring load and elongation.

provided by the amplifiers in the signal conditioning circuits shown in Fig. 6(a). The output voltage is observed on a liquid crystal display during loading. It is also recorded on the y-axis of an x-y recorder that is used to provide an on-line load-elongation record during the tensile test. The output is also digitized and stored on a hard disk. The compliance of the measuring spring was repeatable to within 1%. The point-to-point scatter in the load reading is less than 0.2%. Each point on the plots shown below represents the mean of 20 such readings. The uncertainty in the force measurements is $\pm 1\%$.

The specimen elongation is also sensed with an eddy current transducer, which is mounted in the support block for the fixed platen. Again, the transducer senses the position of the flag attached to the sliding platen. Because the displacement of the flag due to specimen elongation is so small (about one wavelength of light at the yield stress in aluminum), it is necessary to employ a sensor with enhanced sensitivity. This improvement in sensitivity is accomplished in the signal conditioning circuit shown in Fig. 6(b). Note that the log amplifier has been removed. This modification produces a much higher voltage output near the zero position of the sensor, but severely limits the range over which the output is linear (25 μm). The sensitivity of the instrument system is 40 mV/μm, which corresponds to a voltage output of 400 mV for a strain of 1% imposed on the specimens with a gage length of 1 mm. The resolution of the system is specified as 0.0025 μm, which is equivalent to the displacement due to a strain of 0.00025%, acting on a tensile specimen 1 mm long. However, the governing uncertainty turned out to be larger, as noted below.

IV. TESTING PROCEDURES

The specimens are mounted in the microtensile loading device by adhesive bonding. The platens are positioned axially so that both the load and elongation sensors are at the beginning of their linear ranges. Specimen alignment is achieved by positioning the rectangular frame specimen assembly squarely on the platens. Then the specimen is bonded to the mounting plates with an adhesive that polymerizes almost instantly. The specimens are ready to be tested except that the silicon frame which served as a carrier must be removed.

The vertical sides of the frame are effectively removed by fracturing, thus freeing the specimen. The horizontal members of the frame are retained and serve as miniature platens, assuring that the alignment of the specimen array is maintained. The difficulty in fracturing the vertical members is preventing any motion of the sliding platen, which would damage the specimens during the fracturing process. Any slight movement imposed on the sliding platen as the frames are fractured produces large stresses in the specimens and causes premature failure.

To avoid damage to the specimen during fracturing requires that the sliding platen be locked to the fixed platen. A special clamp was fabricated, as shown in Fig. 7, to lock the sliding platen to the fixed platen. This clamp, which bridges the sliding platen, is fastened to the fixed platen with two end positioned screws. The clamping action is applied with other screws that engage the flexure plate and drive it downward onto the sliding platen. The flexure plate limits motion of the

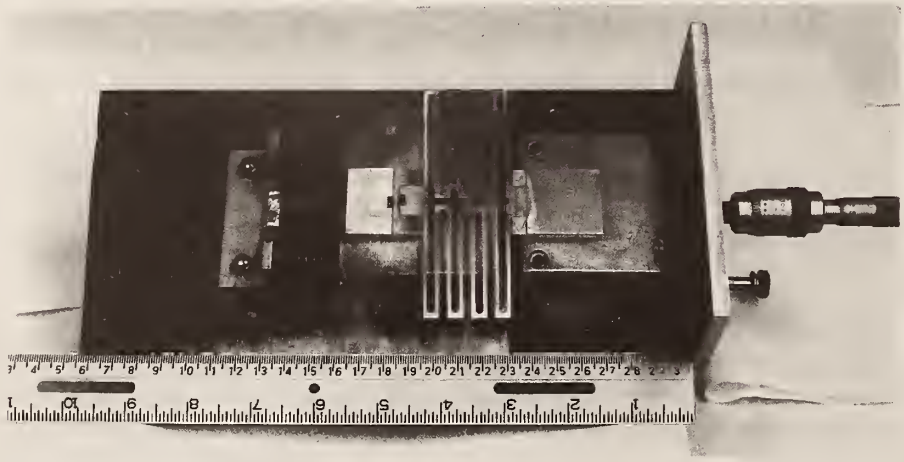

FIG. 5. Photograph of the microtensile loading system.

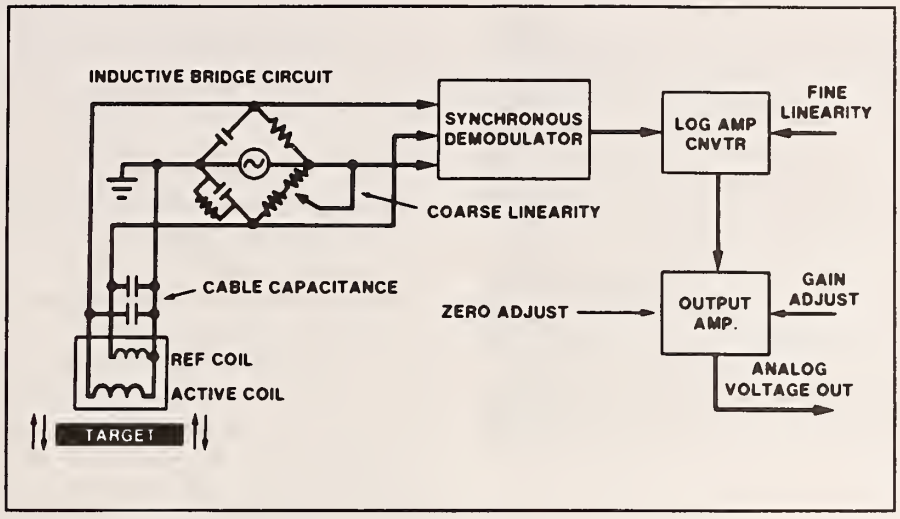

(a)

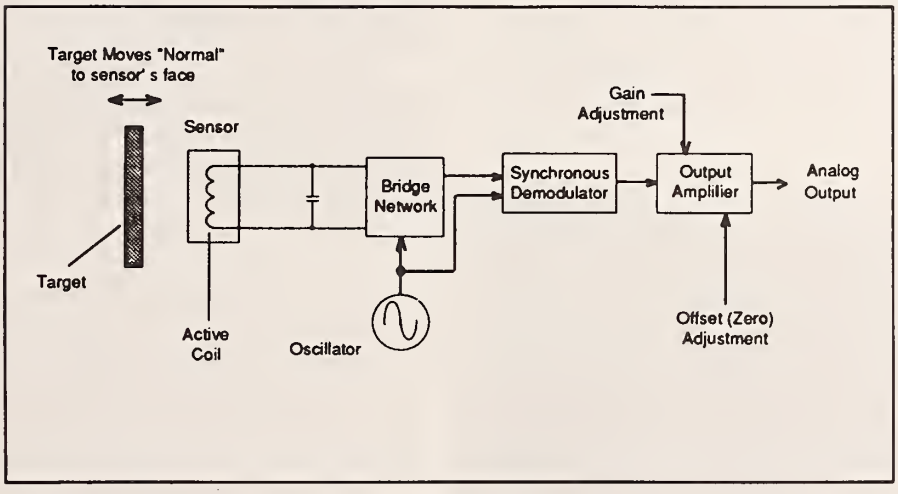

(b)

FIG. 6. (a) Block diagram of electronic components in a conventional eddy current transducer. (b) Block diagram of electronic components in an enhanced sensitivity eddy current transducer.

sliding platen as the clamp is engaged and prevents any movement of the picture frame.

When the clamp is tight and the sliding platen is fixed, the vertical sides of the frame are fractured. We initially fractured the vertical sides by promoting cracks that propagated across the width of each side. This was not reliable because in many instances the cracks were arrested by the thin surface layer of SiO_2, and the relief of the constraint was incomplete. A more effective procedure was to use a fine scribe to break away small pieces of the silicon until a band of material was removed from each of the vertical members. When the breakage was completed, the flexure plate was released and the clamp removed. A photograph showing the specimen and the fractured members of the frames is given in Fig. 8.

The specimen array and frame were examined under high magnification at the conclusion of this process to ensure that no damage had been induced and that the specimens were in perfect alignment. Load was then applied in small increments (about 2% of ultimate load) by extending the spring. The frictional constraints at the sliding platen were relieved by tapping with a light striker after each load increment.

The voltages from the eddy current sensors monitoring load and elongation were recorded on an x-y recorder that could be observed during the test. The

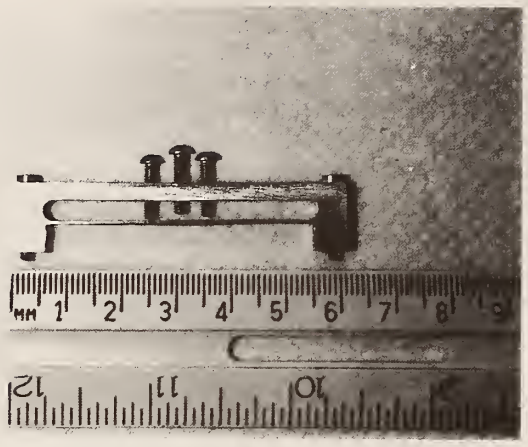

FIG. 7. Clamp, incorporating a flex plate, for locking the sliding platen.

output voltages were also digitized and stored on a hard disk at a rate of four readings per second.

Because of problems with an accurate measurement of the elastic response of these films, the yield strength was determined by using a 0.2% offset with an assumed elastic modulus of 70 GPa, Young's modulus of bulk aluminum.

FIG. 8. Photograph of the specimen array and a broken vertical member on the frame.

The in-plane specimen dimensions were measured using the displacement readouts of the optical microscope. The widths of the miniature coupons, nominally 250 μm, were measured to within approximately ± 2 μm.

The thickness was measured on untested portions of the film using a commercially supplied instrument that records the vertical displacement of a diamond stylus as it is displaced across the edge of the thin film. These measurements were made on the whole film and, after etching away the components one by one, are believed accurate to 5% based on their reproducibility. This uncertainty controls the measurement uncertainty for the stress which is $\pm 5\%$.

Because all the specimens in Table I came from the same wafer, all have the same film thickness. The wafer was mounted 50 cm from the crucible and rotated during deposition, so variations of $\pm 5\%$ in the film thickness on this wafer can be excluded. While the average stress value is uncertain by $\pm 5\%$, this uncertainty is not the primary cause for the scatter in the measured strength.

An uncertainty in the effective gage length results from the persistence of projections of the silicon substrate under the ends of the specimens. These are not exactly the same from specimen-to-specimen and assembly-to-assembly and add an uncertainty of up to -20%, or $\pm 10\%$, to the strain results.

V. RESULTS AND DISCUSSION

Yield and ultimate strengths determined for seven specimens are listed in Table I. The scatter in these results is larger than the measurement uncertainty of 5% and is attributed to variability in the specimens and the specimen material, to be discussed below.

The test conditions enforce equal displacement on the four individual specimens, while the total force is recorded. So the load-displacement record gives the average force (over the four individual coupons in the array) at the indicated displacement. However, because the

TABLE I. Mechanical properties of thin Ti–Al–Ti films.

Specimen identity	Yield strength (MPa)	Ultimate strength (MPa)	Strain at failure (%)
0	[a]	172	[a]
A	121	199	1.18
B	115	186	1.15
C	96.4	191	1.81
D	71.5	156	1.28
E[b]	120	144	0.54
F	91.0	146	0.85

[a]Not measured.
[b]Single specimen rather than an array of four specimens.

loading spring is soft, the test conditions are essentially force-controlled. When one individual specimen of the array fails, the remaining three are unable to sustain the applied force, so the whole array fails. That means the reported strength values correspond to the lowest failure load among the four individual specimens, at the displacement indicated. The force-displacement and stress-strain curves of Fig. 9 indicate average force and stress values at the indicated displacement and strain.

The present technique has not produced acceptable values of Young's modulus because of problems with the accuracy of the displacement measurement. Slight rotations of the sensing flag (Fig. 4) contribute spurious displacements of the order of 1 μm to the measured displacements. Attempts to measure the spurious displacement and calibrate it out produced load-elongation and resulting stress-strain curves, as shown in Figs. 9(a) and 9(b). These stress-strain curves gave varying values of the initial slope, so we did not attempt to derive elastic modulus values.

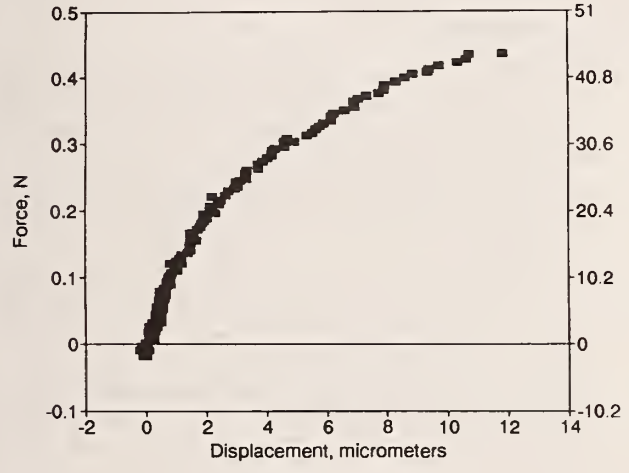

(a)

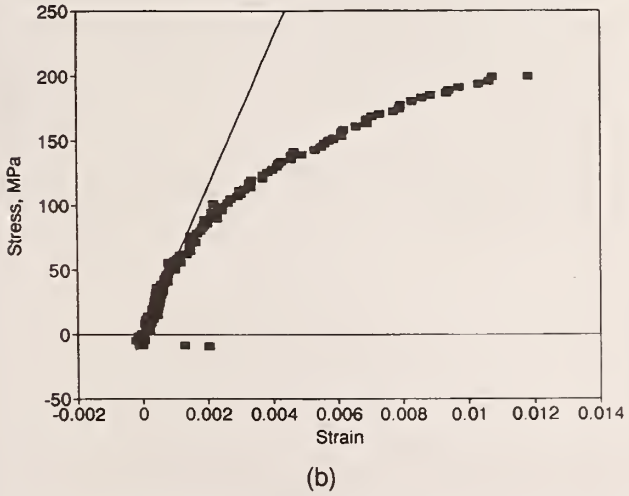

(b)

FIG. 9. (a) A typical force-elongation record for Ti–Al–Ti (0.1–2.0–1.0 μm) films. (b) A typical stress-strain curve for Ti–Al–Ti (0.1–2.0–0.1 μm) films.

However, the qualitative features of the curves shown in Fig. 9 were reproduced in all the tests. We have listed the total elongation to failure of each specimen in Table I. These values, ranging from 0.54% to 1.81%, are much lower than the value of 15% or so that characterizes commercial aluminum alloys. This discrepancy is far too large to be accounted for by the measurement uncertainty of $\pm$10% of the strain to failure. Furthermore, the behavior of the specimens during elongation to failure, as observed in the microscope, was quite different from normal bulk tensile specimens, including specimens of the thin sheet. The behavior appeared quite brittle. The specimens fractured suddenly with no apparent stretching, thinning, or narrowing (Fig. 10).

The brittle fracture strength of a specimen is strongly dependent on its flaws or cracks. Brittle fracture strength is usually measured on different materials than ductile fracture strength, so the variabilities cannot be compared directly. But, usually, the brittle fracture strength, when it is controlled by small flaws or cracks, is more variable than the ductile fracture strength, as measured on replicate specimens of a ductile material.

We conclude that the present thin-film specimens exhibit behavior that is considerably less ductile than bulk commercial aluminum alloys. The low ductility is evident in the low strains to failure and is reflected in the scatter of the strength properties.

Effects of misalignment can be important in tensile testing. The present specimens are too small for the standard alignment check, which requires mounting multiple strain gages around a specimen and checking for equal strains. However, the multiple specimens

FIG. 10. Brittle failure of the thin films near the ends.

in the specimen arrays can be observed through the microscope. Their appearance changes noticeably as they are initially loaded, because they become straighter and, thus, reflect more of the normally incident light back up to the eyepiece of the microscope. Visual observations indicated that all specimens straightened out together, with no systematic side-to-side progress or asymmetry. No systematic order of specimen failure was noted. The interior two specimens showed cracking before fracture to the same degree as the outer two, and the left and right specimens seemed to fail similarly. In addition, the loading spring is soft relative to bending about its tensile axis. In the presence of small misalignments, only a small difference in tensile force across the specimen array would be produced. Therefore, the scatter indicated in Table I is not attributable to misalignment.

VI. CONCLUSIONS

The use of photolithography for fabricating the specimens permits a large number of specimens to be produced with uniform characteristics. With relatively rapid testing, it is possible to gather a significant amount of data and to provide properties with statistical significance. For instance, in the seven measurements of the ultimate tensile strength of the Ti–Al–Ti films, we can report a mean strength of 170.6 MPa and an estimated standard deviation of 22.3 MPa.

The ductility of these films is very low (0.54 to 1.81%) when compared to the ductility of either bulk aluminum or titanium, which are both an order of magnitude higher. The low ductility is due to one or all three of the following factors:

(1) The edges of the specimens were not straight, but contained strain concentrations which produced premature failure.

(2) Flat tensile specimens with a very high ratio of width to thickness, 114 in this case, are incapable of reaching the levels of plastic tensile strain that are seen in specimens with aspect ratios around one.

(3) These metallic films produced by electron beam evaporation are inherently brittle because of their microstructure, which is much different from that of normally processed bulk metals.

The most significant problems in the use of this microtensile loading system are the friction which inhibits the free motion of the sliding platen and the sensor flag rotation which limits the accuracies in measuring elongations at small loads. The most significant problems with specimen fabrication and inspection are an accurate determination of the cross-sectional area and the gage length, and the necessity of the Ti protective layers.

ACKNOWLEDGMENTS

A variety of facilities and apparatus are required for fabricating tensile specimens on silicon. Use of facilities offered by R.E. Harris, leader of the Cryoelectronics Group of the Electromagnetic Technology Division of N.I.S.T., and by William May of the Electrical Engineering Department of the University of Colorado at Boulder is gratefully acknowledged. Paul Glairon is acknowledged for a helpful discussion on etching silicon.

REFERENCES

1. J.E. Steinwall and H.H. Johnson, in *Thin Films: Stresses and Mechanical Properties II*, edited by M.F. Doerner, W.C. Oliver, G.M. Pharr, and F.R. Brotzen (Mater. Res. Soc. Symp. Proc. **188**, Pittsburgh, PA, 1990), pp. 177–182.
2. R.W. Hoffman, in *Thin Films: Stresses and Mechanical Properties*, edited by J.C. Bravman, W.D. Nix, D.M. Barnett, and D.A. Smith (Mater. Res. Soc. Symp. Proc. **130**, Pittsburgh, PA, 1989), pp, 295–306.
3. C.T. Rosenmayer, F.R. Brotzen, and R.J. Gale, in *Thin Films: Stresses and Mechanical Properties*, edited by J.C. Bravman, W.D. Nix, D.M. Barnett, and D.A. Smith (Mater. Res. Soc. Symp. Proc. **130**, Pittsburgh, PA, 1989), pp. 77–86.
4. I. Kim and R. Weil, *Testing of Metallic and Inorganic Coatings*, edited by W.B. Harding and G.A. DiBari (American Society for Testing Materials, STP 947, Philadelphia, PA, 1990), pp. 177–182.
5. T.P. Weihs, S. Hong, J.C. Bravman, and W.D. Nix, in *Thin Films: Stresses and Mechanical Properties*, edited by J.C. Bravman, W.D. Nix, D.M. Barnett, and D.A. Smith (Mater. Res. Soc. Symp. Proc. **130**, Pittsburgh, PA, 1989), pp. 87–98.
6. W.D. Nix, Metall. Trans. **20A**, 2217–2245 (1989).
7. L.S. Fan, R.T. Howe, and R.S. Muller, Sensors and Actuators **A21–A23**, 872–874 (1990).
8. M. Mehregany, R.T. Howe, and S.D. Senturia, J. Appl. Phys. **62**, 3579–3584 (1987).
9. D.B. Lee, J. Appl. Phys. **40**, 4569–4574 (1969).
10. M. Mehregany and S.D. Senturia, Sensors and Actuators **13**, 375–390 (1988).

Appendix B. 1994: Mechanical Behavior of Aluminum and Copper Thin Films

AMD-Vol. 187, Mechanics and Materials for Electronic Packaging:
Volume 2 – Thermal and Mechanical Behavior and Modeling
ASME 1994

MECHANICAL BEHAVIOR OF ALUMINUM AND COPPER THIN FILMS

David T. Read
Materials Reliability Division
Boulder Laboratories
National Institute of Standards and Technology
Boulder, Colorado

James W. Dally
Department of Mechanical Engineering
University of Maryland
College Park, Maryland

ABSTRACT

The mechanical behavior of thin films produced by electron-beam evaporation of Al and Cu and deposited on silicon substrates has been studied experimentally. Thin layers of Ti, similar to adhesion-promoter and diffusion-barrier layers used in microelectronics fabrication, were usually included on the specimen films. Tensile specimens that consisted of four parallel coupons were patterned by microlithography. The gage sections of the specimens were freed by etching away the substrate, leaving the tensile coupons supported by a die-sized silicon frame.. These specimens were tested in a specially designed thin film testing machine mounted under an optical microscope.

Improvements in the apparatus have eliminated a sliding--friction error, greatly reduced spurious contributions to the measured displacement, stiffened the load sensor so that behavior of the specimen past maximum load can be observed, and added closed-loop control of imposed displacement or load.

INTRODUCTION

Motivation: Reliability of thin films in electronic packaging

This study is motivated by the need to improve the general levels of understanding and predictability of the reliability of electronic devices and electronic packaging and interconnect structures. Aluminum thin films are widely used in the manufacture of integrated circuits, to form electrical connections among circiut elements and bonding pads. Aluminum and copper films are used in the manufacture of MCM-D (multi-chip-module--deposited) interconnect structures, and are finding new uses in the MCM-L (multi-chip-module--laminated) structures.

The treatment of the critical issues of manufacturability and reliability of integrated circuits and of packaging and interconnect structures is reaching a new level of sophistication. It has been reported that savings of cost and time-to-market have been achieved through the use of finite element analysis of mechanical behavior, to streamline and focus procedures in design, inspection, and test (Dunn, 1993). This use of finite element analysis has been proved effective in the design and evaluation of high-performance structures such as nuclear pressure vessels, aircraft, and a variety of aerospace structures. Several reports of advanced analyses of the mechanical behavior of electronic packaging and interconnect structures can be found in the literature. A few examples are: Pao *at al*, 1991; Guess and Burchett, 1992; and Lau and Rice, 1992.

A key advantage of the use of advanced mechanical engineering analyses, particularly finite element analysis, is the quantitative link achieved between material properties and structural behavior. Macro-world failure analyses are considered complete only when the predicted failure conditions, based on the material properties, structural geometry, and failure criterion, agree quantitatively with the actual loading at failure. To date this quantitative link has been absent in the analysis of electronic interconnect structures because of the lack of material properties data. In fact, material property values are often taken as variable parameters in analyses of electronic packaging structures. The present study attempts to address this lack of data.

Background: Mechanical behavior of thin films

Many studies of the mechanical behavior of thin films have been reported in the literature. These are reviewed by Hoffman (1966) and Hardwick (1987). Often the principal subject has been the fundamental nature of thin films, or a new testing technique. This literature can be briefly summarized in a few general

statements, although these are clearly oversimplifications of a complex subject:

1. It is necessary to be specific about the meaning of the term "thin film." This study treats films produced by physical evaporation and vapor deposition, with thicknesses in the range from 0.2 to 2.5 micrometers thick. The behavior of metal thin films alone, independent of substrate, is considered here. Direct effects of the substrate on mechanical behavior are excluded by removing the film from the substrate before testing. Indirect effects, such as an influence of the substrate on the microstructure or chemical composition of the deposited thin film, are of interest.

2. Mechanical behavior of metal thin films can be studied experimentally using a variety of special techniques; test procedures designed for bulk materials cannot be used directly (Nix, 1989, Read, 1992).

3. It seems clear that evaporated metal films in the thickness range considered here have the same crystal structure, lattice spacing, and Young's modulus as their bulk metal counterparts. During the course of a series of studies on compositionally modulated films (Baral *et al.*, 1985), it was shown that these three physical properties are the same for pure-metal films as for bulk material. The latest reports (Davis *et al.*, 1992), indicate that compositionally modulated films also have elastic properties nearly identical to those of bulk mixtures with the same average composition.

4. Thin films seem to have low elongation to failure compared to bulk specimens. Reported elongations to failure for thin films are often around 1 percent. Hardwick (1987) indicates that low measured values of ductility may be a consequence of the difficulty of testing suspended thin films. The present study will conclude the opposite: that thin films do in fact have low tensile elongation to failure, and this behavior is not an artifact of measurement.

5. The strength levels reported for thin films are usually higher than for pure bulk specimens of the same chemical element. This is considered to result from some combination of the very small grain sizes often found in thin films and the effect of impurities introduced during the vapor deposition process.

SPECIMEN PREPARATION

The tensile test techniques used here include a specimen preparation procedure that is compatible with the equipment and procedures used in the fabrication of electronic devices. Direct handling of the thin metal film is avoided, uniaxial tensile force-displacement records are produced, and the specimen size can be scaled downward through microlithography. The specimen preparation procedure has been described in detail elsewhere (Read and Dally, 1993) Here a brief description emphasizing recent improvements is given.

Figure 1 shows the Si, SiO_2 , and metal layers in the specimen assembly when it is ready for testing. Substrate preparation begins with oxidized silicon wafers, polished on both sides. We have used wafers that are 50 mm in diameter by 0.3 mm thick, with a [100] orientation. The SiO_2 layer is about 5000 Å thick. The SiO_2 on both sides of the wafer is patterned with photoresist to mask die-sized specimen frames 8 mm square, with a window that is 1 mm by 2 mm in the center, figure 2.. The

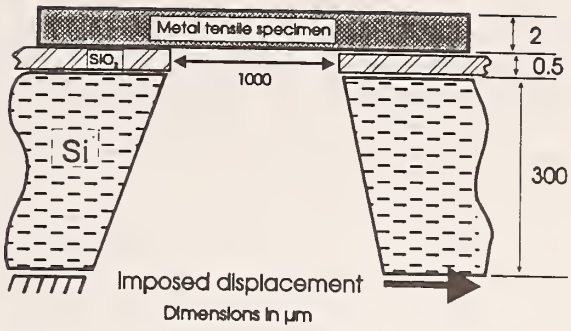

FIGURE 1. SCHEMATIC CROSS-SECTION OF THE SPECIMEN ASSEMBLY AFTER FABRICATION IS COMPLETE.

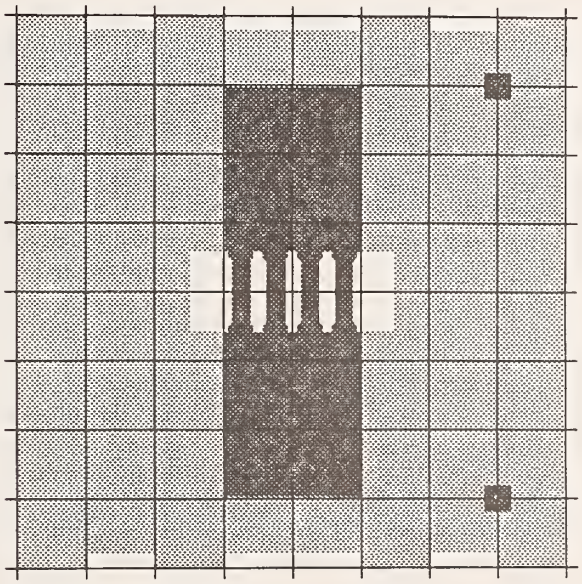

FIGURE 2. PHOTOMASK LAYOUT OF THE SPECIMEN ASSEMBLY. THE GRID SPACING IS 1 mm. THE LIGHTER GRAY IS THE SiO_2 LAYER, AND THE DARKER GRAY IS THE SPECIMEN METAL.

photoresist pattern on the back side of the wafer is aligned to the developed photoresist pattern on the front side, using infra-red illumination. Etching in BOE (buffered oxide etchant) removes the unmasked SiO_2, leaving a pattern of frames with windows in the remaining SiO_2 on both sides of the wafer.

Final plasma-cleaning of the wafer and deposition of the metal film are carried out in a single specially-equipped vacuum chamber. Argon gas at a pressure of 10 to 50 milliTorr forms a plasma. The plasma is driven with 100 watts of electrical power for ten minutes. This cleaning procedure has been found necessary, because poorly-adhering films will be destroyed during the Si etch step. Commercially supplied aluminum and copper of

5 nines purity have been used as specimen materials. The metal is heated in a crucible by an electron beam until the deposition rate reaches the selected level, 3 to 10 Å per second. Evaporation is continued until the desired metal thickness is reached. At 10 Å per second a 2 μm film can be deposited in about half an hour. This paper reports data for specimens with thin titanium layers on top and bottom and for some pure metal specimens. Ti layers 0.05 and 0.1 μm thick have been used.

Grain sizes of thin films are much smaller than those of bulk metals, except for epitaxial films. The grain sizes of the films tested here have been measured to be in the range of 0.5 to 1 μm. Transmission electron microscope (TEM) examination of as-deposited films in the 0.2 to 0.5 μm thickness range reveals typical polycrystalline metal, with clearly defined grain boundaries, a significant population of twins in Cu, and few built-in dislocations outside the grain boundaries.

Next, tensile coupons (strips) are patterned in the metal film, with widths from 14 to 250 μm. Each specimen consists of multiple parallel strips mounted to the same frame. The strips on a frame will all be loaded at the same time; the measured force will be the sum of the forces on each of the individual strips. The 250-μm-wide coupons have gage lengths of about 1 mm. The narrower coupons have proportionally smaller gage lengths, with the ratio of length to width maintained between 3 and 10. The tensile strips are formed using a typical wet-etch lithographic process. Figure 2 shows the design, with the metal layer superposed on the oxide layer. The pattern of the tensile strips is realized on a photomask. Negative photoresist on the specimen wafer is exposed to ultraviolet light through the photomask, after it has been aligned to the frames. The resist is developed and baked, and then the specimens are etched. The aluminum etchant is the usual phosphoric acid solution, used at 40 °C. The same solution is used 35 °C to etch copper. The Ti layers are etched with a dilute solution of H_2O_2 and HF in water. If the solution is old and the H_2O_2 has dissipated, the photoresist can be attacked, causing damage to the specimens. The wet-etch produces edges which have no tears. At high magnification in the SEM, deviations from straightness of a fraction of a μm appear all along the specimen edges.

The wafers are introduced into an aqueous hydrazine solution in a reflux condenser (Mehregany and Senturia, 1988), and etched for 4 hours at 100 °C. This treatment removes the unprotected silicon in the windows under the gage sections of the tensile coupons, and leaves an array of frames containing suspended tensile coupons. These usually have the appearance of being slightly curled out-of-plane in the transverse direction. They do not appear taut, and are probably slightly buckled.

APPARATUS

The testing machine used in the previously reported study (Read and Dally, 1993) has been replaced. The new testing machine consists of a fixed grip and a movable grip, connected by columns that can be expanded, figure 3. The expandable columns are made with heaters to produce thermal expansion, or are made of piezoelectric stacks. The moveable grip is connected to a flexible steel beam that bends in proportion to the applied force. This grip is cantilevered just above the base of the device, so

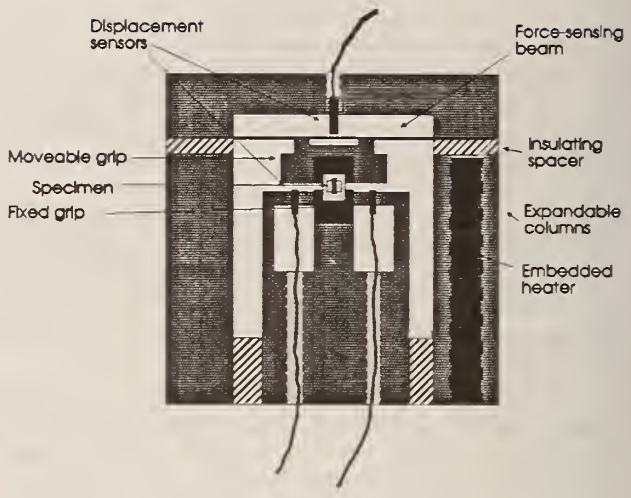

FIGURE 3. SCHEMATIC DIAGRAM OF THE MECHANICAL TESTING DEVICE. THE DEVICE MEASURES ABOUT 14 BY 12 CM.

sliding friction, which was present in our previous apparatus, is eliminated. The testing machine is actuated by current to theheaters or by voltage applied to piezoelectric actuators. The thermal device used aluminum columns with cartridge heaters mounted in holes. The piezoelectric device has two piezoelectric stacks 60 mm tall.

Displacement is imposed at a constant rate, by using a closed loop control control system to apply current to the heaters or voltage to the piezoelectric stacks. The control loop is driven by a computer which accepts input from the sensors and updates the drive three times per second. Displacement is measured at the grips, using noncontacting eddy current sensors, figure 3. The grips are massive and rigid compared to the thin film specimens, so the extraneous displacements are negligible. Two sensors are used, mounted in the plane of the thin film at either side of the grip. These sensors produce 1 mV of signal for each 25 nm of displacement.

Tension on the specimen bends the beam that carries the moveable grip. This bending displacement is detected by a third eddy-current sensor. Several beams have been used. Best results have been obtained with steel beams 0.38 to 0.5 mm thick. These have produced displacements ranging from 5 to 10 micrometers for an applied force of 0.34 N, which is obtained by using a 35-gram test mass. The calibration factors are 1.7 N/V or more, so a 1-mV signal corresponds to 0.0017 N. This load sensor has a stiffness of about 0.063 N/μm. This is about one-fourth of the elastic stiffness of the largest Cu specimen tested; it allows measurement of force-displacement behavior well beyond maximum load for most specimens.

PROCEDURE

The test procedure begins with the mounting of a specimenassembly in the testing machine. The moveable grip is clamped to the base of the device with a special clamp that can be tighted and released with minimal displacement. Some of the 250-μm-wide coupons have been tested individually, by manually cutting off 3 of the 4 coupons in the specimen assembly (fig. 2) at this stage of the test. Then the sides of the silicon frame are chipped out manually using a stylus. This operation usually takes 15 m to ½ h. When the clamp is released, the moveable grip returns to its cantilevered position, so that friction between the moveable grip and the base is avoided. The specimens are usually observed to be slightly buckled at this point. This buckling comes from two sources: buckling present in the specimens before the frame was severed, and additional buckling introduced when the moveable grip is unclamped. The clamp is arranged so that if this grip moves at all upon release, it moves in the direction to compress and buckle the specimen.

In the results tabulated below, the initial specimen area is used in all stress calculations. The areas were determined as the product of specimen thickness and specimen width. The thicknesses were measured with a commercial profilometer of the type commonly used in semiconductor facilities. Specimen widths and gage lengths were measured with a traveling microscope. Reported elongation values are elongation at maximum load. In some tests it seemed like a useful value of the strain to failure could be recorded, but in many tests the load decreased gradually to nothing with increasing imposed displacement. Therefore strain to failure could not be defined from the load-displacement record. A final measurement of the total length of the two parts of the fractured specimens, as is commonly done for bulk specimens, is impossible for these thinfilm specimens, because of large out-of-plane deformations at failure.

RESULTS

Thin Film stress-strain behavior

Stress-strain curves for TiAlTi and TiCuTi layered specimens are shown in figures 4 to 7. The Ti layers make up less than 10 percent of the specimen thickness. Figures 4 and 5 show constant-deformation-rate tests. These stress-strain curves look a lot like bulk metal stress-strain curves; one important difference is that the elongation axis extends only to 2 or 3 percent, instead of the 50 percent or more that would be needed to display the behavior of bulk pure-metal specimens. Figures 6 and 7 show cyclic stress-strain behavior. Nothing in these plots is significantly different from general behavior observable in bulk metals. However, the extent of the imposed cyclic strain was limited to avoid failure.

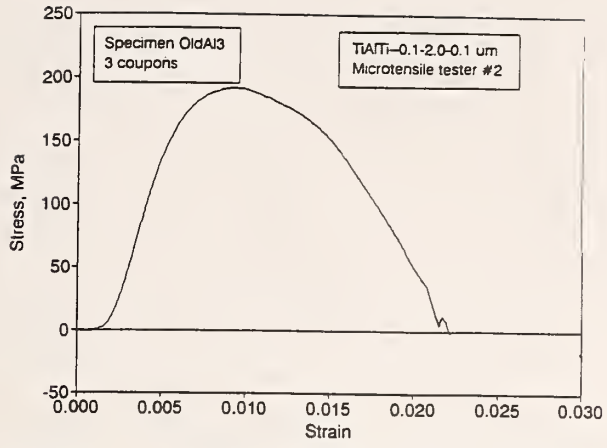

FIGURE 4. TYPICAL STRESS-STRAIN CURVE OF TiAlTi FILM, 2 μm THICK, SHOWING THAT THE STRESS-STRAIN CURVE CAN BE FOLLOWED PAST THE MAXIMUM LOAD, AND THAT THE POINT OF FINAL FAILURE IS NOT CLEARLY DEFINABLE.

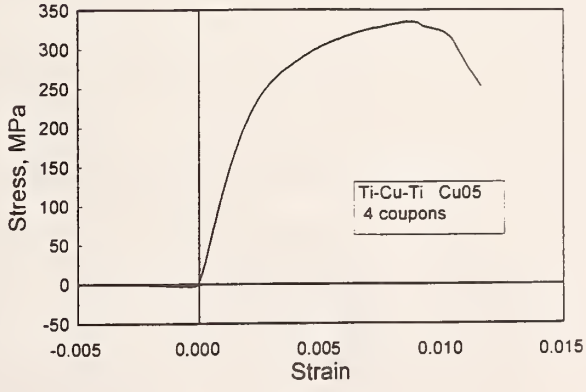

FIGURE 5. TYPICAL STRESS-STRAIN CURVE OF TiCuTi FILM, 1.7 μm THICK, SHOWING THAT Cu FILMS ARE TYPICALLY STRONGER THAN THE Al FILMS, AND HAVE SIMILAR ELONGATION TO MAXIMUM LOAD.

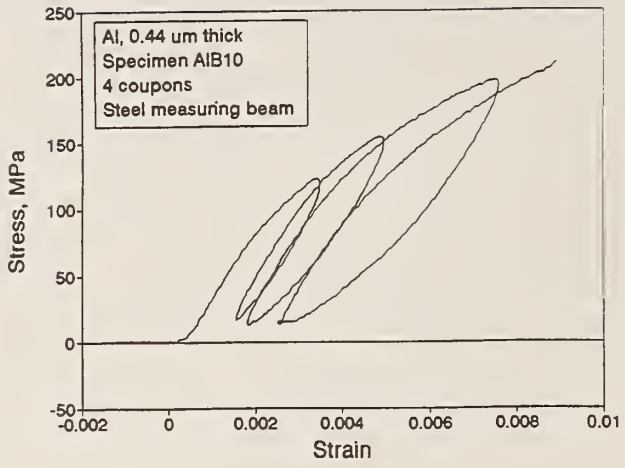

FIGURE 6. CYCLIC STRESS-STRAIN RECORD FOR TiAlTi THIN FILM, SHOWING HYSTERESIS SIMILAR TO WHAT WOULD BE OBSERVED WITH CONVENTIONAL MACROSCOPIC SPECIMENS.

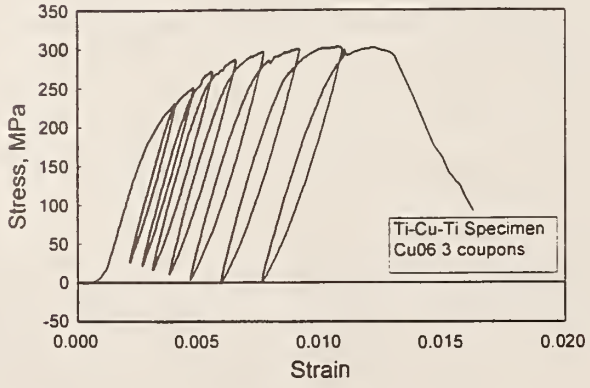

FIGURE 7. CYCLIC STRESS-STRAIN RECORD FOR A TiCuTi FILM, PLOTTED ON A COARSER STRAIN SCALE THAN THE PREVIOUS FIGURE, SHOWING SIMILAR HYSTERESIS AND REPEATABLE CYCLIC BEHAVIOR.

Figure 8 compares the loading and unloading slopes of the same TiCuTi specimen to the Young's modulus of bulk polycrystalline Cu. As noted in the introduction, there is no question but that the thin metal films should have the same elastic moduli as bulk metal. In this figure, the initial modulus, meaning, the apparent modulus for initial loading, is less than the handbook modulus value. This figure illustrates that the final modulus may not be observed on initial loading because of plastic deformation, and that the present apparatus and specimens are capable of producing the correct result.

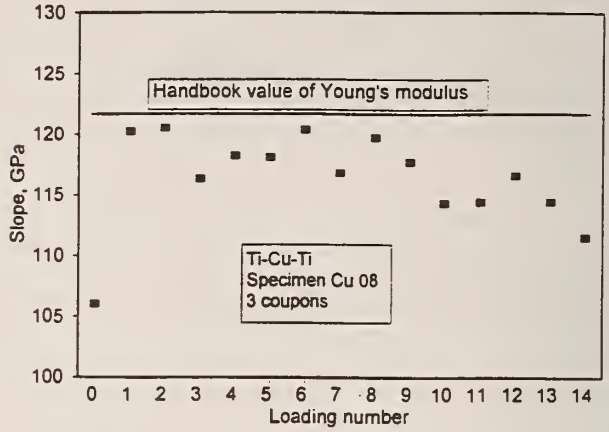

FIGURE 8. SLOPES OF STRAIGHT-LINE PORTIONS OF THE STRESS-STRAIN RECORD SHOWN IN FIGURE 7. THE X-AXIS IS LOADING NUMBER, INCLUDING INITIAL LOADING, UNLOADINGS, AND RELOADINGS.

Copper and aluminum thin films vs bulk metal

The behavior of TiAlTi and TiCuTi films can be compared to that of bulk Al and bulk Ti based on multiple tests. Some of the TiAlTi results were reported previously (Read and Dally, 1993), and are introduced here for purposes of comparison. The testing device on which these data were obtained, called microtensile tester number 1, was more susceptible to errors of displacement measurement than tester number 2, though its load measurement device was quite accurate. Tables 1 and 2 give the TiAlTi and TiCuTi results.

The statistical summary of the TiAlTi and TiCuTi results is given in Table 3. From Table 3 we see that the strength values for TiCuTi are higher than those for TiAlTi. The large standard deviation of the yield strengths of TiAlTi films is believed to result from yield strengths measured in the old tester that are generally too low. The new tester produced higher values. The best average value is believed to be much closer to the higher values produced by tester number 2 than to the average listed in Table 3.

TABLE 1. TENSILE TEST RESULTS FOR TiAlTi FILMS 2.0 μm THICK.

Yield strength, MPa	Ultimate strength, Mpa	Strain at maximum load, %
121*	199*	1.2*
115*	186*	1.1*
96*	191*	1.8*
71*	156*	1.3*
120*	144*	0.54*
91*	146*	0.85*
186	191	0.8
195	197	0.8
*Obtained with microtensile tester number 1.		

TABLE 2. TENSILE PROPERTIES FOR TiCuTi FILMS 1.72 μm THICK.

Yield strength, MPa	Ultimate strength, Mpa	Strain at maximum load, %
207*	240*	1.1*
276*	330*	0.5*
276	308	0.84
302	333	0.87
269	302	0.95
249	270	0.55
264	346	1.8
253	335	1.4
265	323	1.2
*Otained with microtensile tester number 1.		

TABLE 3. AVERAGE AND STANDARD DEVIATIONS OF MEASURED VALUES OF STRENGTHS OF 2-μm-THICK TiAlTi AND TiCuTi THIN FILMS

Material	Value	Yield strength, MPa	Ultimate strength, MPa	Strain at maximum load, %
TiAlTi	Average:	124	176	1.0
	Standard dev:	41	22	0.37
TiCuTi	Average:	262	310	1.0
	Standard dev:	24	33	0.39

Table 4 lists the handbook tensile property values for pure bulk polycrystalline copper, aluminum, and titanium. Literature values for the yield and ultimate strengths of pure copper and aluminum vary. This variability indicates the influence of grain size, very low levels of impurities, and prior deformation on the flow behavior of pure face-centered-cubic metals.

The yield and ultimate strengths of the pure aluminum specimens are given in Table 5, and summarized statistically in Table 6. They agree with those of the TiAlTi specimens within the standard deviations of the measured quantities. Especially since tester number 1 seemed to produce low values of the yield strength, the disagreement between the yield strengths of the pure Al specimens and the TiAlTi specimens does not seem statistically significant. The elongation of the thinner, pure specimens seems lower than that of the thicker, layered specimens, however. It is argued below that this lowered elongation is a real thickness effect.

TABLE 4. HANDBOOK TENSILE PROPERTIES OF PURE POLYCRYSTALLINE Al, Cu, AND Ti.

Material	Source	Yield Strength, MPa	Ultimate Strength, MPa	Elongation, %
Al	ASM Handbook (1979)	15 to 20	40 to 50	50 to 70
	Smithells (1983)	20	55	55
Cu	ASM Handbook (1979)	33	209	60
	Smithells (1983)	48	216	48
Ti	ASM Handbook (1979)	140	235	54
	Smithells (1983)	103	241	55

TABLE 5. TENSILE RESULTS FOR PURE Al FILMS, 0.44 μm THICK.

Yield strength, MPa	Ultimate strength, MPa	Strain at maximum load, %
161	166	0.5
168	174	0.5
110	211	0.3
162	210	0.3

TABLE 6. AVERAGE AND STANDARD DEVIATIONS OF MEASURED VALUES OF STRENGTHS OF PURE Al THIN FILMS 0.44 μm THICK

	Yield strength, MPa	Ultimate strength, MPa	Strain at maximum load, %
Average:	150	190	0.45
Standard dev:	24	20	0.09

Aspect ratio

Figure 9 shows the yield and ultimate strengths of a set of TiAlTi specimens from a single wafer, plotted against cross-section aspect ratio, that is, the ratio of specimen width to specimen thickness. The specimen thickness was constant. The width was varied during specimen fabrication, by subdividing the original wide tensile coupons into arrays of parallel narrower coupons. In testing such arrays, the average strength of the whole array is measured. The figure indicates no strong, consistent trends of strength with aspect ratio. Observations of the appearance of the specimens as they deformed and failed also yielded no indications that the narrower specimens were behaving any differently than the wide ones. Therefore, the strength results reported here are believed to be insensitive to the cross-section aspect ratio, at least over the range tested.

Figure 10 plots elongation to maximum load against the same aspect ratio. The scatter is larger than for the strengths, but again, no consistent tendency is shown for these specimens, which had different widths but the same thickness. The received wisdom from macro-scale studies of thin wide sheets of aluminum seems to be that care is required in maintaining uniform gripping, and in keeping the specimen gage length sufficiently long compared to the width. But, when sufficient care is taken with these items, near-normal values of tensile elongation at maximum load are expected. Dieter (1976) discusses geometric corrections of the conventional elongation to failure, which includes a significant contribution from deformation occuring during necking This contribution, of course, occurs after maximum load.

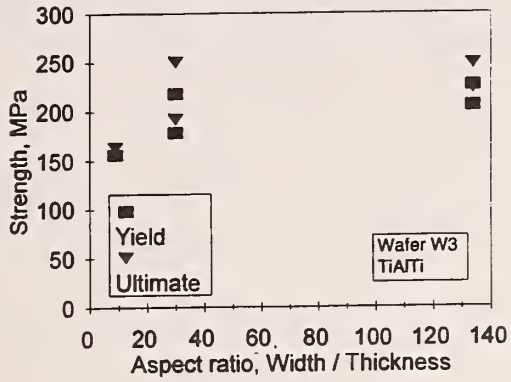

FIGURE 9. YIELD AND ULTIMATE STRENGTHS FOR TiAlTi SPECIMENS FROM A SINGLE WAFER, PLOTTED AGAINST CROSS-SECTION ASPECT RATIO.

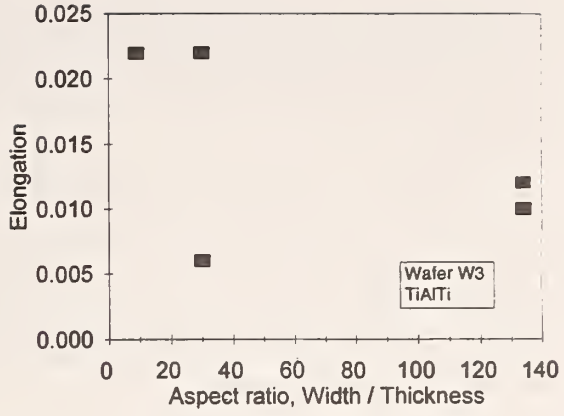

FIGURE 10. ELONGATION TO MAXIMUM LOAD FOR TiAlTi SPECIMENS FROM A SINGLE WAFER, PLOTTED AGAINST CROSS-SECTION ASPECT RATIO.

Most studies of the mechanical behavior of thin films have reported low values of elongation to failure, consistent with the values around 1 % reported here. One study (Steinwall, 1992) found much higher values in some specimens. Those specimens had a lower cross-section aspect ratio than most of those tested here. But, those specimens also had ultra-fine grains, much smaller than those in the specimens used in the present study. The average grain diameter of these ultra-fine-grained specimens was less than 0.1 μm. It is argued below that Steinwall's higher ductility values relative to the present study are a result of his ultra-fine grain sizes, and not a result of his lower cross-section aspect ratio.

DISCUSSION

Why is the measured ductility so low?

Possible causes of the observed low ductility for thin films include: a real thin-film effect, a grain size effect, an aspect ratio effect, non-uniform specimen cross section, rough specimen edges, and other unknown effects or artifacts. The tensile test results presented in this paper indicated low ductility in pure and multilayer thin film tensile specimens of various thicknesses and widths. The thinnest specimens tested had the lowest ductility.

The low ductility values for thin films reported here and in many other studies are believed to be real, and not an artefact of the test procedure or the specimen preparation. Paper after paper on thin film mechanical properties has reported low ductility. The only counterexample known to the authors is found in Steinwall's (1992) results, which showed low ductility for some thin-film specimens with grain sizes similar to those used here, but higher ductility for specimens of ultra-fine grain sizes, prepared and tested by the same procedures.

The argument that low ductility in thin films results from some deficiency in the specimen-preparation procedure must be considered carefully. Evidence against the specimen-preparation argument is that ductilities in the neighborhood of 1 % are found for a variety of specimen-preparation procedures. It is clear that small tears or cracks in thin-film tensile specimens can drastically reduce their elongation to failure. Because the specimens used here are produced by microlithography, the edges contain some undulations on the scale of 1 μm, but no mechanical damage. If these extremely small irregularities were the cause of the low observed ductility, this observation would be significant in itself. However, it is hard to believe that all of the many thin film studies in the literature have been subject to the same sort of edge irregularities.

An additional piece of evidence in favor of the low ductility of thin films is that some studies have found low elongation is some specimens and higher ductility in others, all prepared with similar techniques. Kim and Weil (1989) reported systematic decreases in elongation to failure as they made their monocrystalline nickel electrodeposited specimens thinner. Their plot of elongation results is consistent with values of 1 % near specimen thicknesses of 1 μm. The results of Steinwall (1992) mentioned above also fall in this category, because he found low ductility for films of some grain sizes, but high ductility for others.

The aspect ratio argument was covered above. Though the data are few, it appears that the aspect ratio effect on thin film elongation is weak.

There is good evidence that very fine grain size alone does not reduce ductility to the extent commonly observed in thin films. Studies of the mechanical behavior of very-fine-grained specimens of Cu and of Al have been performed (Merz and Dahlgren, 1975, and Alpas *et al*, 1990). These studies used thin-film deposition techniques, but continued the deposition for extremely long times to produce specimens several hundred μm thick. These studies indicated ductilities approaching 10 %, much higher than the values observed here.

Two factors that strongly influence ductility have been identified: specimen thickness and grain size. A companion study

to this one (Keller, Phelps, and Read, 1994) has shown that intra-grain dislocation generation and motion are suppressed in pure Cu films 0.25 μm thick. This was attributed to the tendency for disloctions to be trapped at grain boundaries, where displacement accumulated, causing the film to literally "unzip" and fail along grain boundaries.

The picture that emerges is that ultra-fine grains (Steinwall, 1992) enhance the grain-boundary slip, and that this deformation mode can provide substantial elongation to failure in thin films. Normally fine grains, of the order of 0.1 to 1 μm, do not allow significant grain-boundary slip. In these films, dislocations accumulate at grain boundaries, causing them to fail with low tensile elongation. The thinner the film, the stronger this effect, and hence the lower the elongation.

CONCLUSIONS

The mechanical behavior of thin films is influenced by their thickness and grain size. Yield and ultimate strengths are elevated over bulk values by the very-fine grain size found in normally-deposited thin films. Impurities trapped in the specimens during the deposition process probably play a role here as well. Ductility is reduced below bulk values because the atomic-scale deformation process is influenced by the thin-film surface.. However, ultra-fine grains can introduce an additional slip mechanism, some sort of grain boundary slip,and thus can have higher elongations than the specimens tested here (Steinwall, 1992). Thinner fine-grained specimensthan those tested here should have even lower ductility.

REFERENCES

Alpas, A. T., Embury, J. D., Hardwick, D. A., and Springer, R. W., 1990, "The mechanical properties of laminated microscale composities of Al/Al_2O_3", *Journal of Materials Science* 25, 1990, pp. 1603-1609.

ASM Handbook Committee, 1979, *Metals Handbook Ninth Edition Volume 2, Properties and Selection: Nonferrous alloys and pure metals*, Americal Society for Metals, Metals Park, Ohio 44073.

Baral, D., Ketterson, J. B. and Hilliard, J. E., 1985, "Mechanical properties of composition modulated Cu-Ni foils," *Journal of Applied Physics, 57*, pp. 1076-1083.

Davis, B.M., Li, D.X., Seidman, D.N., Ketterson, J.B., Bhadra, R., and Grimsditch, M., 1992, "Elastic and nanostructrural properties of Cu/Pd superlattices," *Journal of Materials Research, 7*, Number 6,, pp. 1356-1369.

Dieter, George E., *1976, Mechanical Metallurgy*, Second Edition, McGraw-Hill, New York, pp. 346-348.

Dunn, Robert,1993, Keynote address at ASME International Conference on Electronic Packaging, Binghampton, New York.

Guess, Tommy R. and Burchett, Steven N., 1992, "An experimental / analytical study of strains in encapsulated assemblies," in *Advances in Electronic Packaging 1992, Volume 1*, Proceedings of the First Joint ASME/JSME Conference on Electronic Packaging, EEP-Vol.1-1, Milpitas, California, April 9-12, 1992, edited by W. T. Chen and J. Abe', American Society of Mechanical Engineers, New York, pp. 543-550.

Hardwick, D. A., 1987, "The Mechanical Properties of Thin Films: A Review," *Thin Solid Films 154*, pp. 109-124.

Hoffman, R. W., 1966, "The Mechanical Properties of Thin Condensed Films," in *Physics of Thin Films*, edited by Georg Hass and Rudolf Thun, Academic Press, New York.

Keller, R. R., Phelps, J. M., and Read, D. T., 1994, "Tensile Deformation-Induced Microstructures in Free-Standing Copper Thin Films," *Materials Research Society Proceedings*, in press.

Kim, Ingon and Weil, Rolf, 1989, "The Mechanical Properties of Monocrystalline Nickel Electrodeposits," *Thin Solid Films*, 169, pp. 35-42.

Lau, John H., and Rice, Donald W., 1992, "Thermal fatigue life prediction of flip chip solder joints by fracture mechanics method," in *Advances in Electronic Packaging 1992, Volume 1*, EEP-Vol.1-1, Proceedings of the First Joint ASME/JSME Conference on Electronic Packaging, Milpitas, California, April 9-12, 1992, edited by W. T. Chen and J. Abe', American Society of Mechanical Engineers, New York, pp. 385-392.

Mehregany, Mehran and Senturia, Stephen D., 1988, "Anisotropic Etching of Silicon in Hydrazine," *Sensors and Actuators, 13*, pp. 375-390.

Merz, M. D., and Dahlgren, S. D., 1975, "Tensile strength and work hardening of ultrafine-grained high-purity copper," *Journal of Applied Physics 46*, pp. 3235-3237.

Nix, W. D., 1989, "Mechanical Properties of Thin Films," *Metallurgical Transactions, 20A*, pp. 2217-2245.

Pao, Yi-Hsin, Chen, Kuan-Luen, and Kuo, An-Yu, 1991, "A nonlinear and time dependent finite element analysis of solder joints in surface mounted components under thermal cycling," *Materials Research Society Symposium Proceedings Vol. 226*, Materials Research Society, Pittsburgh, pp. 23-28.

Read, D. T., 1992, "In situ measurements of strength and ductility of thin films", in *Advances in Electronic Packaging 1992, Volume 1*, EEP-Vol.1-1, Proceedings of the First Joint ASME/JSME Conference on Electronic Packaging, Milpitas, California, April 9-12, 1992, edited by W. T. Chen and J. Abe', American Society of Mechanical Engineers, New York,, pp. 463-468.

Read, D. T. and Dally, J. W., 1993, "A new method for measuring the strength and ductility of thin films," *Journal of Materials Research, 8*, No. 7, pp. 1542-1549.

Smithells, 1983, *Smithell's Metals Refrence Book*, Sixth Edition, edited by Eric Brandes, Butterworths, London.

Steinwall, J. E., 1992, *Microfabrication and Mechanial Properties of Free Standing Thin Films*, Ph.D. thesis, Cornell University.

Appendix C. 1995: Fatigue of Microlithographically-Patterned Free-Standing Aluminum Thin Film Under Axial Stresses

David T. Read
Materials Reliability Division,
National Institute of Standards
and Technology,
Boulder, CO 80303

James W. Dally
Mechanical Engineering Department,
University of Maryland,
College Park, MD 20742

Fatigue of Microlithographically-Patterned Free-Standing Aluminum Thin Film Under Axial Stresses*

Fatigue life as a function of number of stress cycles has been determined for three-layer titanium-aluminum-titanium thin-film specimens. For nominal stresses ranging from 50 to 90 percent of the upper-bound ultimate strength, the fatigue lives ranged up to 76 cycles. In all specimens, active cracks were observed after only a few stress cycles. These cracks grew with repeated cycling. The fatigue life was reached when the specimen could no longer sustain the maximum cyclic stress.

Introduction

This study is motivated by the need to extend the methods of fatigue-life prediction [1–5] to thin films. Deterministic evaluations of the reliability of multilayered thin-film structures require an understanding of the fatigue lives of the individual layers. One source of stresses in multilayered structures is differential thermal expansion in adjoining materials. Electronic devices are commonly subjected to thermal cycling during a manufacturing screening test to reveal defective devices. Manufacturing screening is from 1 to 20 cycles, while operation can involve thousands [6–8] of cycles.

The specimens tested here were free-standing, as will be described below, and so their behavior does not directly simulate that of films adhering to substrates. The tensile stress in free-standing films is easier to apply and control than stresses in films on substrates. These results are presented as a simpler first step toward understanding the more complicated cases of films on substrates and thin films in multilayer structures. They may also be relevant to cases where free-standing films are used in special devices.

In these experiments we used a relatively new technique [9], which enabled us to conveniently fabricate and test a series of thin-film specimens that were nearly identical. However, because of the extremely small size of these specimens, and because the specimens were produced by vapor deposition, the experimental procedure differed from the current practice of strain cycling to investigate the fatigue behavior of bulk materials at low cycle life. The differences were: we could not use a standard specimen geometry, for example, hourglass-shaped; we could not impose compressive stresses, because the films were free-standing; and we controlled the applied cyclic stress, whereas in conventional testing strain is often controlled. In these experiments, we controlled the cyclic stress applied to the specimens, and observed the number of cycles to failure in the range of 1 to 100 cycles.

The prediction of fatigue life of conventional structures with macroscopic dimensions has reached a high state of development [1–5]. However, the methods are based entirely on empirical observations of the fatigue resistance of either uncracked or cracked specimens. Two typical descriptions of the fatigue life of initially uncracked specimens are commonly used: low-cycle fatigue and high-cycle fatigue. The tests reported below were carried out according to the general methods of high-cycle fatigue testing, in that the control parameter was stress, and the stress was restricted so that the elastic part of the strain was generally greater than the plastic part. However, the resulting cycle lives were much less than those typical of high-cycle fatigue.

In this paper, we describe: (*a*) the techniques used to prepare thin-film specimens; (*b*) the loading system that was designed to accommodate these very small specimens; and (*c*) the procedures used in testing the films. The results are presented in the form of a segment of an *S-N* curve. We also discuss the relationship of these results to the context of a modern treatment of fatigue resistance.

Specimen Preparation

The techniques used to prepare specimens are relatively new [9]. In a batch-production process, each thin film sample is fabricated on a silicon frame, which supports it until it is ready to be tested. The specimen structures, consisting of films suspended from supporting frames, are referred to as specimen assemblies. The thin film on each frame is patterned to form four parallel tensile strips or coupons. Each coupon has a gage section 1 mm long by 0.25 mm wide by 2.45 μm thick. The central Al layer is 2.25 μm thick. The two titanium layers on the specimen surfaces are each 0.1 μm thick. The gage sections

*Contribution of the U.S. National Institute of Standards and Technology; not subject to copyright in the U.S.

Contributed by the Electrical and Electronic Packaging Division for publication in the JOURNAL OF ELECTRONIC PACKAGING. Manuscript received by the EEPD August 11, 1992; revised manuscript received December 20, 1994. Associate Technical Editor: A. Dasgupta.

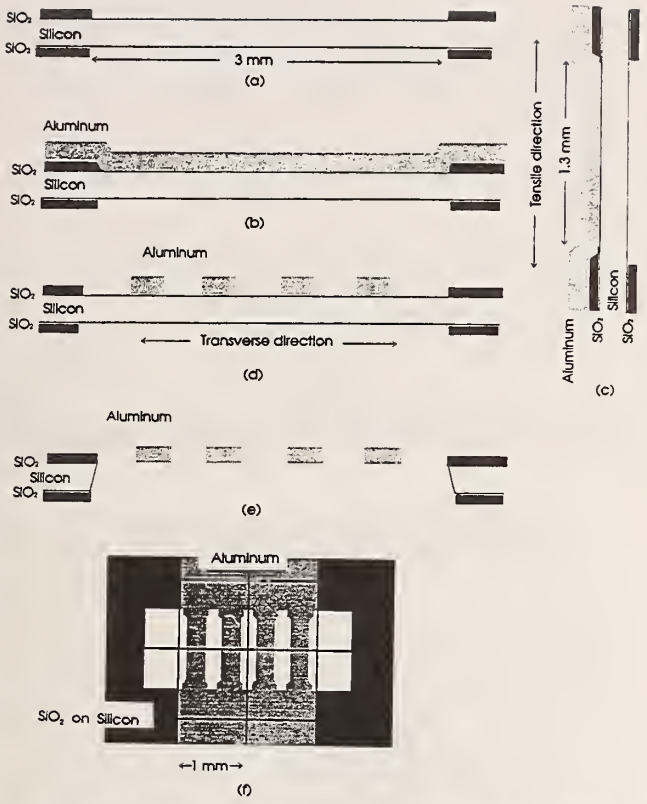

Fig. 1 Schematic diagrams showing specimen preparation sequence. Thicknesses of SiO_2 and aluminum films are exaggerated relative to the thickness of the silicon wafer. (a) Window patterned in the SiO_2 on the silicon wafer. (b) Aluminum thin film deposited over the whole wafer. (c) Cross section along the tensile direction showing the aluminum film covering the whole wafer. (d) Tensile coupons within the windows on the silicon wafer. (e) Tensile coupons suspended on the frame, after removal of the silicon within the window. (f) Plan view of specimen assembly, at a smaller scale.

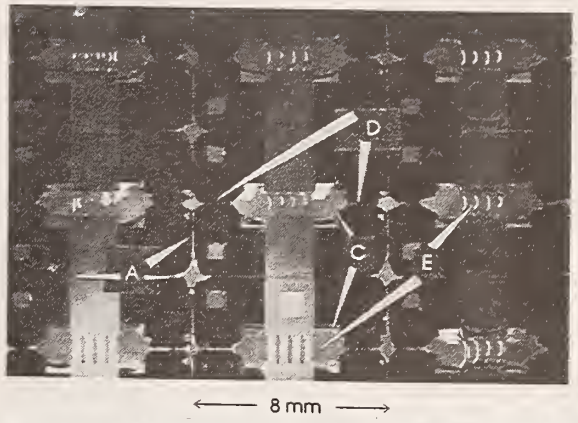

Fig. 2 Portion of the completed wafer with 9 specimen assemblies, each supporting four parallel tensile coupons. A: Etched grooves separate individual specimen frames. B: Aluminum thin film. C: Windows etched through the silicon wafer. D: Lines where frames will be fractured to allow testing of the free-standing films. E: Aluminum tensile coupons suspended from the supporting frames.

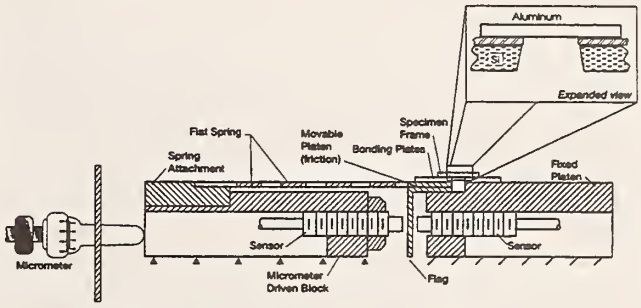

Fig. 3 Drawing of loading system used for the fatigue tests

of the tensile specimens are freely suspended across the interior of the frame. Thirty-six of these frames are produced on a single 51 mm (2 in.) diameter silicon wafer.

The specimens were prepared by employing a number of processes common to the microelectronics industry. Figure 1 shows the specimen preparation steps schematically. We began with a 51 mm (2 in.) diameter silicon wafer, polished and oxidized on both sides. The first step, Fig. 1(*a*), was to pattern, by semiconductor-style microphotolithographic techniques, windows in the SiO_2 on both sides of the wafer. We then deposited the metal film by successive electron-beam evaporation of controlled amounts of titanium, aluminum, and again titanium. The base vacuum was 10^{-6} torr. The evaporation rate was set at 10 Å per s for aluminum, and 3 Å per s for titanium. Figures 1(*b*) and 1(*c*) show the metal film, labeled "aluminum" for simplicity, covering the whole wafer, including the bare silicon in the previously defined windows, and the silicon still coated with SiO_2 surrounding the windows. We then defined the geometry of the individual tensile coupons by another standard lithography step. Figure 1(*d*) shows the transverse cross section of the individual tensile coupons. The pattern in the metal film is aligned to the windows in the SiO_2 layer using a mask aligner. The manual aligner we used is, at best, capable of alignment to within a few μm. We estimate that we aligned to better than 10 μm. This was more than adequate for our specimens, which had a length over 1 mm. Finally, the wafer was etched in aqueous hydrazine to remove areas of silicon not protected by SiO_2. Figure 1(*e*) shows the suspended films in cross section. Figure 1(*f*) shows a plan view of the specimen assembly.

Figure 2 shows a portion of the completed wafer with nine specimen assemblies, each supporting four parallel tensile coupons.

Loading System

The loading system was designed for tensile testing of thin-film specimens [9], and was adapted for low-cycle-life fatigue experiments. The loading system has two special features. First, is the ability to rigidly clamp the specimen frame while it is severed and then to release it without imposing tensile displacements that produce loading. This control of displacements during the frame fracture process is a stringent requirement because extension to failure of the thin-film tension specimens is only about 10 μm. The second special feature is the ability to impose very small forces that are precisely controlled.

The mechanical features of the loading system, illustrated in Figs. 3 and 4, include a fixed platen and a sliding platen with a pair of specimen-mounting plates, a calibrated spring, and a series-connected pair of micrometers. The mounting plates are fixed to the two platens with small screws so that they can be removed and recycled. After alignment, the specimen frame is bonded to the mounting plates with a quick-setting methyl-2-cyanoacrylate adhesive. The load is applied by displacing one end of the spring with one or the other of the two micrometers. One micrometer is a differential type with graduations of 1 μm, and the other is a conventional type with graduations of 10 μm. The other end of the spring is fastened to the sliding platen. As the spring is extended, the spring force is transmitted through the sliding platen to the specimen array. For these tests, only the single-screw micrometer was used, so that the

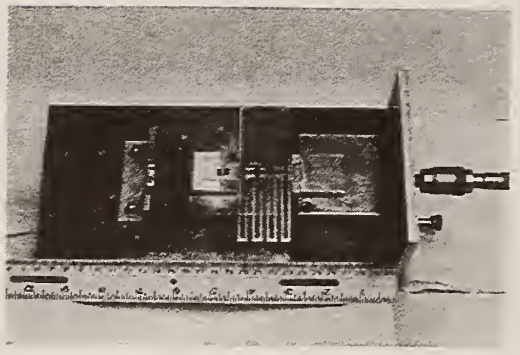

Fig. 4 Photograph of the loading system used for the fatigue tests

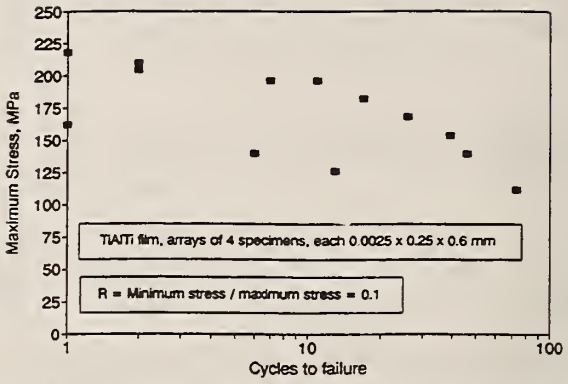

Fig. 5 S-N_f curve for TiAlTi thin-film specimen array, showing the maximum cyclic stress as a function of number of cycles to failure

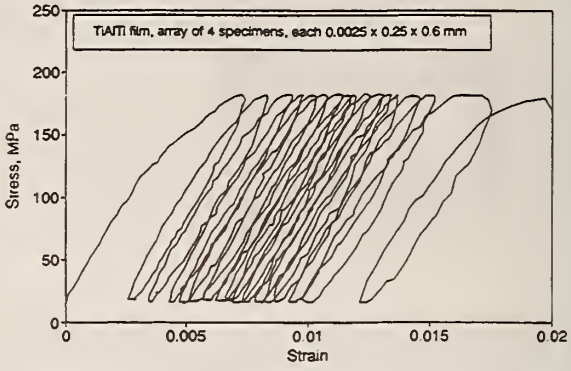

Fig. 6 Stress-strain record for a TiAlTi specimen array that failed on the 17th cycle

loads were imposed with a precision of about 5 mN, or 1 percent of the ultimate strength.

The travel of the sliding platen was retarded by friction; however, this effect was mitigated by continually tapping the support structure of the fixture with a light striker during the loading cycle. Measurements of the remaining frictional forces showed that these were less than 1 mN.

The extension of the loading spring was measured using an eddy-current sensor that was fixed to the micrometer-mounted end of the spring. Its target was an aluminum flag attached to the sliding platen. With this mounting arrangement, the sensor is insensitive to simple translation of the spring as a whole, but responds to spring extension.

The tensile elongation of the specimen was measured using a second eddy-current sensor mounted to the fixed platen. The same flag served as the target for this sensor. It was required to be much more sensitive, because of the very low tensile elongations of these specimens, around 10 μm. The tapping of the fixture to mitigate friction limited the resolution of the sensor to ±0.25 μm, although the specified precision of the instrument system is ±0.0025 μm. During the test the signals for load and displacement were digitized and stored 4 times per second. Pairs of successive readings were averaged for analysis and for plotting force-elongation curves. The whole loading system, shown in Fig. 4, was mounted under an optical microscope equipped with a closed-circuit television system.

Test Procedures

The test procedure, adapted from that developed previously for tensile testing [8], was to adhesively bond a specimen assembly to the sliding and fixed platens, and then to clamp the sliding platen in place. We next fractured the frame at the locations D indicated in Fig. 2 and released the clamp. Finally, the specimen was inspected to ensure that the specimen was undamaged and that the frame was completely severed.

The fatigue loads were applied by turning the single-action micrometer by hand. The specimen was first loaded to a preselected maximum fatigue load, then cycled between this maximum and the minimum load, which was 10 percent of the maximum load. Each load cycle required approximately 1 min. Hysteresis loops were recorded on an xy plotter, and the measured values of applied force and specimen extension were stored on the hard disk of a laboratory computer. Specimen failures could be observed in the microscope, and recorded on videotape. The system was stress-controlled, so once a specimen could no longer sustain the maximum load, it failed catastrophically. The failure was by high-velocity crack propagation.

Results and Discussion

Two specimens were tested to determine the tensile strength and 12 other specimens were tested in fatigue. Loads were selected to ensure that failure occurred in 100 cycles or less. The results, given in Fig. 5, show the number, N_f, of cycles to failure as a function of the maximum applied stress S. There were clearly imperfections in the specimen geometries. We often observed crack-like features even before loading.

The results of Fig. 5 show a bimodal pattern with 11 of the 14 tests giving a S-N_f curve with relatively small scatter. The remaining three points are also consistent but indicate lower strength by about 30 percent. We will divide the data into two populations (high and low strength) for the discussion. The S-N_f curve for the high-strength population shows a knee at about 16 cycles.

Stress-Strain Behavior. The stress-strain behavior of one thin-film specimen under cyclic load is illustrated in Figs. 6, 7, and 8. The important features in each of these plots are the stress-strain hysteresis loops. As noted above, the force-displacement data were acquired as discrete readings, at a rate of 4 readings per second. For plotting, these were smoothed by interval averaging over two readings, or approximately ½ s. In Figs. 6–8, the discrete data points were connected by straight lines. The duration of each loop is 1 minute or more.

In Fig. 6, a continuous record of stress-strain is shown over 17 cycles of loading. We observe two important features in these results. First, a hysteresis loop occurs, and the size of the loop changes with the number of cycles—large, smaller, then large again. Second, a ratchetting occurs because a permanent strain is imposed on the specimen with each cycle of load. Stability of the cyclic stress-strain curve was not achieved in these tests, where the cyclic loading was stress-controlled and the life was always less than 100 cycles. The irreversible part of the strain in Fig. 6 is attributed entirely to plastic strain in the specimen. The distribution of this strain over the gage length

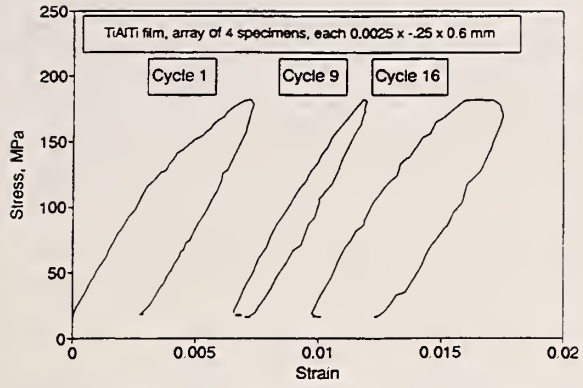

Fig. 7 Stress-strain record for the same specimen as Fig. 6, showing cycles 1, 9, and 16

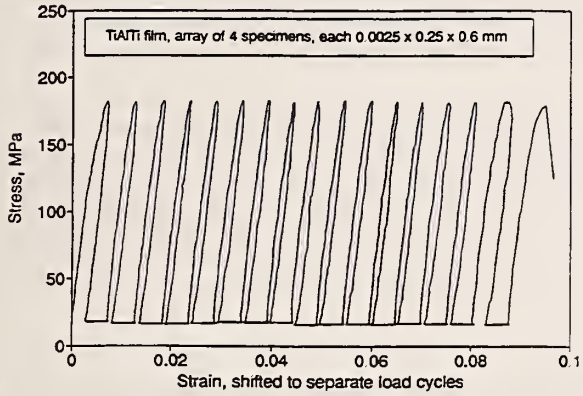

Fig. 8 Test record for the same specimen as Figs. 6 and 7, with individual cycles offset to higher strains to show all cycles separately

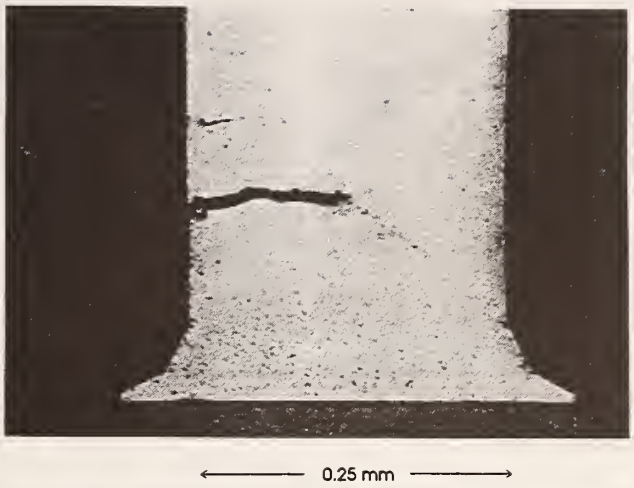

Fig. 9 Crack in thin-film fatigue specimen prior to failure

was not measured; however, the specimens were observed using the optical microscope. No sign of inhomogeneous deformation was observed. Standard alignment checks, such as loading a specimen with four gages situated around its tensile axis, were not possible in the present test procedure. However, the fixture was compliant to lateral motion of the sliding grip; this provided some self-alignment. Also, certain observations not available in standard fatigue tests were possible here. These specimens would be expected to buckle or wrinkle if significant nonaxial loading occurred. For example, the out-of-plane settling of the specimens when the silicon frame was broken was often evident from their appearance. Furthermore, four individual tensile specimens were present in each test. Nonaxial loading would be expected to load the individual specimens differently. But no sign of nonaxial loading or in-plane bending was observed. The two interior specimens behaved just the same as the two to the outside. Figures 6–8 are believed to represent axial strains only, with no detectable contributions from misalignment or bending.

The changes in the hysteresis loop are more clearly depicted in Fig. 7, where the loops corresponding to only the first, ninth, and sixteenth cycles are shown. In the first cycle, we see a stress-strain curve that is representative of a tensile test, except that the specimen was not loaded to failure. In spite of the discontinuities in the curves due to friction, we observe a linear elastic region, followed by a plastic region with significant strain hardening. Precise measurements of the constitutive constants such as the elastic modulus and the strain hardening coefficient are not possible for several reasons. The flag, which translates with the moving end of the specimen, also rotates, introducing an error into the strain measurement. Also, the thin-film specimens are not flat: after etching a transverse curl is evident.

Returning to Fig. 7, the hysteresis loop is much smaller for load cycle 9 than it was for cycle 1. Strain hardening has occurred, and the yield strength of the thin film has been enhanced by cyclic stressing above the original yield strength.

The hysteresis loop for the sixteenth cycle, which was the last complete cycle before the specimen failed, has markedly increased in size over the ninth. This increase is due to cracks which initiated during previous cycles and extended during the 16th cycle. The crack extension at the maximum applied stress results in large apparent strains. The elastic recovery curve for all three hysteresis loops was nearly identical.

Another display of the stress-strain curves for this specimen is presented in Fig. 8. In this representation, the individual loops have been separated by adding an artificial offset to the strain for each cycle. These results show the marked reduction of the size of the hysteresis loop on the second cycle, compared to that of the first. The loops remained essentially constant in size until the fourteenth cycle. At this point, cracks, which had apparently initiated during previous cycles, began to extend. These cracks, as shown in Fig. 9, increased the compliance of the specimen and produced permanent extensions in the gage length. Crack growth was very large on the sixteenth cycle and specimen failure occurred just as the maximum stress was reached on the seventeenth cycle. Figure 9 is typical of the observations available during the tests. Cracks were seen to initiate early in the tests, and to grow gradually to the size (half the width of the specimen) shown in Fig. 9. Failure occurred soon after the cracks reached this size.

The slopes of the initial portion of the loading curves in these figures do not agree with handbook values of Young's modulus for the specimen materials. We attribute this to problems with the design of the testing device, specifically, with the measurement of strain. Here we report no results that are based on measurement of strain. We note that the difficulty of measuring accurate values of Young's modulus in tensile testing is well-known even in tests of macroscopic specimens. These difficulties are even more severe here, where the total elastic elongation is approximately one wavelength of light. Our force data are much more accurate than our displacement data, because we used a soft spring, described above, to convert force to a displacement for measurement.

Comparison With Bulk Material Behavior. These results cannot be compared directly to typical results for the behavior of bulk metals in fatigue, because the test procedures used

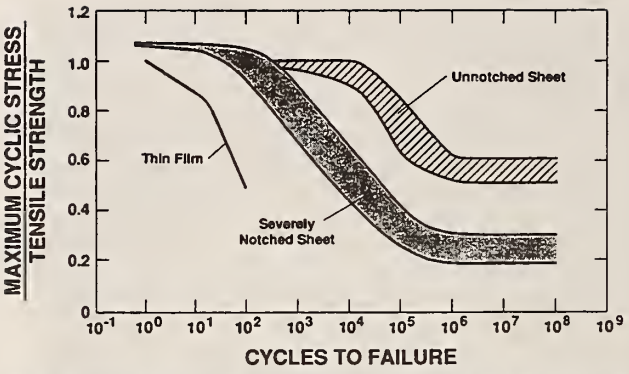

Fig. 10 Comparison of the present results for TiAlTi thin-films to results for fatigue of thin sheets of aluminum and stainless steel with stress concentrations [4]

here are unconventional. The size and thickness of the specimens and the available loading system precluded both conventional low-cycle and high-cycle fatigue test procedures. Also, because of the manual loading fixture, cycle lives beyond 100 cycles were impractical.

The present results are compared to previous results [4] on the fatigue life of axially loaded notched and unnotched sheet specimens of aluminum and stainless steel in Fig. 10. The notched specimen results included stress concentration factors of 2 and 4. The normalized *S-N* curves exhibited a knee similar to that seen in the present results for thin-films. For the unnotched comparison specimens the knees occurred generally between 10^3 and 10^4 cycles. For the severely notched specimens, the knee occurred between 10 and 100 cycles. The present thin-film results show normalized failure strengths that are significantly lower than the bulk sheet results [4] for cyclic life in excess of 5 cycles. The thin-film *S-N* curve is also below the scatter band for axially loaded cylindrical specimens [4]. We conclude that the S-N_f curve for this set of thin-film specimens in tension-tension fatigue is lower than that in bulk material by a factor of about 2.

Low Versus High-Cycle Fatigue. In low-cycle fatigue, the plastic strain range $\Delta\epsilon$ plays the decisive role, whereas in high-cycle fatigue the stress is regarded as the controlling factor. Analysis of the cyclic $\Delta\epsilon$-N curve by Sandor [1] shows that for a typical aluminum alloy the plastic and elastic parts of the strain were equal at a fatigue life around 1500 cycles. So in Sandor's example alloy, 7075-T6 aluminum, the boundary between low-cycle fatigue and high-cycle fatigue can be taken as a fatigue life of 1500 cycles. For this alloy, the monotonic plastic strain to failure is 11 percent [10].

For the thin-film TiAlTi specimens tested here, the strains involved are much different. The average tensile strain to failure is about 1 percent, and that includes elastic strains, plastic strains, and crack-opening displacements that produce apparent strains. The force-extension curves in the present set of tests show that elastic strains are larger than the plastic strains on all cycles after the second. This result holds even if the elastic strain is calculated from the cyclic stress and the Young's modulus of bulk Al, rather than as the reversible part of the stress in Fig. 7, and if an effective gage length of 0.6 mm is used. For the specimens that failed on the second cycle, the nonelastic strains were comparable to the elastic strains.

We think that the extremely short low-cycle fatigue life of the thin-film specimens is related to their brittle tensile behavior, that is, to the lack of an extended range of plastic strain before failure in tension. The elongation of these films is much lower (0.54 to 1.81 percent) than the elongation of either bulk aluminum or titanium, which are an order of magnitude higher [10]. The mechanical behavior of thin films has been reviewed by several authors [11–13]. Values of elongation to failure of around 1 percent or even less are typical in free-standing films, in both uniaxial and biaxial tests. The cause of this behavior is not understood.

The fatigue lives of the thin films tested in this study were much less than might have been expected from bulk behavior, as indicated above in Fig. 10. The cause must be sought in two main areas: intrinsic thin-film behavior; and, artifacts of the specimen-preparation process. The mechanical behavior of thin films is known to be different from that of bulk material [11–13]. Hoffman [11] notes observations of localized plastic deformation leading to cracking and failure in tensile tests. However, fatigue failures are extremely sensitive to defects, and the thin-film specimens tested here could not be subjected to conventional specimen-preparation, including careful removal of surface irregularities by polishing. Therefore the present results cannot now be regarded as characteristic of thin films in general. Additional testing is needed to clarify the mechanism of crack initiation in thin-film testing, and the role of intrinsic thin-film behavior in the fatigue resistance of thin films.

The process used here for fabricating the thin-film specimens is advantageous for an engineering assessment of thin-film fatigue characteristics. In particular, four elements of the present experimental procedures may affect the fatigue strength of these films: the etch in a hydrazine solution; the high ratio of specimen width to thickness; possible damage induced during fracture of the frame; and added stress due to vibration from the tapping used to mitigate frictional effects.

Summary

Techniques previously developed for preparation and testing of tensile specimens of thin films [9] have been successfully adapted for fatigue testing. The low-cycle fatigue life of TiAlTi thin film specimens has been measured under stress-controlled cycling. The consistency of the results given in Fig. 5 indicates that it is possible to prepare a set of nearly identical thin-film specimens and to test them under cyclic tensile stresses. Typical low-cycle fatigue behavior was not observed after 16 cycles. To achieve a life of 50 cycles, it was necessary to lower the applied stress to 65 percent of the ultimate strength. The specimens used here clearly contained imperfections, and so the observed fatigue life behavior may not be characteristic of thin films in general.

Acknowledgments

A variety of facilities and apparatus were required for fabricating tensile specimens on silicon. Use of facilities offered by R. E. Harris, of the Cryoelectronics Group of the Electromagnetic Technology Division of NIST, and by William May of the Electrical Engineering Department of the University of Colorado at Boulder is gratefully acknowledged.

References

1 Sandor, Bela I., *Fundamentals of Cyclic Stress and Strain*, University of Wisconsin Press, Madison WI, 1972.

2 Fuchs, H. O., and Stephens, R. I., *Metal Fatigue in Engineering*, Wiley, New York, 1980.

3 Dieter, George E., *Mechanical Metallurgy*, Second Edition, McGraw-Hill, New York, 1976, pp. 403–447.

4 Hardrath, H. F., Landers, C. B., and Utley, E. C., "Axial Load Fatigue Tests on Notched and Unnotched Specimens of 61S-T6 Aluminum Alloy, Annealed 347 Stainless Steel and Heat-Treated 403 Stainless Steel," *Nat. Adv. Co. Aero. Tech. Note 3017 (1953)*, reviewed in Forrest, P. G., *Fatigue of Metals*, Pergamon Press, Oxford, 1962, p. 162.

5 Manson, S. S., "Fatigue: A Complex Subject—Some Simple Approximations," *Experimental Mechanics 5*, No. 7, July 1965, p. 193.

6. Dally, James W., *Packaging of Electronic Systems,* McGraw-Hill, New York, 1990, p. 382–383.

7 Mandel, C. E. Neil, Jr., "Environmental Stress Screening," *Electronic Materials Handbook, Vol. 1 Packaging,* C. A. Dostal et al., eds., ASM International, Metals Park, OH, 1989, p. 876, 882.

8 Robock, Paul V., and Nguyen, Luu T. "Plastic Packaging," *Microelectronics Packaging Handbook,* R. R. Tummala and E. J. Rymaszewski, eds., Van Nostrand Reinhold, New York, 1989, p. 631.

9 Read, David T., and Dally, James W., "A New Method for Measuring the Constitutive Properties of Thin Films," *Journal of Materials Research,* Vol. 8, 1993, pp. 1542–1549.

10 American Society for Metals, *Metals Handbook Ninth Edition, Vol. 2,* American Society for Metals, Metals Park, OH, 1979.

11 Hoffman, R. W., "The Mechanical Properties of Thin Condensed Films," *Physics of Thin Films, Vol. 3,* edited by G. Hass and R. E. Thun, eds., Academic Press, 1966, pp. 211–273.

12 Brotzen, F. R., Rosenmayer, C. T., and Gale, R. J., "Mechanical Behavior of Aluminum and Al-Cu(2%) Thin Films," *Thin Solid Films,* Vol. 166, 1988, pp. 291–298.

13 Doerner, Mary F., and Nix, William D., "Stresses and Deformation Processes in Thin Films on Substrates," *CRC Critical Reviews in Solid State and Material Sciences,* Vol. 14, 1988, pp. 225–268.

Appendix D. 1997: Tension-tension Fatigue of Copper Thin Films

TENSION-TENSION FATIGUE OF COPPER THIN FILMS

D. T. Read
Materials Reliability Division
National Institute of Standards and Technology
Boulder, Colorado 80303

Tension-tension, load-controlled fatigue results extending to over 100,000 cycles for electron-beam-evaporated copper are reported. The specimen is fabricated as a single tensile coupon with hundreds of grains across the width but only one or few through the thickness, supported on a silicon frame. These specimens had measured values of Young's modulus lower than literature values for bulk polycrystalline values, but had high values of the yield and ultimate strengths. Closed-loop feedback control of the piezoelectric actuators allowed load-controlled fatigue tests with a cycle duration of 15 s. Stress-endurance results for this set of copper films is reported and compared to previous results.

Key words: Closed-loop testing, cyclic, displacement, endurance, force, piezoelectric, S-N curve, servo, strain, stress.

INTRODUCTION

Electronic devices are tested for reliability by thermal cycling. Modeling of the potential failure modes in such devices requires data on material behavior. These data are lacking for many of the unique materials that are used in electronic devices, especially thin-film materials. Several excellent reviews on thin-film mechanical behavior have appeared recently [1-8]. However these works have concentrated on test methods and general behavior, rather than on specific property values. The data presented here on the resistance of copper thin-films to failure by tension-tension fatigue are intended to be useful in modeling the reliability of electronic interconnects made of copper thin-films and subjected to cyclic loading.

A previous paper on fatigue behavior of aluminum thin-films [9] reported unexpectedly low fatigue resistance. In the present study, the fatigue resistance of copper thin-films is found to be considerably better than was reported for the aluminum films. However, the data cannot be unambiguously interpreted to mean that copper thin-films have better fatigue resistance than aluminum, because of changes in the test procedures. The present test procedures are improved over those used for the aluminum, in that the cyclic loads are applied under closed-loop feedback control [10], and tensile strips are tested individually, instead of in groups of 4.

SPECIMENS

All the specimens in this study came from the same silicon wafer substrate. Windows were produced in the oxide layer on a 50-mm diameter silicon wafer by microphotolithography. The substrate was clamped to a plate held at room temperature by flowing cold water. Copper of 5-nines purity was evaporated from a graphite crucible, using an electron beam in a chamber that had been pumped to a base vacuum of less than 10^{-6} torr. The deposition rate averaged 10 Å per second, as monitored by a quartz-crystal thickness gauge. The specimen film consisted of an adhesion layer of 0.05 μm of Ti, 1.1 μm of Cu, and a second, cap, layer of 0.05 μm of Ti. These specimens are designated as EBE Ti Cu Ti in the figures.

Microphotolithography was used again to subtractively pattern the film into tensile coupons. Then the wafer was etched in aqueous hydrazine at 100 °C for approximately 4 h to remove the Si from the regions behind the tensile strips, leaving them suspended across windows in the silicon wafer. Aqueous hydrazine is a hazardous material because it is highly toxic and corrosive. It is not explosive.

Each finished specimen consists of a Si frame about 8 by 3 mm, with a window through the center about 1 mm long by 1.5 mm wide. Suspended across the window is a single tensile strip. The suspended strips hve a gage section 200 μm wide by 600 μm long and wider sections at the ends. The Si frame protects the specimen from damage during handling, and allows the specimen to be aligned to the tensile axis before the frame is glued to the grips of the tensile apparatus. Figure 1 shows a schematic of the specimen, including the silicon frame and the suspended tensile strip. Figure 2 shows the design of the tensile coupon.

The last step in preparing the specimen for testing is the removal of the sides of the Si frame. We simply chip out the Si manually with a sharp tool. This must be done slowly and carefully, but it can be done with a success rate that is well over 50 percent, and takes up to half an hour per specimen. Specimens that were ruined during this step are reported as ruined during preparation.

Material evaporated under similar conditions was examined in cross-section by transmission electron microscopy (TEM) and found to have an average grain size of 0.98 μm. Figure 3 is a tracing of a TEM micrograph showing the grain morphology of the cross-section. The 200-μm-wide tensile specimens have hundreds of grains across the width, but only one or a few through the thickness. The distribution of grain size in as-deposited thin-films is discussed in detail by Zielinski, Vinci, and Bravman [11]. The distribution is generally quite broad.

APPARATUS

The microtensile tester used in these tests was constructed according to a new design especially for closed-loop testing of thin-films. It uses two piezoelectric stacks as actuators. Each stack is 60 mm long by 15 mm in diameter. The moving grip is carried on a flexible load-sensing beam, which is attached at its ends to a reference beam, which is analogous to the moving crosshead of a conventional full-size tensile testing machine. All the moving parts are cantilevered, so that there is no friction. The tester is mounted in an optical microscope, so that the specimens can be observed during testing.

Two non-contacting eddy-current sensors measure the displacement of the moving grip relative to the fixed grip. These are mounted in the plane of the specimen. Another like sensor measures the displacement of the load-measuring beam relative to the reference beam. A closed-loop control system is formed by routing the sensor outputs to a computer, which maintains target values for the control parameter, which in this series of tests was load. An analog output from the computer controls the voltage applied to the piezoelectric actuator. The

computer program calculates the difference between the desired load and the actual load, and changes the piezoelectric voltage to eliminate the error. This update occurs about 40 times per second.

TECHNIQUE and OBSERVATIONS

Load control was selected because reversible strain control requires compression as well as tension, and these freely suspended thin-films could not be compressed. The fatigue cycles were tension-tension with a minimum load nominally equal to 10 percent of the maximum load. Before each test a value of the maximum load was selected, with the goal of filling in the complete S-N curve. These load values ranged generally from 40 to nearly 100 percent of the ultimate tensile strength.

Voltages corresponding to load and grip displacement are recorded about 4 times per second for the beginning of the test. The duration of each fatigue cycle was 15 s. For tests above a few tens of cycles, it became impractical to store every force-displacement data point. Therefore, an alternative recording schedule was adopted where the maximum and minimum force, displacement, and piezoelectric voltage were recorded for each fatigue cycle. This produced a manageable volume of data, while still recording the important quantities in the test.

Failure was indicated when, after many cycles of loading to the target value and unloading to 10 percent, the load first failed to reach the target value. In seeking for the target load value, the closed-loop control routine would increase the voltage output to the piezoelectric drivers to the maximum capacity, which was 250 V, as indicated by the manufacturer of the piezo stacks. Thus, failure was unmistakable.

Plastic ratchetting occurred in all the fatigue tests, because the specimens were continually in tension. The specimen strain would increase on each load cycle, and would not fully recover. This effect was more pronounced at the higher load levels.

Some problems were experienced with specimens failing in the grip section at the edge of the frame. The failures seemed to occur more often when the specimen was fully loaded within the first few cycles. Therefore a preconditioning procedure was adopted in which the specimens were cycled for 10 cycles at 1/3 of the full load, then cycled for 10 cycles at 2/3 of the nominal load, and then cycled at the full load. The successful tests performed before this explicit preconditioning procedure was adopted also experienced a similar preconditioning, because the load was increased gradually over several cycles to the

preselected value. As the tests became more routine, the ramp-up to the selected load was quicker, and failures at the frame became more common. And, all failures at the frame were excluded from the final results. Therefore, the preconditioning is not believed to contribute any detectable degree of variability to the final results.

Some specimens survived many fatigue cycles only to fail through an obvious malfunction of the test equipment. For example, in one case, a test had to be stopped because the computer's disk was getting filled. During the restart, the specimen was inadvertently overloaded and failed. In another case, the data file was not properly recorded, so we relied on manual notes of the endurance, which were made every few hours. The actual fatigue failure occured at an unknown cycle number, but the notes allowed us to report a lower limit on the endurance in that test. One test was intentionally terminated after over 100,000 cycles. All these tests that were stopped before a fatigue failure are designated as runouts, to indicate that the test result provides only a lower limit of the endurance for that specimen at its load level.

After failure we noted the location of the failure using the microscope included in the test apparatus. Specimens that failed in the gauge section, including those near the change in width at the end of the gage section shown in Figure 2, were accepted. Specimens with the failure at or outside the change in width were excluded as failing outside the gage length. Table 1 shows the outcome distribution for all the specimens that we tested or tried to test.

Table 1. Outcome distribution for all specimens.

Test outcome	**Count**
Fatigue failure (endurance result)	15
Runout (lower-bound endurance result)	3
Used for tensile test	3
Failed outside gage length (not reported)	3
Ruined during preparation (not reported)	3
Failed during preconditioning (not reported)	3
Total	36

RESULTS and DISCUSSION

Typical values of force-displacement and stress-strain for this set of specimens are shown in Figure 4. Table 2 gives the tensile properties. The magnitudes of force and displacement evident in Figure 4 are much smaller than those found in conventional tensile testing. Clearly, special equipment is required to test thin-films. The strains displayed in Figure 4 are derived from grip-to-grip displacement, and therefore overestimate the actual elastic behavior of the specimen. The displacement within the gage section of a specimen that had been loaded and unloaded several times was measured by electronic speckle pattern interferometry (ESPI); this measurement gave a more accurate value of the Young's modulus, which is shown in Table 2. The strength of this material is much higher than values of yield and ultimate strength for pure Cu found in handbooks. This finding is typical of thin-films, and is explained by the very fine grain size of these specimens as compared to that of pure bulk Cu. The low values of elongation are characteristic of thin-films tested in tension. Results of the tensile test results are listed in Table 2, including results for a specimen that endured over 150,000 fatigue cycles at a maximum stress of 197 MPa.

Table 2. Tensile test results for electron-beam-evaporated thin-film tensile specimens.

Condition	Young's modulus, GPa	Yield strength, MPa	Ultimate strength, MPa	Elongation to failure, percent
New	107			
"		332	423	1.6
"		345	423	1.3
"		314	364	1.2
Average, new		330	399	1.4
After 152,098 fatigue cycles at 197 MPa		343	400	1.2

The fatigue results are shown in Figure 5. Plastic ratchetting occurred in all of the fatigue tests, to a much greater degree in the specimens tested at the higher loads. Even though these tests were all run under load control, the fatigue failures at the highest loads appeared to be of the low-cycle-fatigue type. The specimens failed when the plastic strain ratchetted up to a sufficiently high value. Failure strains were generally consistent with the tensile test results, typically around 1.4 percent, as shown in Table 2.

The progress of a typical high-load test was as follows. As the specimen was cycled, the total displacement increased. Some hysteresis was recorded, especially in the earlier cycles. As the test progressed, the appearance of the surface of the specimen changed. The originally flat and shiny surface became rougher, and many short, linear, crack-like features gradually appeared. Eventually, these would grow, looking more and more like cracks. Finally, the specimen would fail.

At lower loads, the appearance would change much more gradually, but in a similar fashion.

Comparison to previous work

Figure 6 compares the present results to a trend curve given by Chalmers[12] as generally representative of the stress-controlled fatigue of metals. The present results appear to fit the trend, with some scatter. Several sets of room-temperature fatigue data for copper bars are summarized by Reed [13]. Unfortunately most of these only include data for 10^5 cycles and higher. For most cases, the fatigue strength at 10^5 cycles is about 200 MPa, and still declining. Figure 6, above, shows a similar fatigue strength at 10^5 cycles. It might be argued that since the present specimens have a higher tensile strength than the typical material, around 400 MPa for the present material *vs* about 300 MPa for many of the materials reported by Reed, the present specimens should also have a higher fatigue strength. This seems not to be the case.

Figure 7 compares the results of the present work for Cu thin-films with previous results for Al thin-films [9], and literature results for sheet metal [14]. These thin-films of Cu clearly have better fatigue resistance than that previously reported for a set of Al specimens. The present Cu data fall between the data for unnotched and notched stainless steel and Al sheet metal. The present results appear to indicate an endurance limit at around half of ultimate, similar to the data for unnotched sheet metal. The notched (k_t = 4) sheet metal had an endurance limit of around one quarter of ultimate. In the present data the plasticity decreases significantly as the stress drops from around 3/4 to 1/2 of ultimate. This occurs at an

endurance of about 5000 cycles. Thus, the transition between low cycle and high cycle fatigue can be estimated to lie somewhere in the neighborhood of 5000 cycles for this set of specimens.

The results shown in Figure 5 have variability at both low ahd high loads, in comparison to data such as those presented by Oshida and Chen [15]. However, Oshida and Chen were able to use fully-reversed bending, their Cu films were supported by thicker polymer layers, and they report their results as a function of strain. In the present study, the variation in endurance as a function of stress at high stresses can be understood through consideration of the stress-strain curve (Figure 4). The high stresses are in the region of plastic strain, where small changes in stress produce large changes in strain. It is anticipated that if the cyclic strain in the present films could be controlled, the apparent scatter in Figure 5 would be transformed into a dependence of endurance on strain range, with less scatter.

For low stresses, the variability in the present study appears to be consistent with expectations. However, the endurance limit, converted to strain, is lower than 0.2 percent, while Oshida and Chen report a value around 0.6 percent at comparable cycle counts. The causes for this difference is are believed to lie both in the specimen material and in the test technique. The electrodeposited specimens [15] were 13 μm think, while the present specimens are 1.2 μm thick. The present specimens are electron-beam-evaporated, while Oshida and Chen's were electrodeposited. And, Oshida and Chen used bending of Cu layers reinforced by by polymer layers, while the present study used tension of unsupported films.

Specimen Geometry

Specimens as shown in Figure 2, with sharp changes in width at the ends of the gauge section, might be expected to fail consistently at the corners. However, the microphotolithography process used to fabricate the specimens produces rounded corners in the actual specimens. Furthermore, slight defects too small to characterize occur along the length of the specimens. These real-world effects, rounded corners and other defects, explain the relatively low number of failures at the end of the gauge section.

Microstructural Phenomena

These specimens were different from bulk sheet metal specimens in that they have only one or a few grains through the thickness. Although a full investigation of the detailed metallurgical behavior during these tests is beyond the scope of this paper, some observations are presented here. Surface

features that appear during fatigue of these specimens, as shown in Fig. 8. The density of the crack-like features and the rumpling of the surface appear correlated with accumulated plastic strain. Similar features, but not as clear or dense, appear in tensile testing. However, transmission electron microscopy (TEM) of a fatigued specimen, Fig. 9, revealed that the microcracks shown in Fig. 8 are in the surface layer only, and not in the Cu. In this figure, the black region is a cross section through the fatigued specimen, and the gray surface layer is the thin layer of Ti on the specimen surface. The openings in the Ti layer correspond to the visible surface microcracks in Fig. 8.

Figure 10 shows a TEM of the fatigued specimen. Two significant types of features are seen: a few individual dislocations; and bands of debris lying at approximately 45° to the plane of the specimen. No dislocation cells as reported in [16] were seen in this specimen. The size of such cells is typically 5 μm, which is much larger than the present specimen thickness. A previous paper [17] presented observations of dislocations in tensile tests of thinner Cu films produced in the same way as those reported here. In that paper it was noted that although only a few dislocations were seen, the density of dislocations was reasonable for the level of plastic strain and the volume of material observed. Similarly, a few dislocations can be seen here in the fatigued specimen. It is believed that the debris bands are remnants of interactions between mobile dislocations and obstacles to their motion.

The absence of clear steps on the specimen surfaces, combined with the absence of dislocation cells in the fatigued material, indicate that the dislocations move individually or in small groups and escape at the specimen surface. This is different from the behavior of bulk materials, where slip bands and dislocation cells are commonly reported.

SUMMARY

A set of electron-beam-evaporated Cu thin-film specimens have been tested in load-controlled tension-tension fatigue. The fatigue resistance is superior to that previously reported for a set of Al thin-film specimens, and intermediate between unnotched and notched sheet metal results found in the literature. The transition from high cycle to low cycle fatigue occurred at around 5000 cycles, accompanied by a decrease in the stress from three-fourths to half of ultimate. Transmission electron microscope observation suggest that dislocations associated with the plastic strain traverse the specimen in a direction at approximately a 45° angle to both the load axis and the through-thickness direction, and then escape from the specimen surface. No cells or walls of dislocations were observed.

ACKNOWLEDGEMENTS

Xochitl Zamora-Thompson performed many of the tests reported here. John Phelps made the TEM observations. This work was supported financially by the Office of Microelectronics Programs of NIST.

REFERENCES

1. D. A. Hardwick, "The Mechanical Properties of Thin-films: A Review," *Thin Solid Films* **154**, 1987, 109-124.

2. P. S. Alexopoulos and T. C. O'Sullivan, "Mechanical Properties of Thin-films," *Ann. Rev. Mater. Sci.* **20**, 1990, 391-420.

3. F. R. Brotzen, "Mechanical testing of thin-films," *International Materials Reviews* **39**, No. 1, 1994, 24-45.

4. Jan-Ake Schweitz, "Mechanical characterization of thin-films by micromechanical techniques," *Materials Research Society Bulletin* July 1992, 34-45.

5. A. Fartash, Ivan K. Schuller, M. Grimsditch, "Vibrating membrane elastomer for reliable measurement of mechanical properties of metallic films," *Rev. Sci Instrum.* **62** (2), February, 1991, 494-501.

6. J. A. Ruud, D. Josell, F. Spaepen, A. L. Greer, "A new method for tensile testing of thin-films", *J. Mater. Res.* Vol. 8, No. 1, Jan. 1993, 112-117.

7. W. D. Nix, "Mechnical Properties of Thin-films," *Metallurgical Transactions A* **20A**, November 1989, 1989-2217.

8. I. Kim and R. Weil, "The Mechanical Properties of Monocrystalline Nickel Electrodeposits," *Thin Solid Films* **169**, 1993, 35-42.

9. D. T. Read and J. W. Dally, "Fatigue of Microlithographically-Patterned Free-Standing Aluminum Thin-film Under Axial Stress," *Journal of Electronic Packaging* **117**, March 1995, 1-6.

10. D. T. Read, "Piezo-Actuated Microtensile Test Apparatus", submitted to *ASTM Journal of Testing and Evaluation.*

11. E. M. Zielinski, R. P. Vinci, and J. C. Bravman, "Effects of barrier layer and annealing on abnormal grain growth in

copper thin films," *Journal of Applied Physics* **76**, 1994, 4516-4523.

12. B. Chalmers, *Physical Metallurgy*, John Wiley and Sons, New York, 207.

13. R. P. Reed and R. P. Mikesell, *Low Temperature Mechanical Properties of Copper and Selected Copper Alloys: A Compilation from the Literature*, National Bureau of Standards Monograph 101, U. S. Government Printing Office, 1967.

14. P. G. Forrest, *Fatigue of Metals*, Pergamon, Oxford, 1966, 162.

15. Y. Oshida and P. C. Chen, "High and Low-Cycle Fatigue Damage Evaluation of Multilayer Thin Film Structure," *Journal of Electronic Packaging* **113**, 1991, 58-62.

16. C. Laird, P. Charsley, and H. Mughrabi, "Low Energy Dislocation Structures Produced by Cyclic Deformation," *Materials Science and Engineering* **81**, 1986, 433-450.

17. R. R. Keller, J. M. Phelps, and D. T. Read, "Tensile and fracture behavior of free-standing copper films," *Materials Science and Engineering* **A214**, 1996, 42-52.

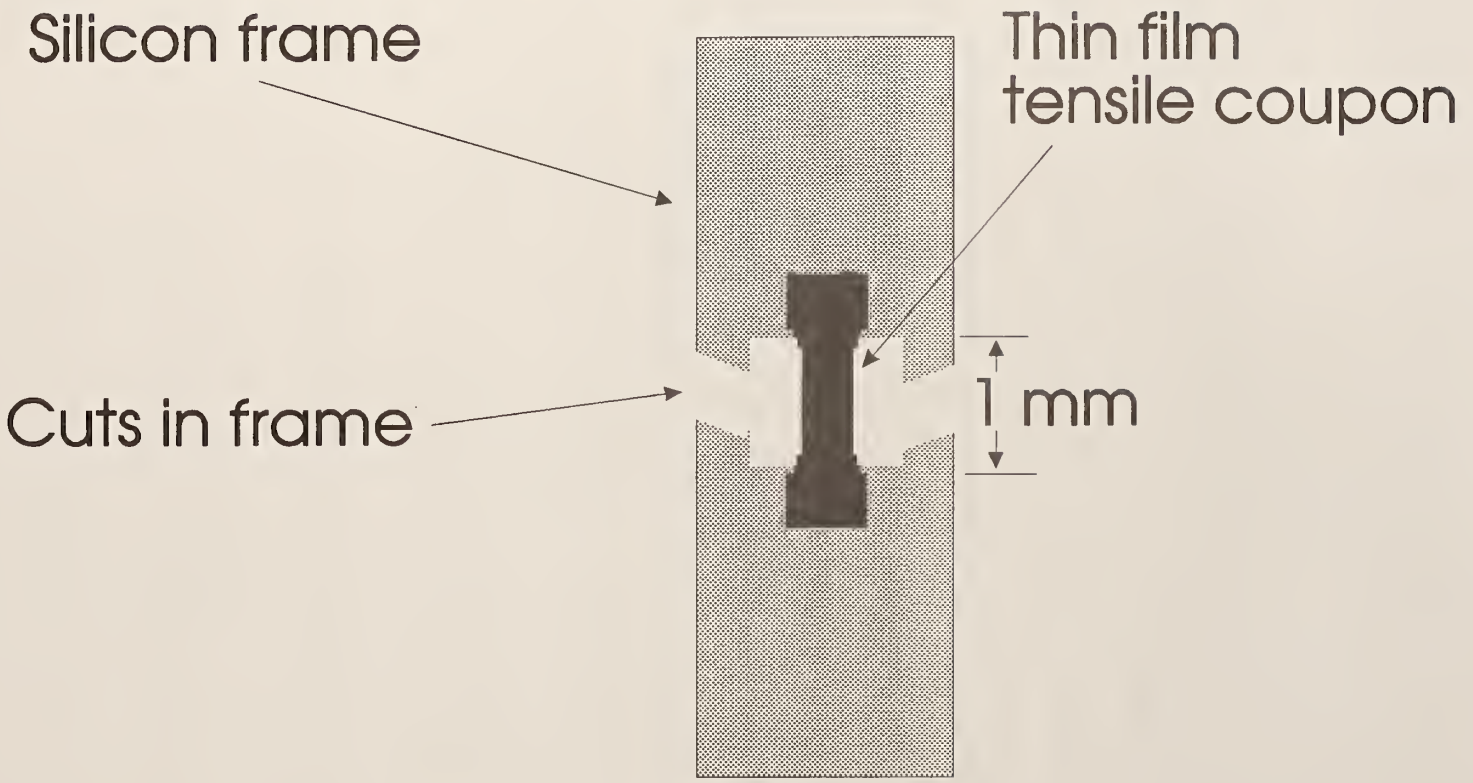

Figure 1. Specimen assembly including silicon frame and thin-film tensile coupon. The frame is shown cut, its condition when it is already mounted to the grips, just before testing.

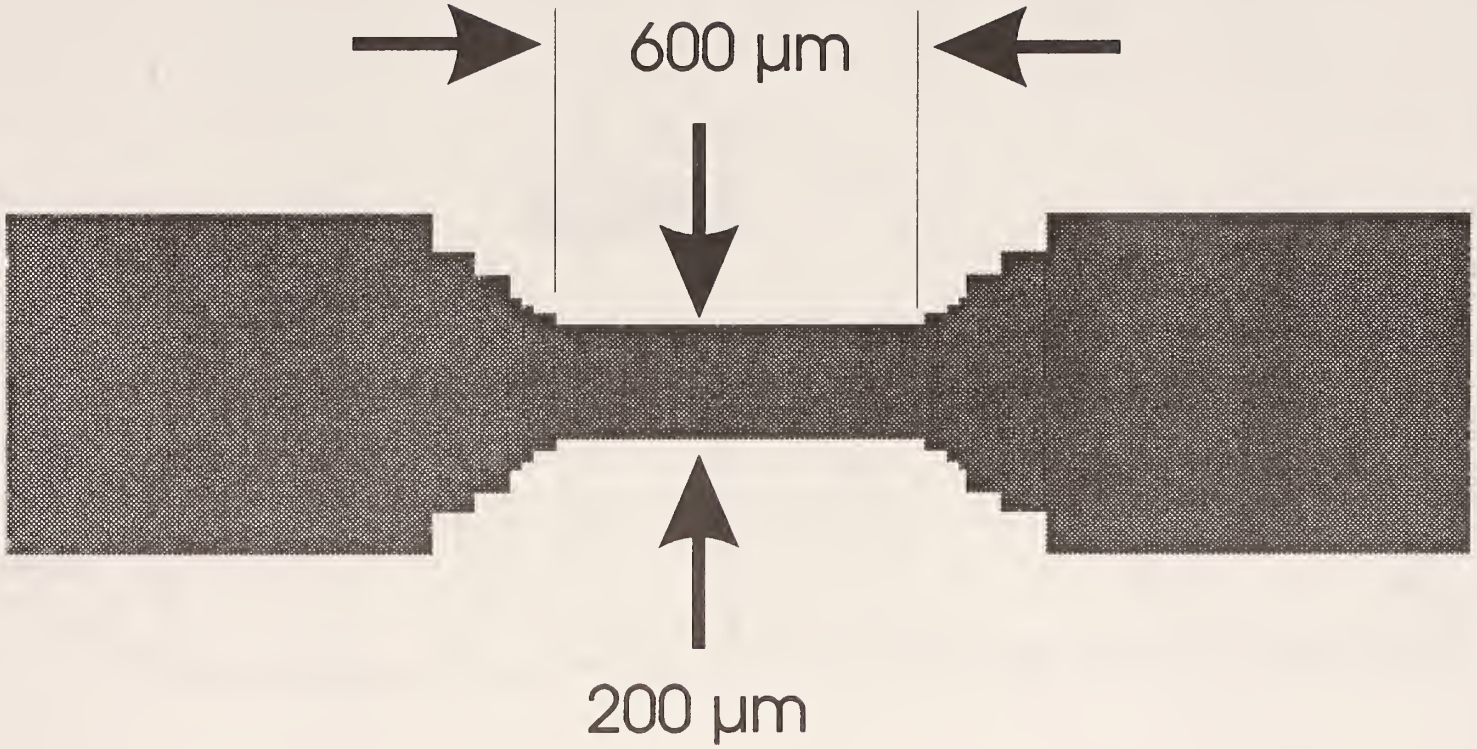

Figure 2. Plan of the tensile coupon.

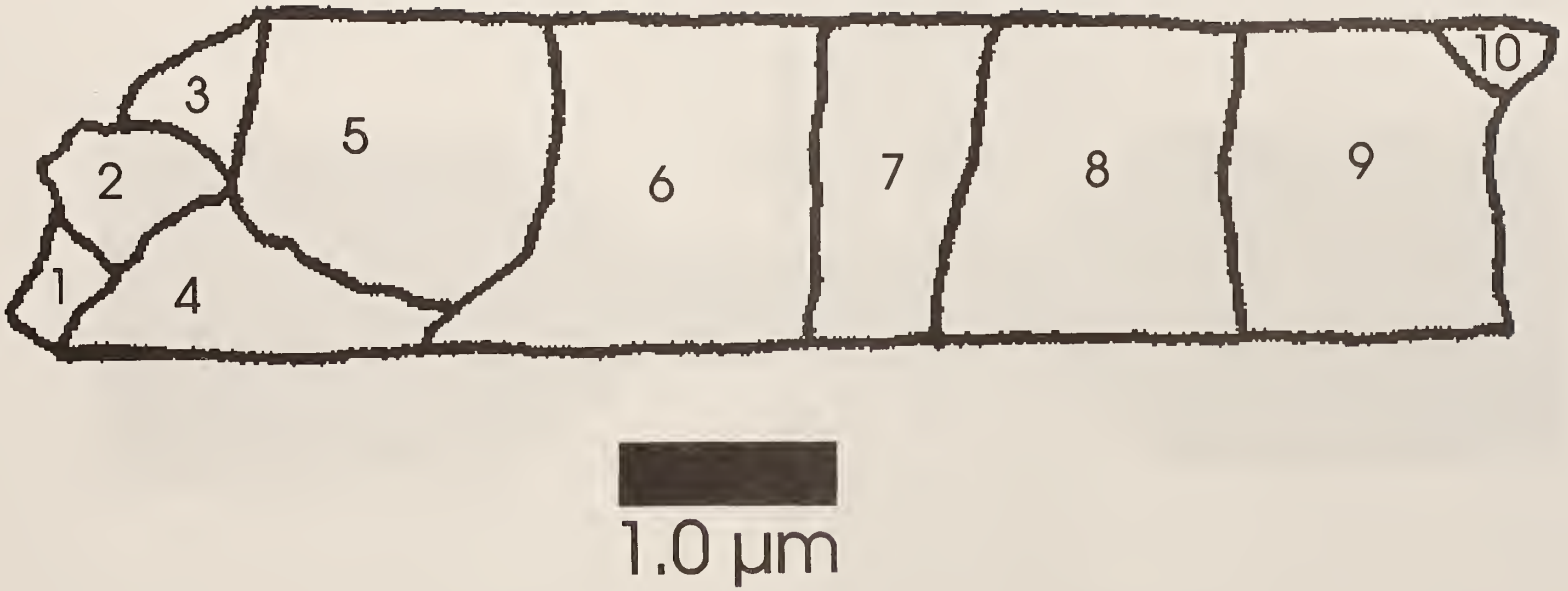

Figure 3. Microstructure of a similar electron-beam-evaporated thin-film, traced from a cross-sectional TEM micrograph.

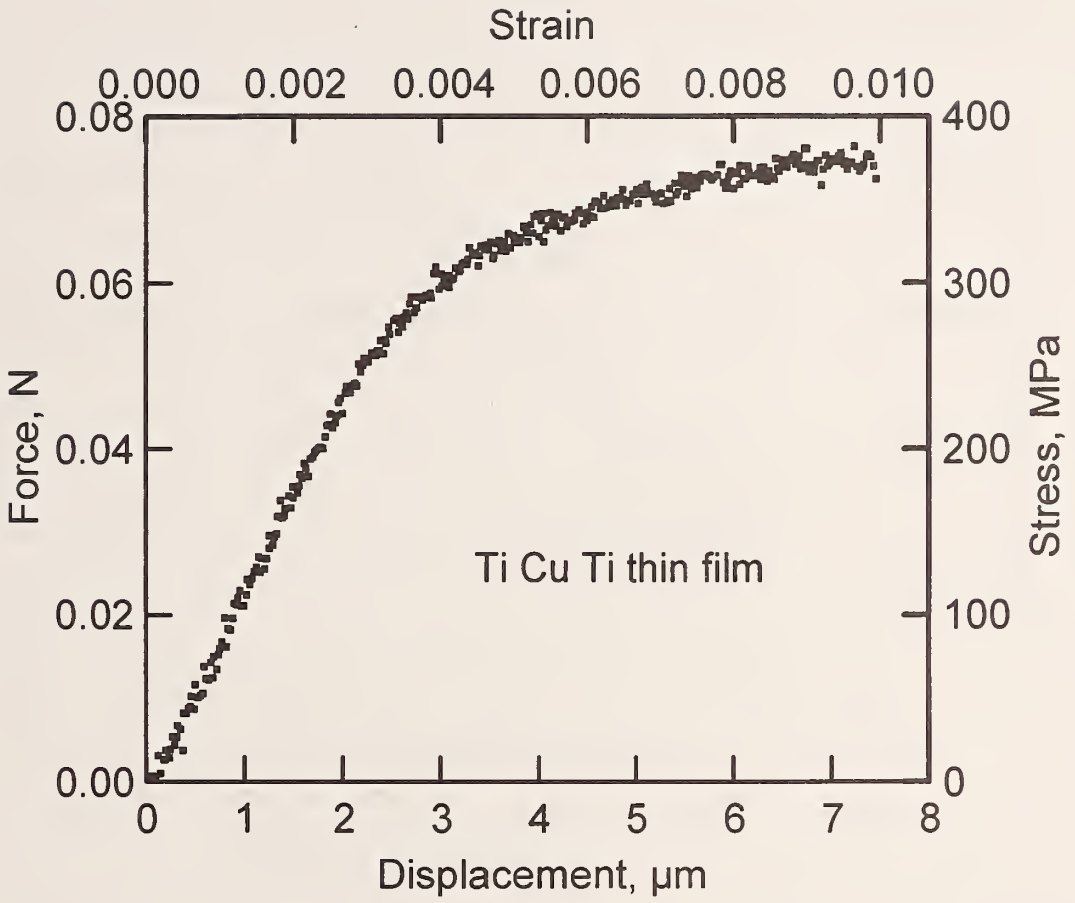

Figure 4. Typical force-displacement and stress-strain record of a thin-film from this set of specimens. One N is about 100 gram-force. The 0.2 percent yield strength, the ultimate tensile strength, and the failure point are indicated.

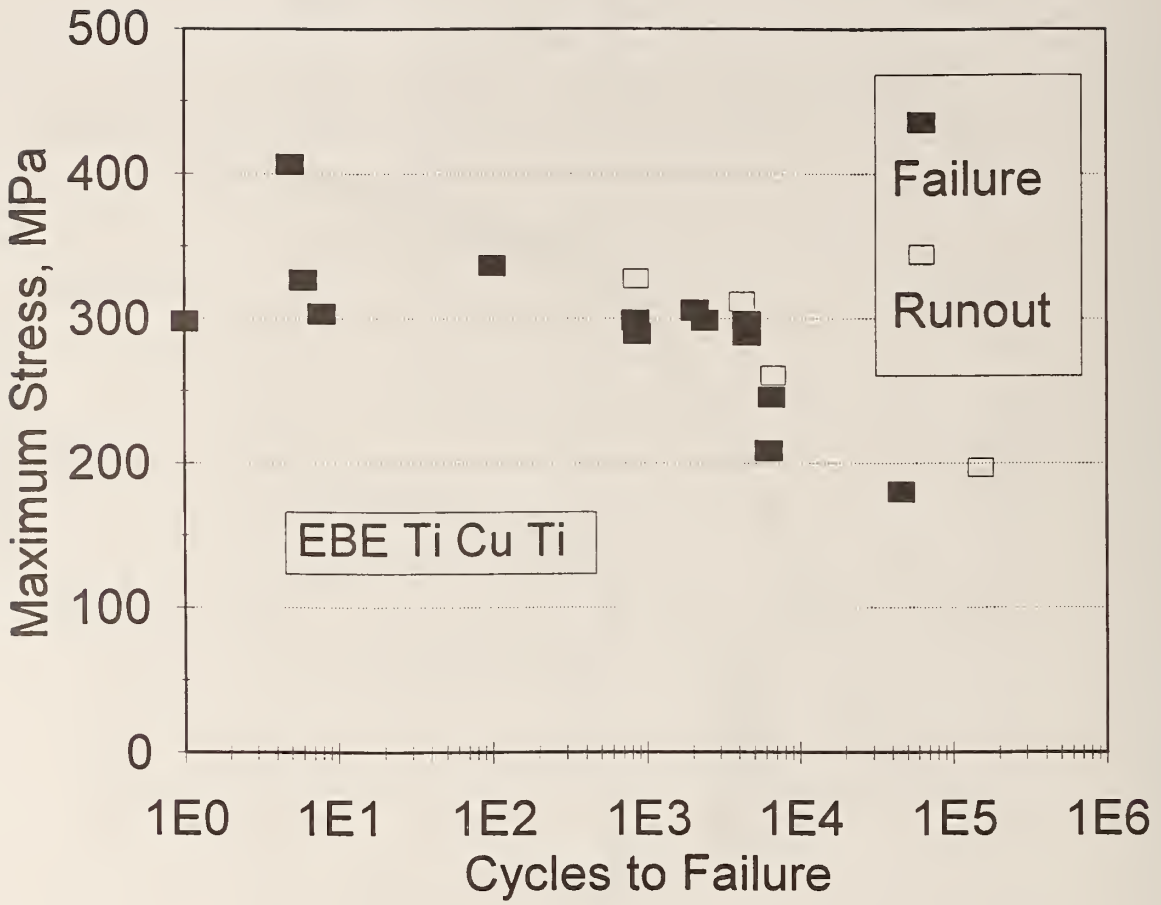

Figure 5. Plot of maximum cyclic stress against number of cycles to failure (S-N plot) for electron-beam-evaporated copper thin-film specimens.

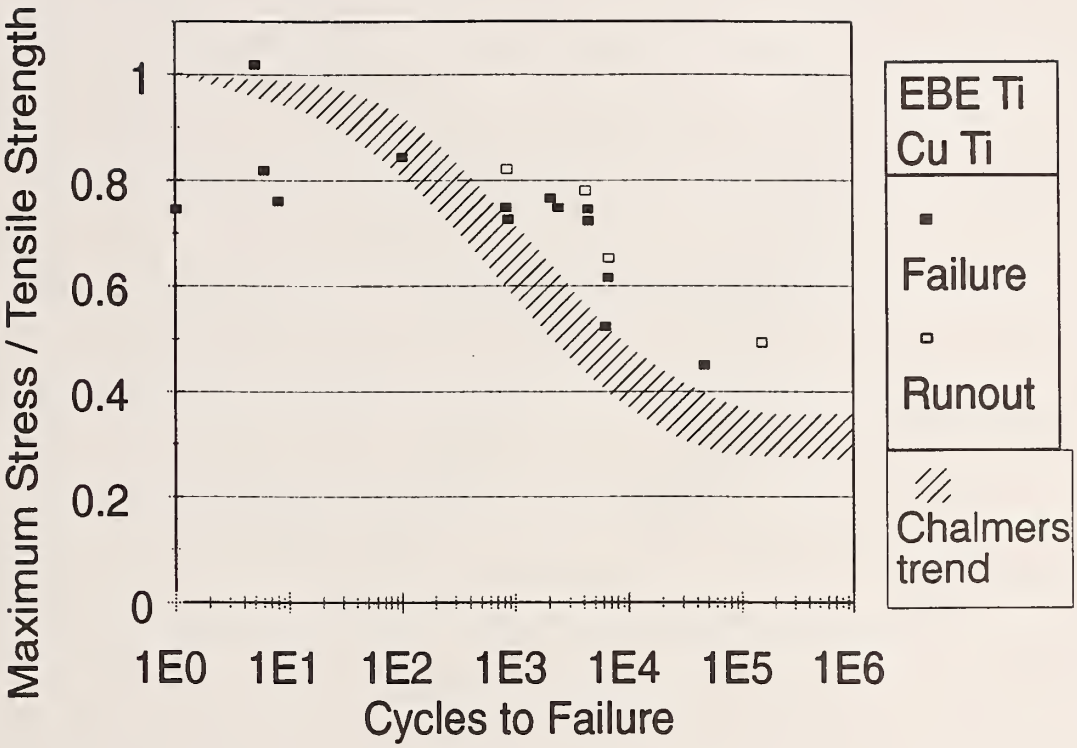

Figure 6. Cyclic stress normalized to ultimate tensile strength plotted *versus* cycles-to-failure for electron-beam-evaporated Cu (present study), compared to the general trend for metals given by Chalmers[12].

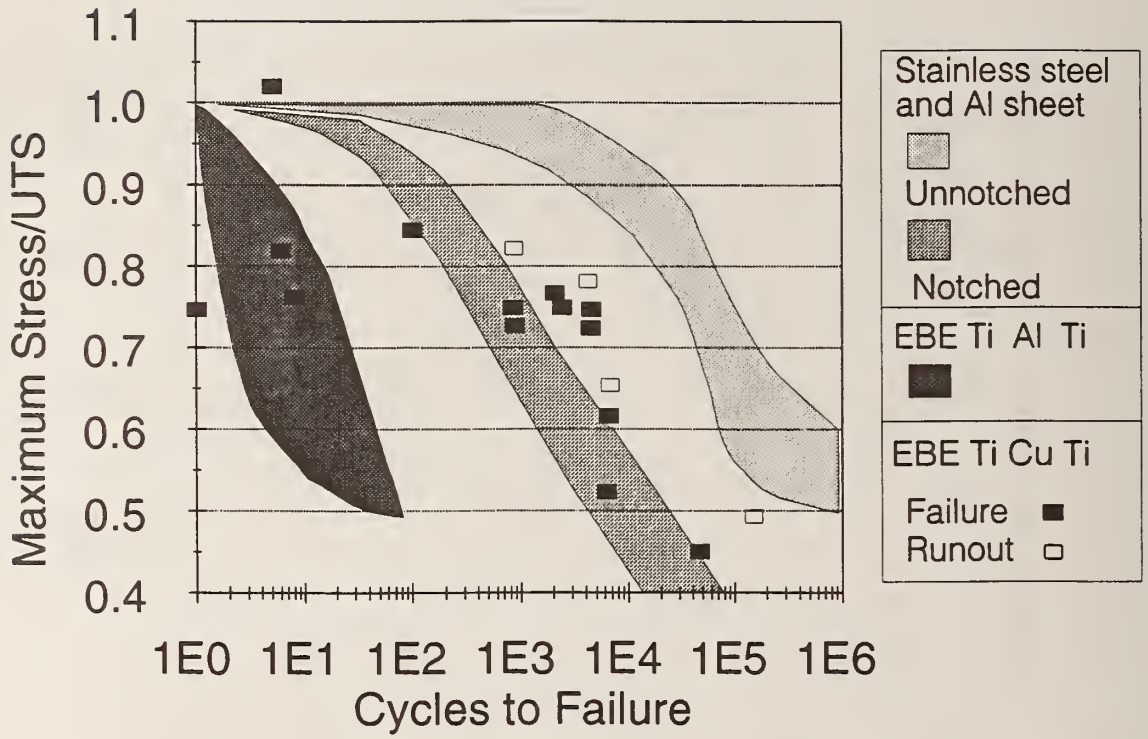

Figure 7. Cyclic stress normalized to the ultimate tensile strength *versus* cycles-to-failure for electron-beam-evaporated Cu (present study), electron-beam-evaporated Al[10], and unnotched and notched sheet metal specimens[14].

Figure 8. Optical micrograph of the surface of a Ti-coated Cu specimen after fatigue.

Figure 9. Transmission electron micrograph of a cross- section of a Ti-coated Cu specimen after fatigue. The large dark region is Cu. The light gray at the surfaces is Ti. The openings in the Ti are not correlated with cracks or notches in the Cu.

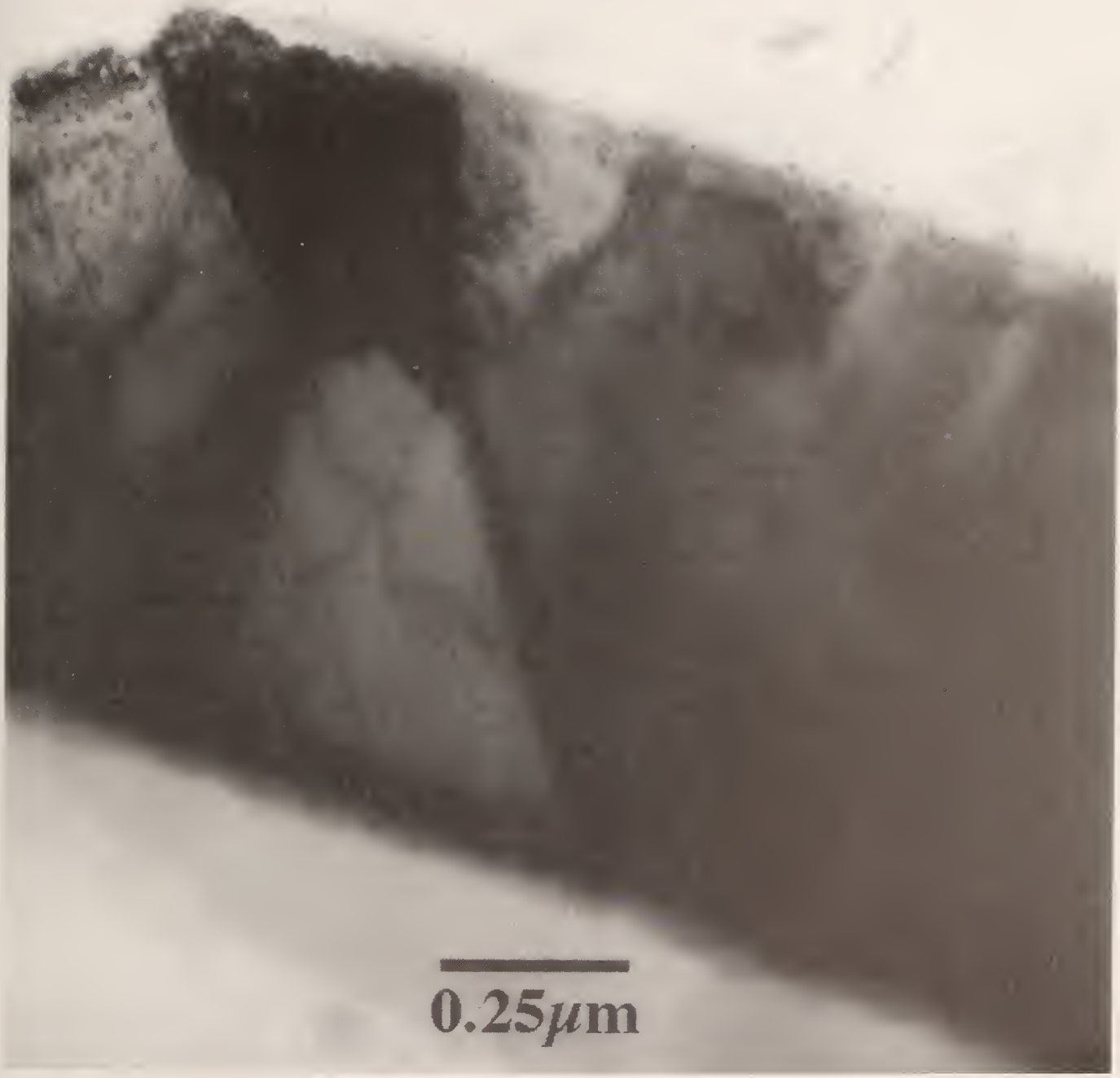

Figure 10. Transmission electron micrograph of a cross-section of a fatigued specimen.

Appendix E. 1997: Piezo-Actuated Microtensile Test Apparatus

PIEZO-ACTUATED MICROTENSILE TEST APPARATUS

David T. Read
Materials Reliability Division
National Institute of Standards and Technology
Boulder, Colorado 80303

ABSTRACT

The design and performance of a microtensile test device designed for measuring the mechanical properties of thin films are reported. The moving grip is cantilevered to avoid friction. Piezoelectric actuation allows precise control of the applied tension. Force is measured indirectly using an eddy-current sensor near a flexible measuring beam, and grip displacement is measured using two similar displacement sensors. The apparatus is constructed for use with specially designed specimen assemblies in which the thin film to be tested is suspended across a silicon frame. The apparatus is rigid enough that the frames can be cut without applying tension to the thin-film tensile specimen. The tester is run in closed-loop control through a laboratory computer, which records force, displacement, and other parameters 5 times per second. Key capabilities are: stroke, 50 μm; maximum force, 1 N; minimum cycle time, 2 s; displacement resolution, ±20 nm; and force resolution, ±200 μN.

Key words: Closed loop, displacement, force, piezoelectric, servo, strain, stress, thin film.

INTRODUCTION

This paper describes a piezo-actuated microtensile test machine suitable for testing specially fabricated thin-film specimens. A variety of microtensile test devices have been described in the literature, with varying advantages and disadvantages. A detailed review is beyond the scope of this report. Several excellent recent papers on thin-film mechanical properties include discussions of the apparatus and additional references [1-5]. Reported approaches to measuring the mechanical properties of thin films can be classified generally as to whether or not the specimen film must be manually parted from the substrate and placed on the grips, and whether the stress applied is pure tension, biaxial, or more complex. For example, Ruud *et al.* [6] parted their specimens from the substrate for mounting in a tensile device that applied pure tension, while Small *et al.* [7] used silicon-framed membrane specimens in a hydraulic bulge-test device that applied biaxial stress.

The problem of safely handling very small specimens has been addressed for both metal and silicon specimens by including a removable reinforcement in the specimen design. Kim and Weil [8] used electrodeposited metal films with a reinforcing section. Ding, Ko, and Mansour [9] tested silicon-framed silicon. A previously reported microtensile test apparatus [10], abbreviated MT-I, was the first device shown to be capable of testing silicon-framed metal thin-film tensile coupons, where the thin film to be tested is suspended across a silicon frame for convenient placement and alignment in the test fixtures. This design eliminates the need to manually part the specimen from the substrate, at the cost of a wet etch to remove the substrate from underneath the gage section of the specimen. Detailed descriptions of this specimen and the steps involved in fabricating it have been given previously [10, 11]. The difficulty with this procedure is that the frame has to be cut before the specimen is tested. The operations involved in cutting the frame can easily allow uncontrolled tension to be applied to the specimen, destroying it. Imposed tensile displacements of as little as 2 μm can produce plastic deformation in a thin-film tensile specimen. Such displacements may require forces as small as 0.01 N (1 gram-force), and thus can easily occur when a cutting tool is applied to the frame or when the frame rebounds after being cut. All known specimen grips mass at least 1 g, so the specimen cannot support the weight of the grips against gravity, as is normal in testing bulk specimens. MT-I used a special clamp to hold the frame while it was cut. Upon its release, this clamp left the specimen exactly in place, without applying any force in the tensile direction.

Few piezo-driven microtensile devices have been described. The current microtensile tester (MT-II) is piezo-driven, preserves the main advantage of the previous one (MT-I)[11], and overcomes its main disadvantages. The main disadvantages of MT-I were: friction between the moving grip and its support plate; off-axis displacement measurement leading to possible errors; high compliance of the spring used for force measurement; and actuation by a manual micrometer.

MT-II overcomes these disadvantages by: cantilevering the moving grip, so it moves without friction; using a much stiffer beam-type spring for load measurement; using two displacement sensors, one on each side of the specimen; and using piezoelectric actuation. Details are described below.

MT-II can be reproduced at a low cost. The mechanical parts of MT-II include less than a dozen simple mechanical components that were made from ordinary materials to ordinary tolerances in a conventional machine shop, and the commercially purchased piezoelectric stacks. These are driven with a commercial 500 V DC power supply. The sensors were also purchased commercially. The electrical signals from the instruments are connected directly to the input terminals of a commercially available analog-to-digital conversion board in a personal computer. The tester fits into an elementary analytical probing station designed for testing of electrical circuits on silicon wafers. Such devices are widely used in the electronics industry. The probing station microscope has a long working distance that allows manipulation of the specimen and a trinocular head that allows observation and photography of the specimens during testing.

MECHANICAL DESIGN

The design of MT-II is shown in Figure 1. An enlarged schematic of a silicon-framed tensile specimen, with the frame cut, is shown in Figure 2. The specimen differs from the version reported previously in that only one coupon is used, rather than four parallel strips. The gage section length is 700 μm, and the width is 200 μm. The fabrication techniques were reported previously [10, 11] and will not be repeated here.

The piezoelectric stacks are 20 mm in diameter and 60 mm long. They are restrained by eight nylon rods that hold the moving head assembly to the base of the device. The moving head assembly includes the reference beam, the force-measuring beam, and the moving grip; these are all cantilevered above the base plate to avoid friction. The clearance is about 25 μm and is not critical. (The term "grip" is used loosely here. The grips are really more like platforms, as shown in Figure 3. In practice the specimen frame is glued onto aluminum plates that are screwed

to flat surfaces on both the fixed part and the moving part of the device.)

The device is 25 mm thick. The grip surfaces are centered vertically, as are all the sensors and the clamp screws. A small aluminum plate is attached with screws to each of the grips. The specimen frame is glued to these plates. The plates can be removed and cleaned or replaced between tests. The clamp screws can be run in against the measuring beam to prevent displacement while the specimen frame is being cut.

The displacement of the moving grip is measured using the commercially-supplied eddy-current displacements sensors [10] shown in Figure 1. The tension applied to the specimen is measured using a third displacement sensor, through the displacement of the force-sensing beam shown in Figure 1. This beam is fixed at both ends, and bends elastically in response to force applied to the moving grip. This bending can be characterized by a single spring constant relating applied force and displacement, and therefore this part of the tester can be thought of as a force-measuring spring. The calibration procedures and sensitivities of these measuring devices are discussed below.

CONTROL SYSTEM

The eddy current displacement sensors were described previously [10]. The analog output of the displacement sensors is introduced to the input of a commercially available analog-to-digital board (A-to-D board) in a laboratory computer. Eight double-ended channels with 16-bit precision are available. Three channels are used for the two displacements and the load. Two others are used for the current and voltage in a resistance thermometer, and another is used to monitor the actual voltage applied to the piezoelectric elements.

A custom-written program running on the computer manages data acquisition and storage, and control of the device. The microtensile tester is operated in digital closed-loop control. This is necessary even in the displacement-controlled modes because the piezoelectric stacks exhibit hysteresis and creep in their response to applied voltage. The program currently offers a choice of fixed value ("set point"), ramp, sine wave, or square wave control of the displacement, the force, or the applied voltage. The program evaluates the error as the difference between the programmed value of the control quantity and its actual measured value. The voltage applied to the piezo-stacks is changed by the sum of a proportional response, a rate response, and an acceleration response. A separate factor relates each response component to its corresponding error. An analog voltage proportional to the error is generated by a D-to-A

converter on the A-to-D board. This voltage is introduced to the control input of a high voltage power supply. The maximum allowed voltage is 250 V.

CALIBRATION

Force is calibrated routinely by tipping the device to a vertical position and placing a known mass on the moving grip. A typical value of the calibration factor is 1.5 N/V. Experiments with springs, turning the device upside down to reverse the effect of the weight of the moving grip, and so on indicate differences of 3 percent or less between this calibration factor in the range where it is calibrated and the range where data are taken. A typical displacement of the measuring beam over the course of a test is 2.5 μm or less, while the thickness of the measuring beam is 500 μm. Although this procedure shifts the effective zero-point of the force calibration range by the weight of the moving grip, which is about 0.35 N, it is superior to other methods that we have tried. Experiments with conventional pulleys to convert gravitational force on known weights to horizontal force have errors at least this large. Calibrated springs in the proper range of force and displacement are not commercially available.

Displacement calibration is performed using a commercially available displacement-measurement system utilizing a timed scanned laser beam. The displacement calibration factor is 25.4 μm/V to within better than 1 percent.

PERFORMANCE

The total stroke of MT-II is about 50 μm. Changing the restraining rods from stainless steel to nylon improved this value considerably. This stroke is sufficient to test to failure thin metal films produced by physical vapor deposition (PVD). Some electrodeposited films thicker than 5 μm have strains to failure approaching 10 percent, and so specimens with a 700 μm long gage section could not be tested to failure in this device.

There are a variety of rates involved in the data acquisition and closed loop control cycles. The fastest rate is the rate of conversion of individual analog voltages to digital values. With the equipment now in use, each conversion requires about 10 μs. These conversions proceed independently ("asynchronously"), under control of the A-to-D board. At the same time, the program is updating the control voltage based on the previous readings.

The control voltage is updated 50 times per second with the current laboratory computer, which is rated at a processor speed of 25 MHz. Ten raw readings are averaged to get the "control"

values used to derive the error signal. Voltages are reported 5 times per second. Each reported value is the average of 10 control values. The reported values are stored on hard disk for later retrieval.

The eddy-current displacement sensors have a sensitivity of 25 μm/V and are operated with ± 2 V full scale. The raw voltage readings have standard deviations of up to about 3 mV, corresponding to 75 nm in the displacement measurement and 5 mN in the force measurement.

The standard deviations for the reported displacements, with the machine at rest, are 20 nm and 0.2 mN (0.02 gram-force). Of these, the error in force is more significant. An improved supplemental force sensor is being developed.

The response of the device to a step in the imposed voltage is shown in Figure 4. The voltage setting was switched from 20 to 40 V. The power supply responded with a time constant of about 0.1 s. The displacement followed, with a time constant of about 0.45 s. These values were obtained by fitting the measured response, indicated by the data points, to a simple exponential function proportional to 1 - exp(-t / T), where t is time after the switch and T is the fitted time constant. Additive and proportional factors and a starting time were also used in this fit. The response of the device is slow because it is extended physically, the measuring spring has some compliance, and the piezo-stacks can exhibit hysteresis and creep. The minimum cycle time quoted above, 2 s, was taken as four times the machine time constant. For smooth sinusoidal cycles with about 100 data points, a cycle time of about 20 s would be required.

No "overdriving" was used in this measurement. The actual response of the mechanical system is shown, with no optimization from the control system. The response time could have been reduced by overdriving, that is, by applying a high voltage momentarily to accelerate the motion of the device, then reducing the voltage to its steady state value. The response in that case would depend on the control parameters.

The response of the tester was documented by using a spring in the form of a small steel "snap-ring", about 1 cm in diameter, as a dummy specimen. This was found to be much more convenient and reproducible than other possibilities such as fine wires in tension or small coil springs. A wire with the appropriate compliance would have to be less than 25 μm in diameter. It would be delicate and difficult to mount, and its elastic response would be difficult to verify. Small coil springs also seemed difficult to mount in the tester. Snap-rings are commonly found in mechanical systems such as automobile carburetors, and are readily available in various sizes. Snap-

rings are compliant and springy in the diametral direction. In normal use a snap-ring is forced open slightly, put in place in a groove around a shaft, and released. It springs back to its normal diameter and is retained by the groove. The ears of the snap-ring were easily adapted to mount to the grips of the tester, so that it provided a load that varied linearly with imposed displacement.

Figure 5 shows the force on such a spring as a function of time under load control. The force data are indistinguishable from the sine function, while the piezo-voltage is seen to decrease slightly over the time of this sample data.

Figure 6 shows a plot of force against displacement for the spring for one cycle. The slight differences between the loading and unloading records are due to friction and hysteresis in the mounting of the spring, not in the testing machine.

SAMPLE RESULTS

Some sample test results are shown in Figures 7-9. These results will be discussed in more detail elsewhere and are included here to demonstrate the performance of the microtensile test device.

Figure 7 shows the force-displacement record for an electron-beam-evaporated (EBE) thin film of Cu with Ti layers on both sides. The film is 1.2 μm thick; the two Ti layers are each 0.05 μm thick. This plot demonstrates some of the difficulties involved in testing thin films, because the elastic displacement is less than 2 μm, the total displacement is less than 10 μm, and the ultimate tensile force is less than 100 mN (10 grams-force).

Figure 8 shows the engineering stress-strain plot from the same test. Because the strains are so small, the engineering strain accurately represents the true strain. The lines on the plot indicate the loading slope, the yield strength, and the ultimate tensile strength. The loading slope shown in this plot does not represent the handbook value of Young's modulus for two reasons: first, the strain is calculated from the grip displacement, and so some deformation outside the gage length is included; and, second, more accurate measurement of the strain in the gage length, reported separately, indicates that the Young's modulus of this specimen is less than the handbook value for bulk copper. This film was deposited slowly on a substrate held at room temperature, and such films have been reported to contain many small voids. Such voids or other microstructural differences between PVD films and bulk metal may lead to differences in their elastic constants.

Figure 9 shows a set of fatigue data for the same thin-film material. These data were obtained in load-controlled tension-tension fatigue. In the two longest tests, one specimen failed at about 45 000 cycles, and one survived over 100 000 cycles.

DISCUSSION

The microtensile tester described above has been used for tensile tests of PVD thin films and for electrodeposits. It has been used for a series of load-controlled fatigue tests, the longest of which ran for over 100 000 cycles. Its advantages include mechanical rigidity that allows testing of silicon-framed specimens, piezoelectric actuation for fine control, cantilevered moving parts for frictionless operation, and closed loop control so that load and displacement rates can be accurately controlled and changed.

The tester as described here has two main shortcomings. One is that it measures the grip displacement, whereas the interesting quantity is the strain in the gage length. The other is the limited resolution of the force measurement. Work is in progress on using ESPI (electronic speckle pattern interferometry) to measure the specimen displacement. This approach appears to work and will be reported separately. The load resolution is limited by the resolution of the eddy-current displacement sensor and the stiffness of the force-measuring beam. Reducing the rigidity of the beam would make it much more difficult to break the specimen frame without damaging the specimen. A more sensitive displacement-measurement technique using an optical lever is being tested.

ACKNOWLEDGEMENTS

Xochitl Zamora-Thompson performed many of the tests reported here. This work was supported financially by the Office of Microelectronics Programs of NIST.

REFERENCES

1. D. A. Hardwick, "The Mechanical Properties of Thin Films: A Review," *Thin Solid Films* **154** (1987), 109-124.

2. P. S. Alexopoulos and T. C. O'Sullivan, "Mechanical Properties of Thin Films," *Annual Review of Matererials Science* **20**, 1990, 391-420.

3. F. R. Brotzen, "Mechanical testing of thin films," *International Materials Reviews* **39**, No. 1, 1994, 24-45.

4. Jan-Ake Schweitz, "Mechanical characterization of thin films by micromechanical techniques," *Materials Research Society Bulletin* July 1992, pp. 34-45.
5. A. Fartash, Ivan K. Schuller, M. Grimsditch, "Vibrating membrane elastomer for reliable measurement of mechanical properties of metallic films," *Review of Scientific Instruments* **62** (2), February, 1991, 494-501.

6 J. A. Ruud, D. Josell, F. Spaepen, A. L. Greer, "A new method for tensile testing of thin films", *Journal of Materials Research* Vol. 8, No. 1, Jan. 1993, pp. 112-117.

7. Small, M. K., Daniels, B. J., Clemens, B. B., and Nix, W, D., "The elastic biaxial modulus of Ag-Pd multilayered thin films measured using the bulge test," *Journal of Materials Research* **9**, No, 1, January, 1994, 25-30.

8. I. Kim and R. Weil, "The Mechanical Properties of Monocrystalline Nickel Electrodeposits," *Thin Solid Films* **169**, 1993, 35-42.

9. Ding, X., Ko, W. H., and Mansour, J. M., "Residual Stress and Mechanical Properties of Boron-doped p^+-Silicon Films," *Sensors and Actuators* **A23**, 1990, 866-871.

10. D. T. Read and J. W. Dally, "A new method for measuring the strength and ductility of thin films," *Journal of Materials Research* **8**, No. 7, July 1993, 1542-1549.

11. D. T. Read and J. W. Dally, "Fatigue of Microlithographically-Patterned Free-Standing Aluminum Thin Film Under Axial Stress," *Journal of Electronic Packaging* **117**, March 1995, 1-6.

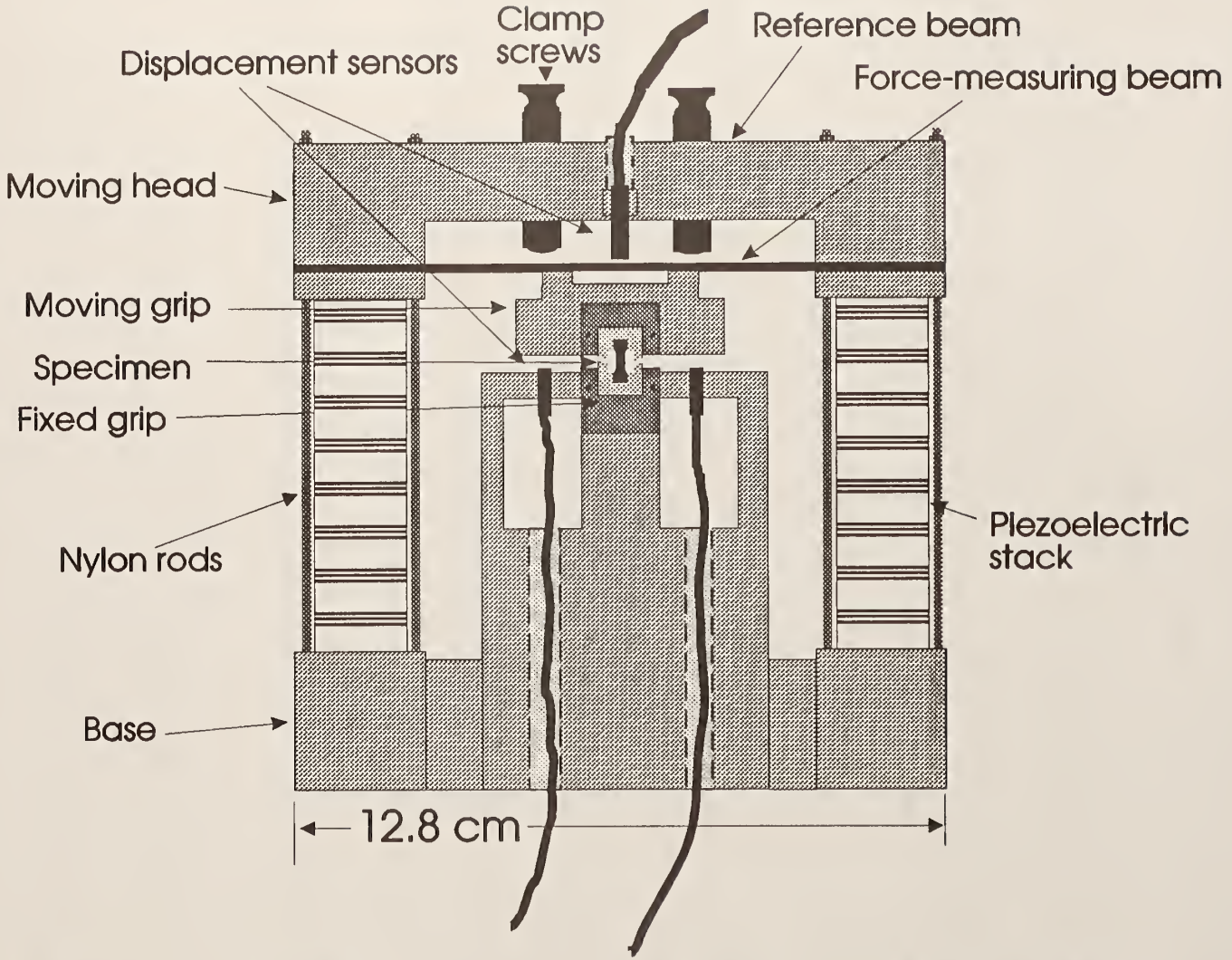

Figure 1. Schematic drawing of microtensile test device (MT II).

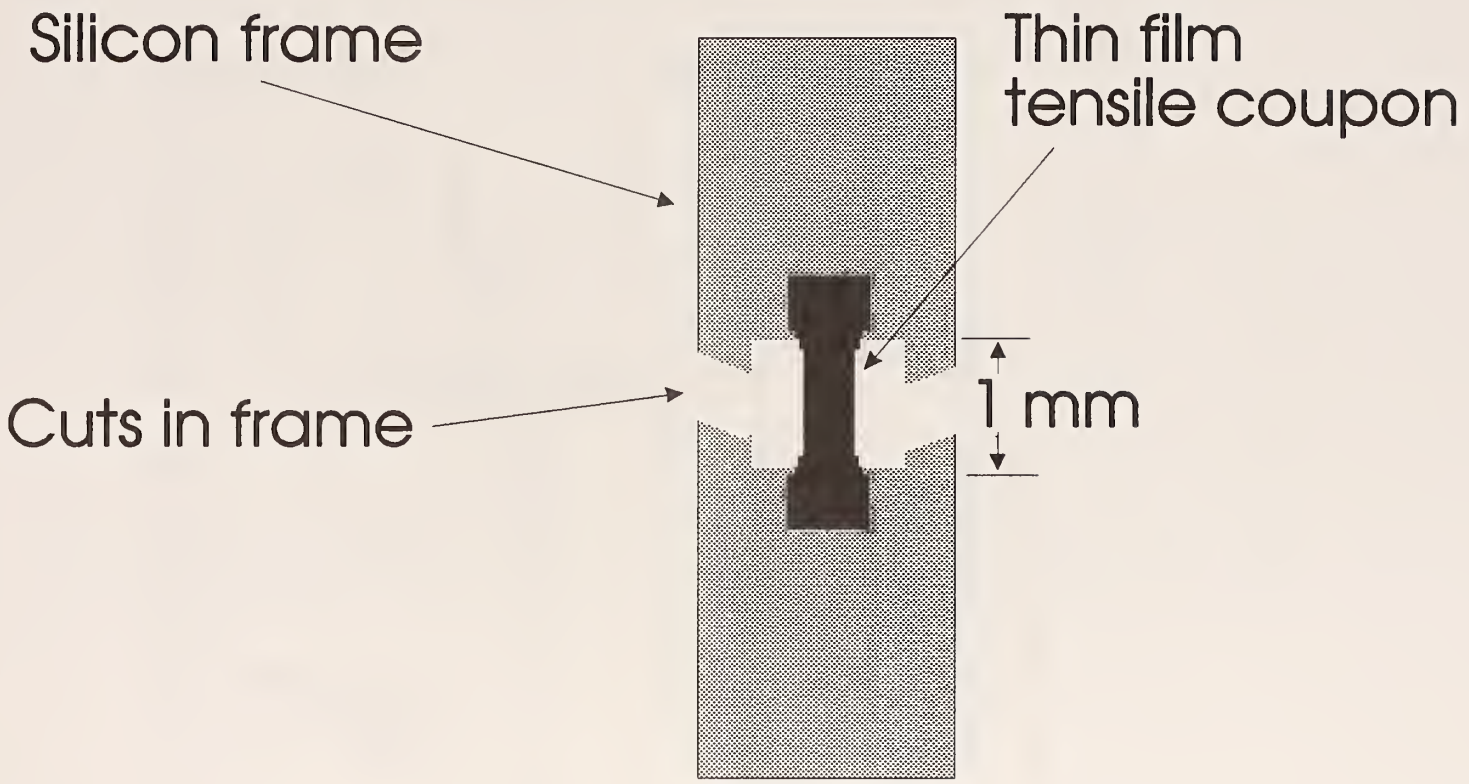

Figure 2. Detail of silicon-framed thin film tensile specimen, after the frame has been cut and before testing.

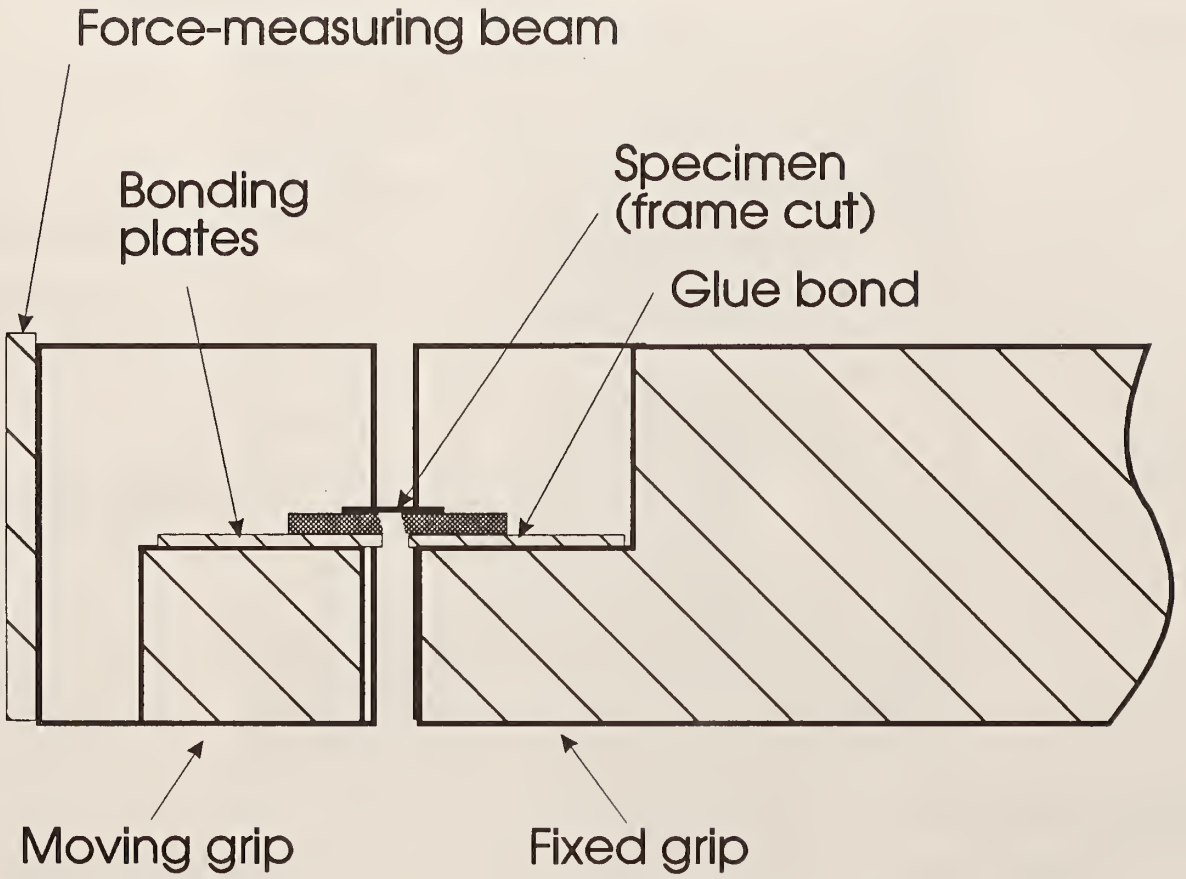

Figure 3. Cross section of the grips, showing how the specimen is mounted.

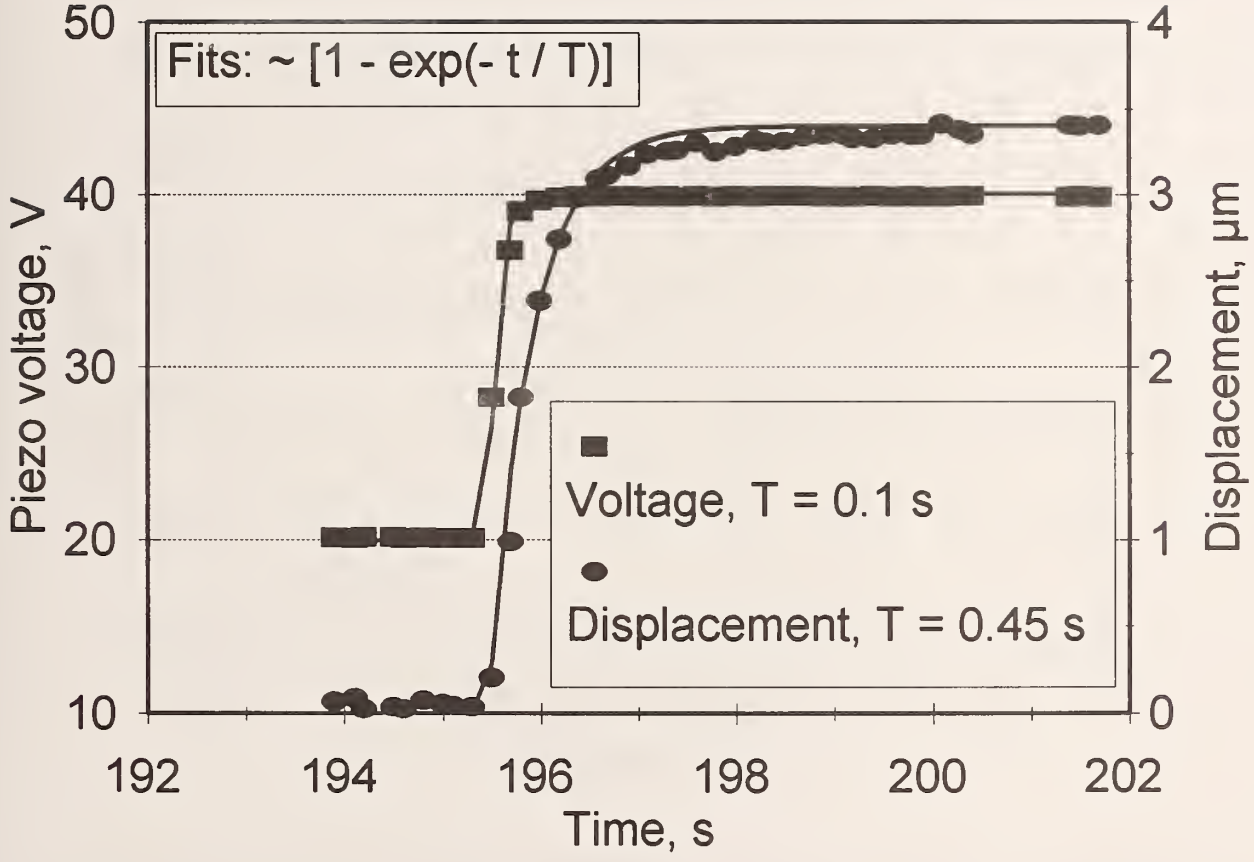

Figure 4. Plot of piezo-stack voltage and moving grip displacement against time, showing the response to a voltage step.

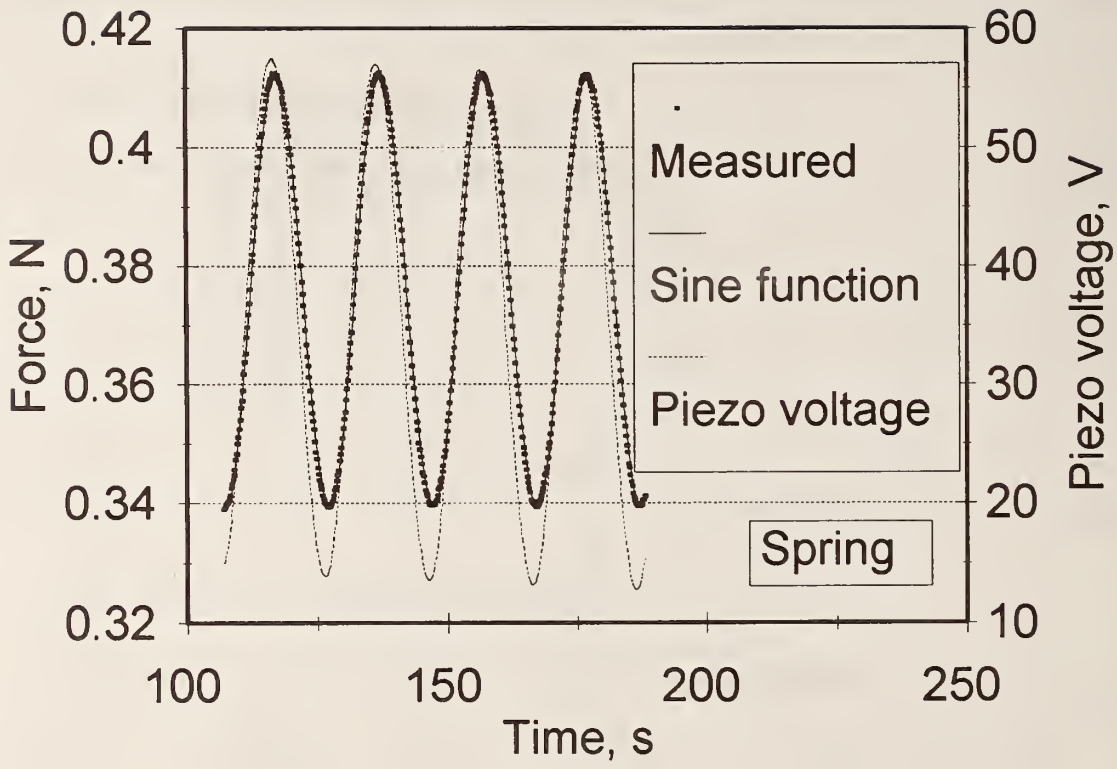

Figure 5. Plot of force on a spring against time obtained with the device in load control. The maximum and minimum values of the force remain constant, while those of the voltage change slightly. The time dependence is indistinguishable from a true sine function.

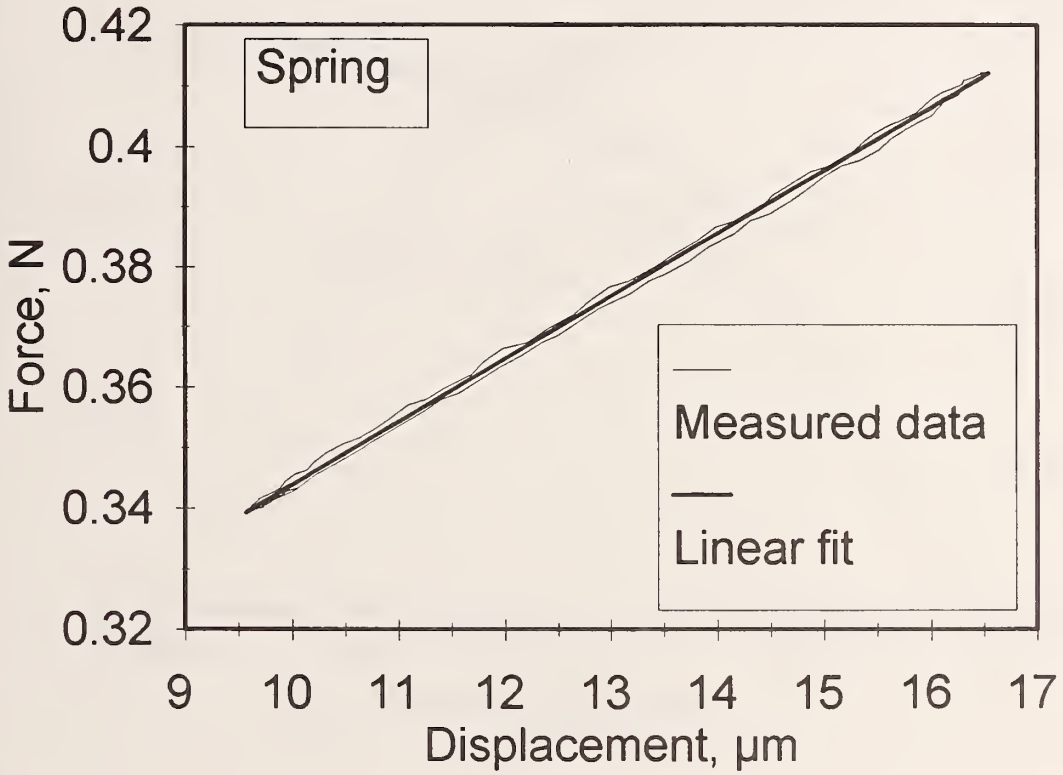

Figure 6. Plot of force against displacement for the spring. The spring is clearly linear. The small deviations result from noise and friction in the mounts of the spring, not in the test device.

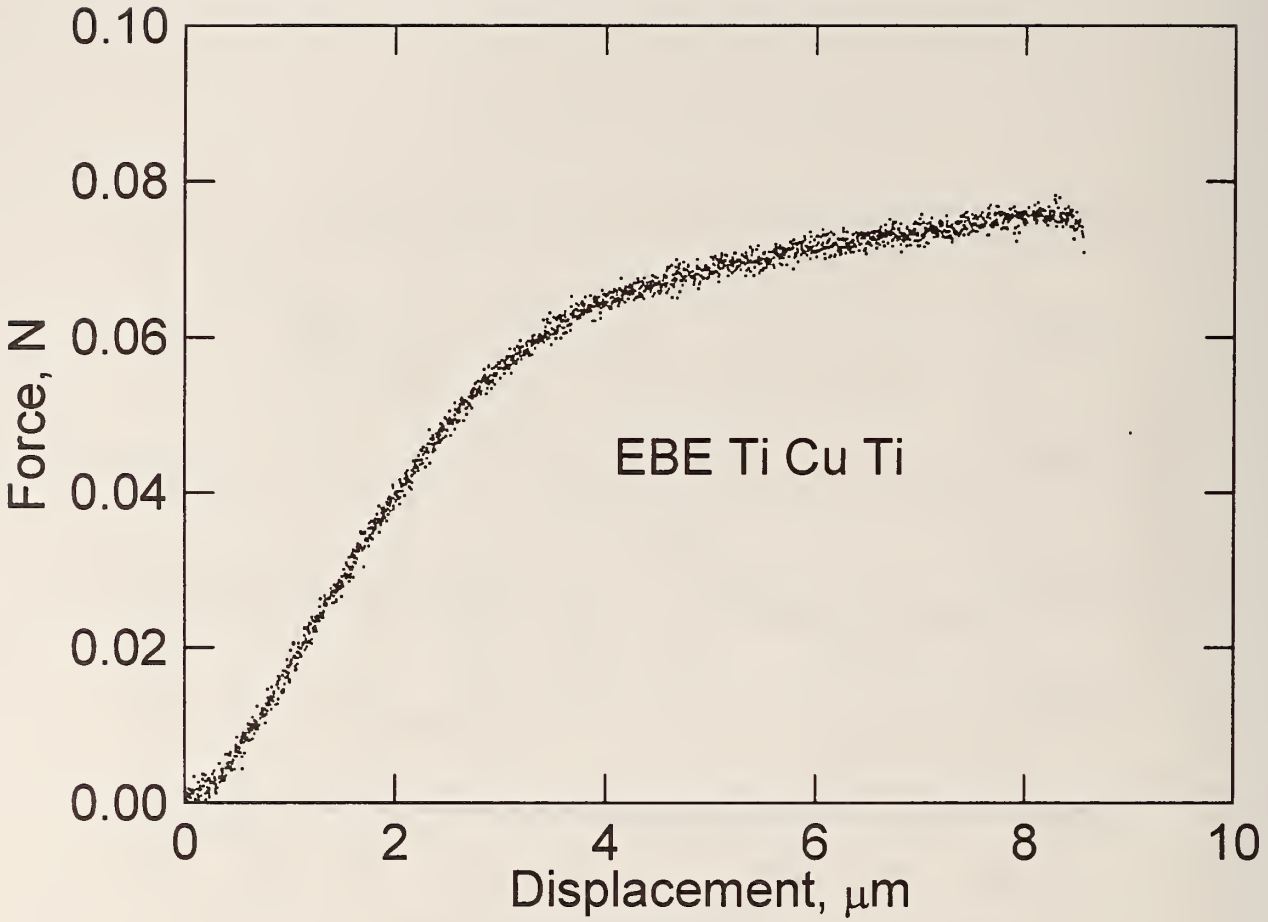

Figure 7. Force-grip displacement record for a tensile test of an electron-beam-evaporated (EBE) thin-film trilayer of Ti, Cu, and Ti. The total thickness is 1.2 μm; the Ti layers are 0.05 μm thick.

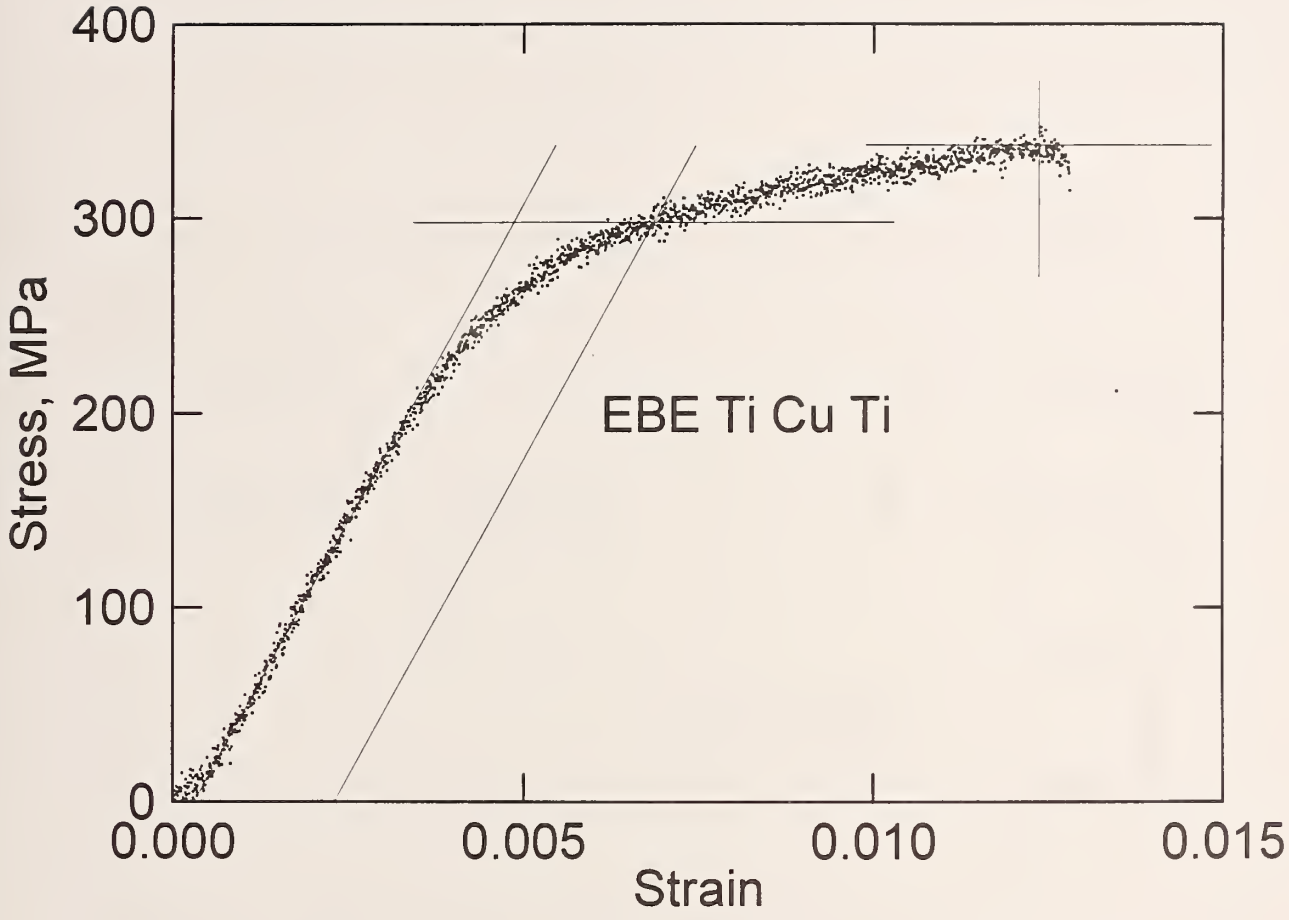

Figure 8. Stress-(engineering)strain record for a tensile test of an electron-beam-evaporated (EBE) thin film trilayer of Ti, Cu, and Ti. The total thickness is 1.2 μm; the Ti layers are 0.05 μm thick.

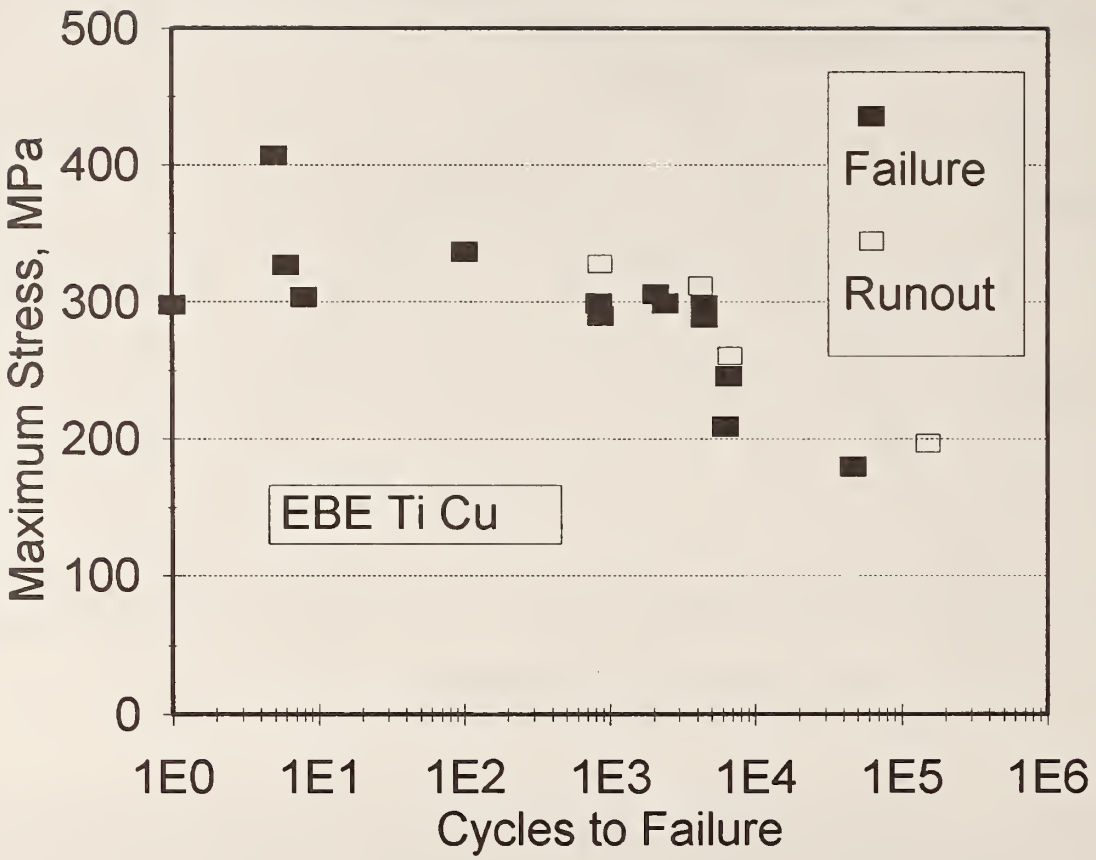

Figure 9. S-N curve for tension-tension fatigue of the TiCuTi films. The minimum load was held at one tenth of the maximum load. One specimen endured over 100 000 cycles without failure.

Appendix F. Drawings

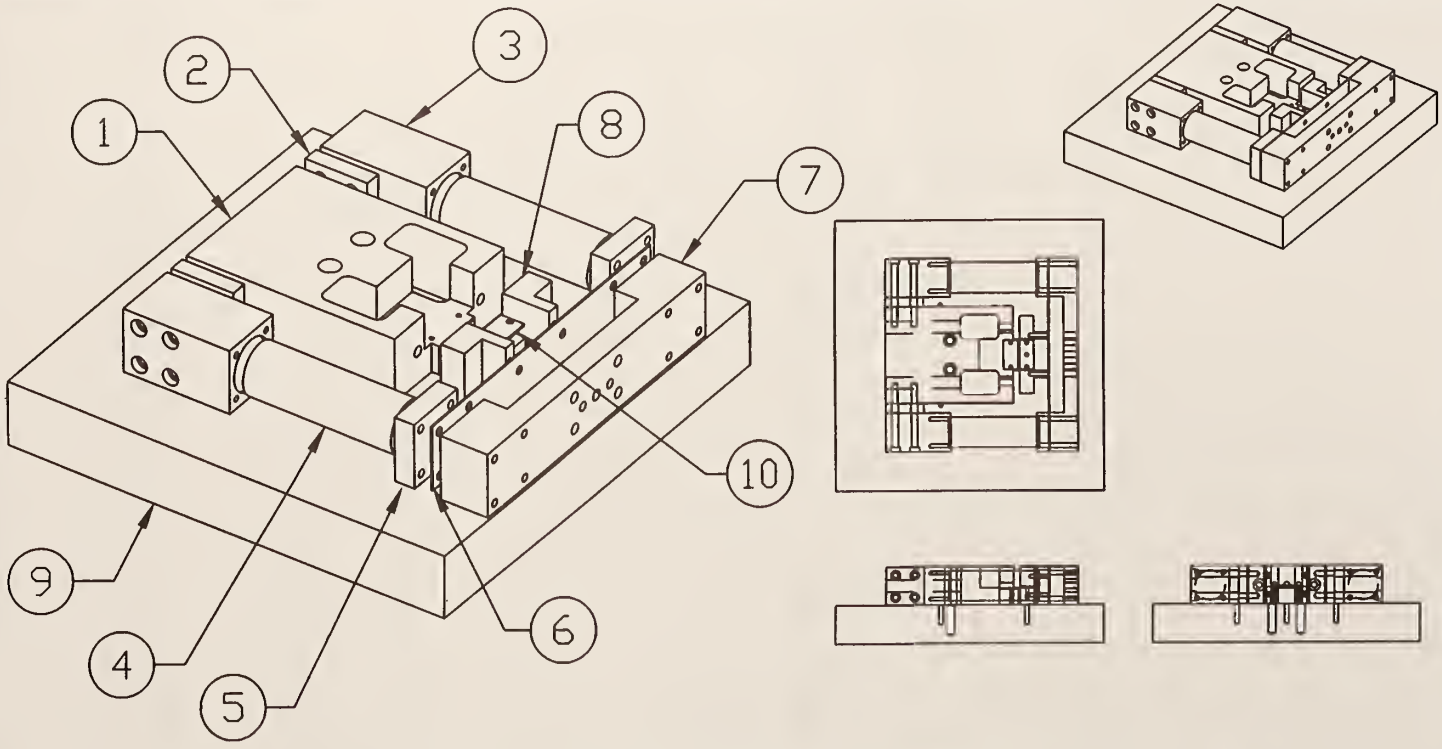

ITEM	QTY	NAME	ITEM	QTY	NAME
6	1	PART2	1	1	PART7D
7	1	PART1	2	2	PART6
8	1	PART8	3	2	PART5
9	1	PART10	4	2	PART4
10	2	PART11	5	2	PART3

All dimensions are in inches unless otherwise specified.

TOLERANCES UNLESS OTHERWISE SPECIFIED:

FRACTIONAL	± 1/64
.X	± .015
.XX	± .010
.XXX	± .005
.XXXX	± .0005
ANGULAR	± 1/2°

NIST UNITED STATES DEPARTMENT OF COMMERCE NATIONAL INSTITUTE OF STANDARDS AND TECHNOLOGY	TESTER	Scientist or Eng.: David T. Read	Scale: 1:1	Date: 10/22/97
	Drawn by: DTR	File Name: testerc.dwg	Quantity: NA	Material: NA

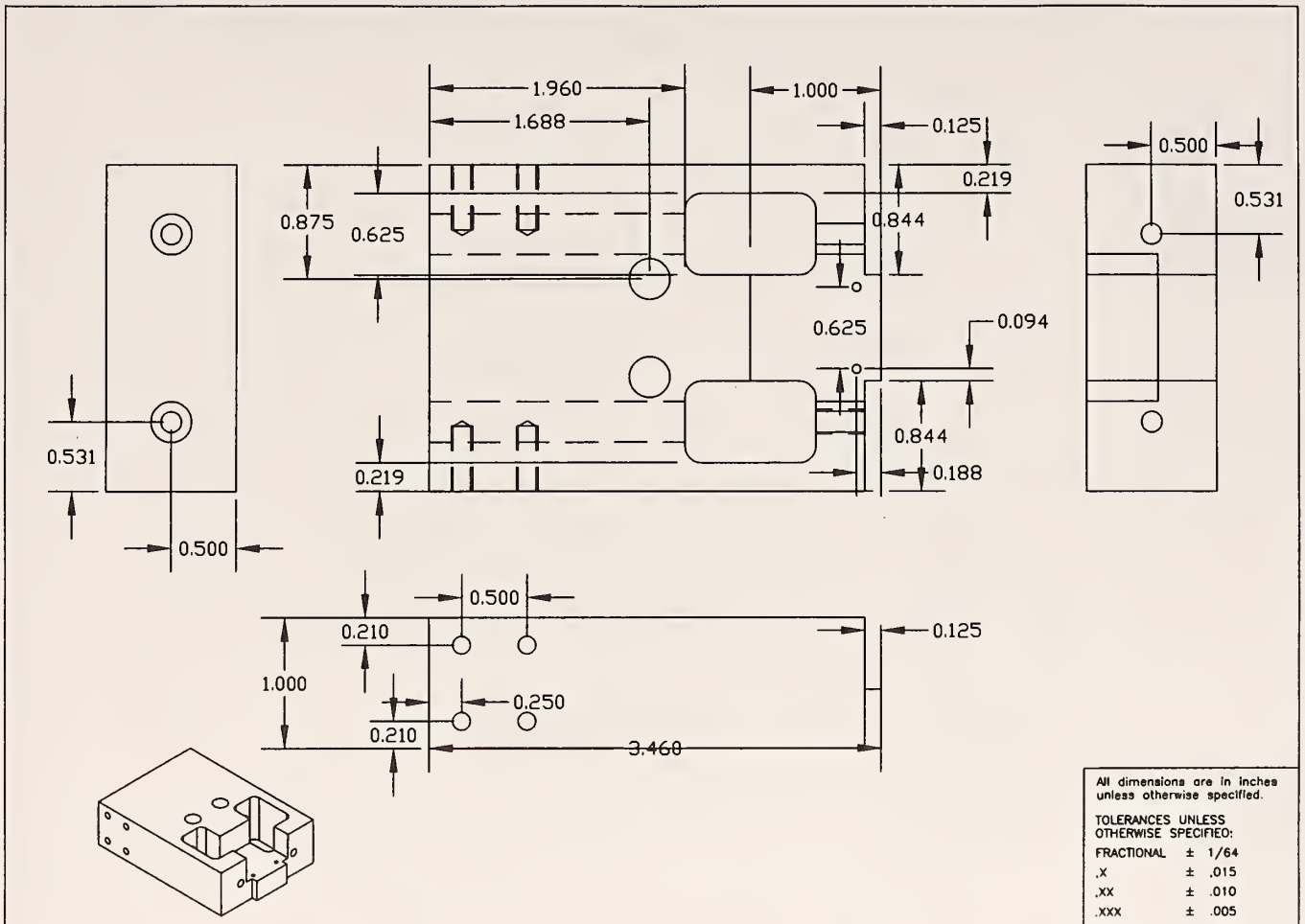
1.960
1.688
1.000
0.125
0.219
0.844
0.875
0.625
0.094
0.625
0.844
0.188
0.219
0.531
0.500
0.500
0.531
0.500
0.210
0.125
1.000
0.250
0.210
3.460
All dimensions are in inches unless otherwise specified.
TOLERANCES UNLESS OTHERWISE SPECIFIED:
FRACTIONAL ± 1/64
.X ± .015
.XX ± .010
.XXX ± .005
.XXXX ± .0005
ANGULAR ± 1/2°
UNITED STATES DEPARTMENT OF COMMERCE NATIONAL INSTITUTE OF STANDARDS AND TECHNOLOGY
Main Body
Drawn by: DTR
Scientist or Eng.: David T.Read
File Name: part7d.dwg
Scale: 1:1
Quantity: 1
Date: 10/22/97
Material: Al

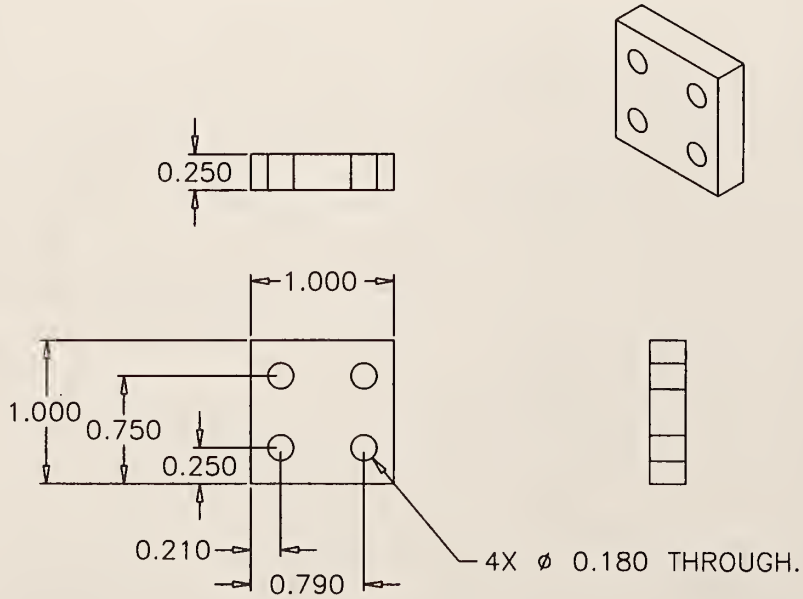

All dimensions are in inches unless otherwise specified.

TOLERANCES UNLESS OTHERWISE SPECIFIED:

FRACTIONAL	± 1/64
.X	± .015
.XX	± .010
.XXX	± .005
.XXXX	± .0005
ANGULAR	± 1/2°

UNITED STATES DEPARTMENT OF COMMERCE NATIONAL INSTITUTE OF STANDARDS AND TECHNOLOGY	Part 6 Al spacer	Scientist or Eng.: David T. Read	Scale: 1:1	Date: 10/2/97
	Drawn by: DTR	File Name: Part6b.dwg	Quantity: 2	Material: Aluminum

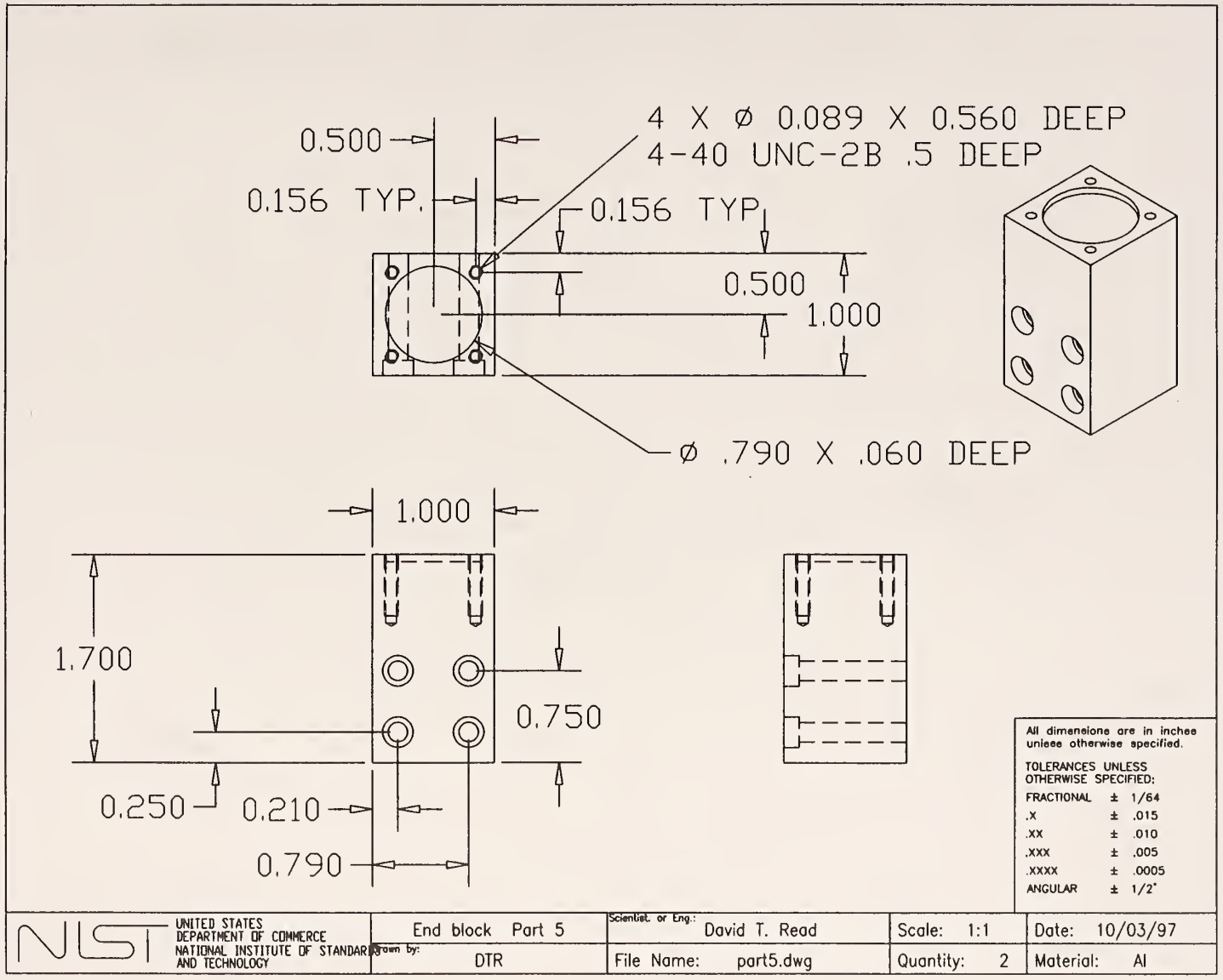
4 X ø 0.089 X 0.560 DEEP
4-40 UNC-2B .5 DEEP
0.500
0.156 TYP.
0.156 TYP
0.500
1.000
ø .790 X .060 DEEP
1.000
1.700
0.750
0.250
0.210
0.790
All dimensions are in inches unless otherwise specified.
TOLERANCES UNLESS OTHERWISE SPECIFIED:
FRACTIONAL ± 1/64
.X ± .015
.XX ± .010
.XXX ± .005
.XXXX ± .0005
ANGULAR ± 1/2°
UNITED STATES DEPARTMENT OF COMMERCE
NATIONAL INSTITUTE OF STANDARDS AND TECHNOLOGY
End block Part 5
Scientist or Eng.: David T. Read
Scale: 1:1
Date: 10/03/97
Drawn by: DTR
File Name: part5.dwg
Quantity: 2
Material: Al

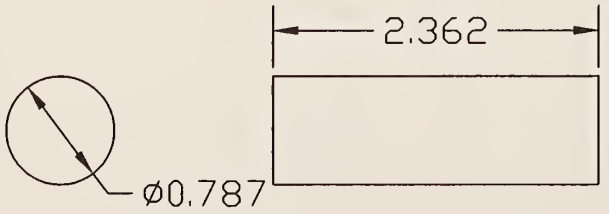

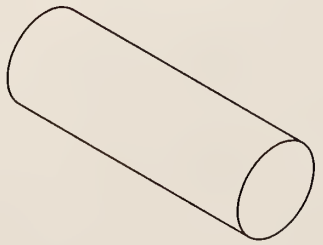

All dimensions are in inches unless otherwise specified.

TOLERANCES UNLESS OTHERWISE SPECIFIED:

FRACTIONAL	± 1/64
.X	± .015
.XX	± .010
.XXX	± .005
.XXXX	± .0005
ANGULAR	± 1/2°

UNITED STATES DEPARTMENT OF COMMERCE NATIONAL INSTITUTE OF STANDARDS AND TECHNOLOGY	Part 4 -- dummy actuator	Scientist. or Eng.: David T. Read	Scale: 1:1	Date: 10/16/97
	Drawn by: DTR	File Name: part4.dwg	Quantity: 2	Material: Al

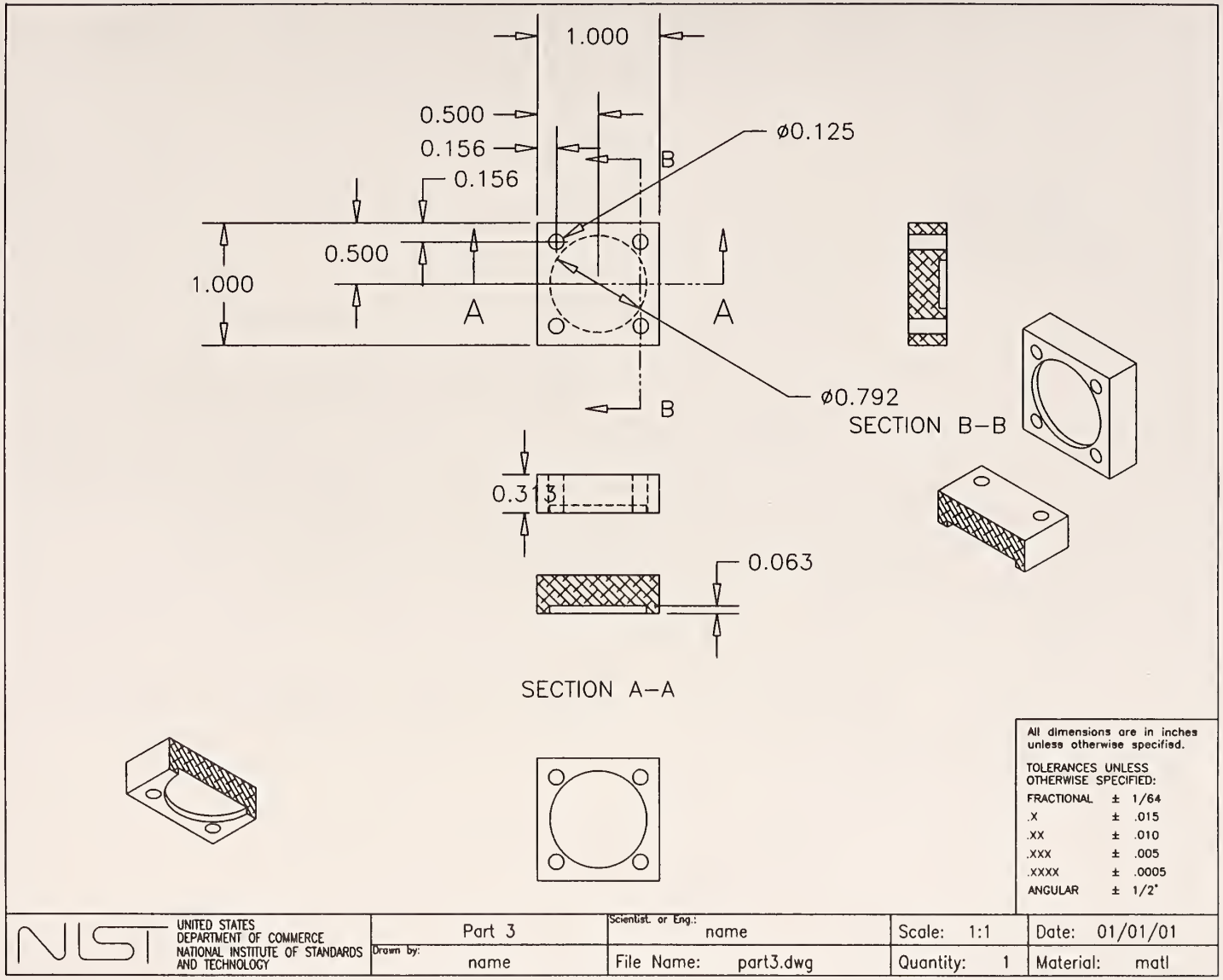
1.000
0.500
0.156
0.156
ø0.125
B
1.000
0.500
A
A
B
ø0.792
SECTION B–B
0.313
0.063
SECTION A–A
All dimensions are in inches unless otherwise specified.
TOLERANCES UNLESS OTHERWISE SPECIFIED:
FRACTIONAL ± 1/64
.X ± .015
.XX ± .010
.XXX ± .005
.XXXX ± .0005
ANGULAR ± 1/2°
UNITED STATES DEPARTMENT OF COMMERCE
NATIONAL INSTITUTE OF STANDARDS AND TECHNOLOGY
Part 3
Drawn by: name
Scientist or Eng.: name
File Name: part3.dwg
Scale: 1:1
Quantity: 1
Date: 01/01/01
Material: matl

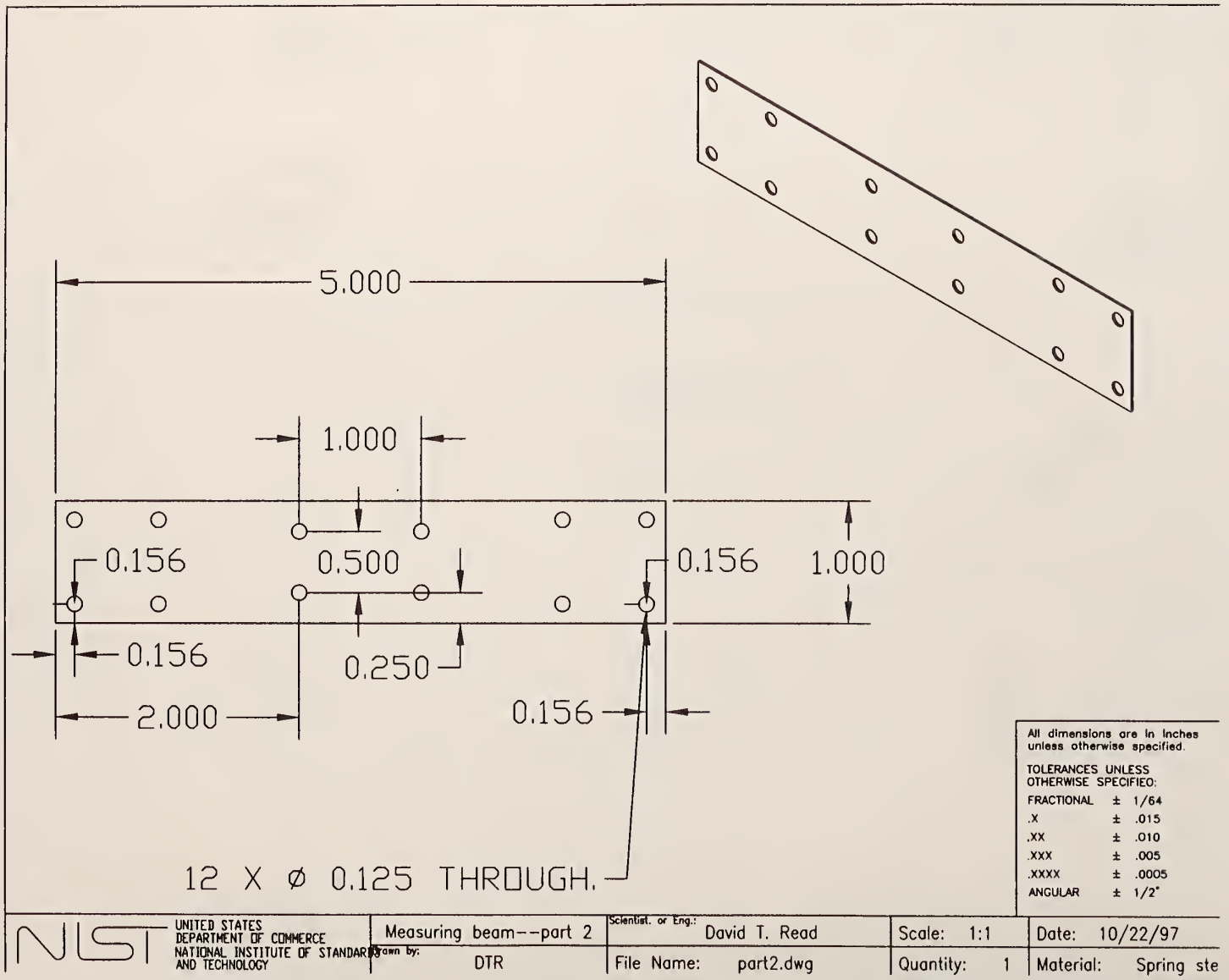

All dimensions are in inches unless otherwise specified.

TOLERANCES UNLESS OTHERWISE SPECIFIED:

FRACTIONAL	± 1/64
.X	± .015
.XX	± .010
.XXX	± .005
.XXXX	± .0005
ANGULAR	± 1/2°

NIST UNITED STATES DEPARTMENT OF COMMERCE NATIONAL INSTITUTE OF STANDARDS AND TECHNOLOGY	Measuring beam--part 2	Scientist. or Eng.: David T. Read	Scale: 1:1	Date: 10/22/97
	Drawn by: DTR	File Name: part2.dwg	Quantity: 1	Material: Spring ste

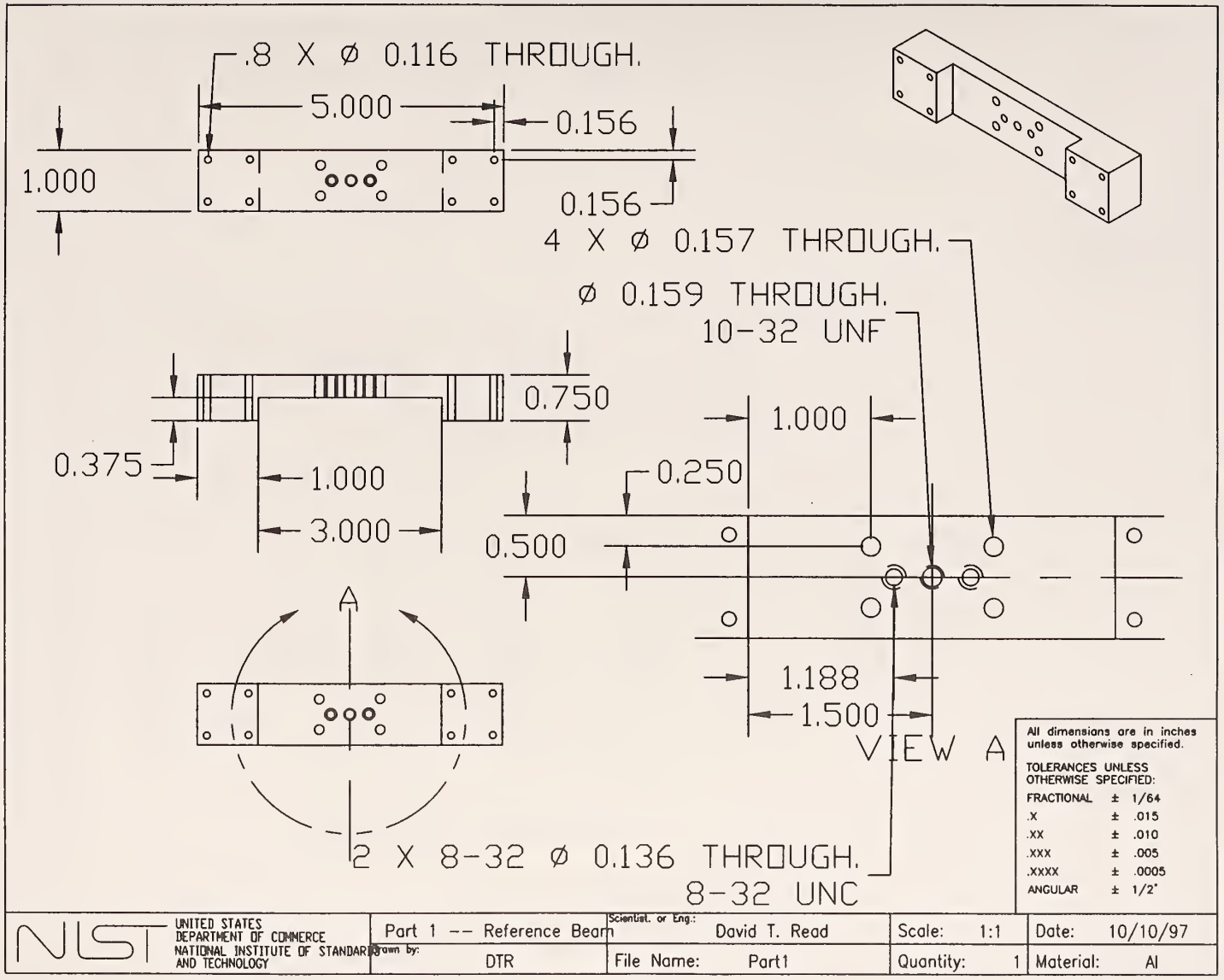
.8 X ø 0.116 THROUGH.
5.000
0.156
1.000
0.156
4 X ø 0.157 THROUGH.
ø 0.159 THROUGH.
10-32 UNF
0.750
0.375
1.000
3.000
1.000
0.250
0.500
A
1.188
1.500
VIEW A
2 X 8-32 ø 0.136 THROUGH.
8-32 UNC
All dimensions are in inches unless otherwise specified.
TOLERANCES UNLESS OTHERWISE SPECIFIED:
FRACTIONAL ± 1/64
.X ± .015
.XX ± .010
.XXX ± .005
.XXXX ± .0005
ANGULAR ± 1/2°
NIST
UNITED STATES DEPARTMENT OF COMMERCE
NATIONAL INSTITUTE OF STANDARDS AND TECHNOLOGY
Part 1 -- Reference Beam
Drawn by: DTR
Scientist. or Eng.: David T. Read
File Name: Part1
Scale: 1:1
Quantity: 1
Date: 10/10/97
Material: Al

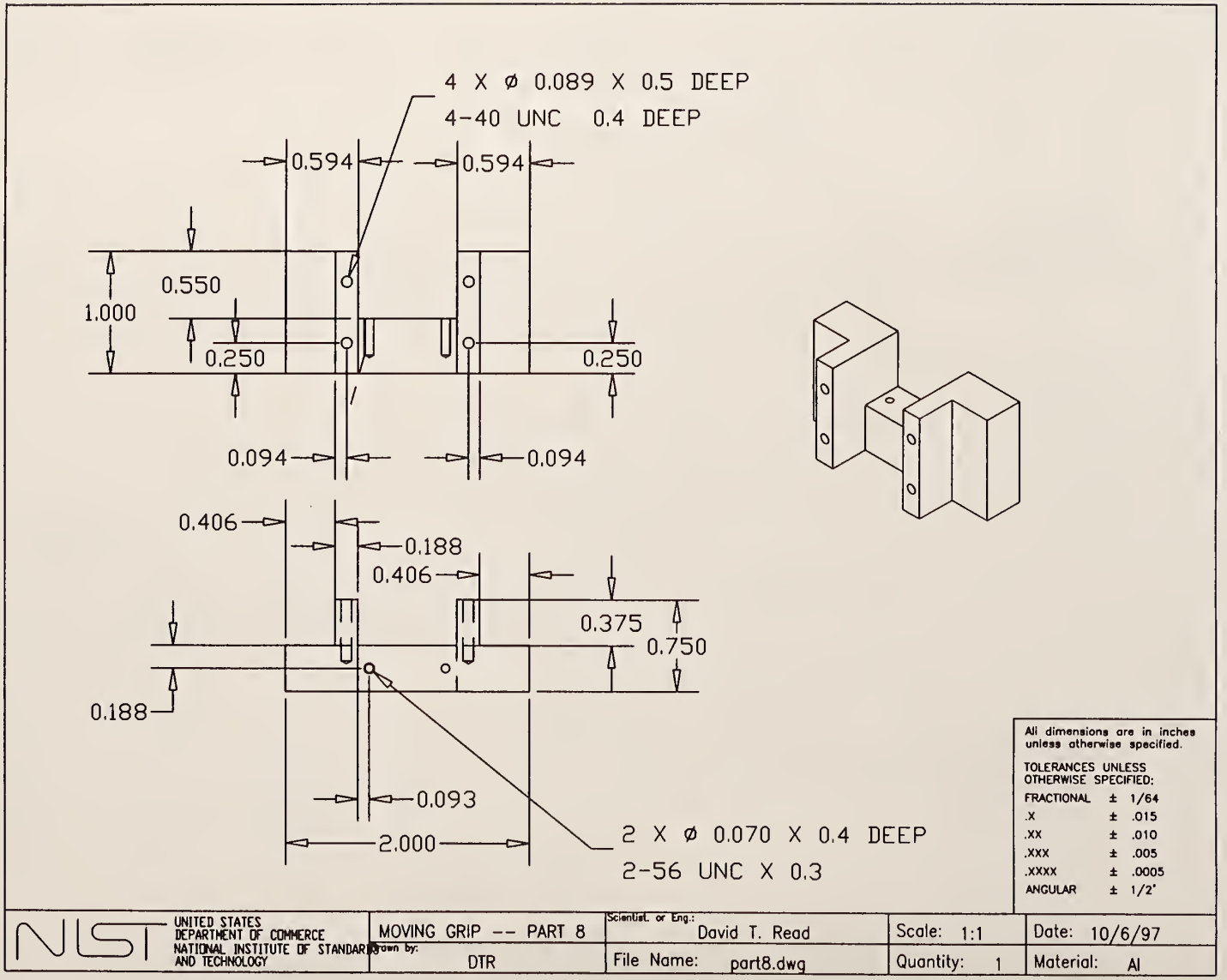
4 X ø 0.089 X 0.5 DEEP
4-40 UNC 0.4 DEEP
0.594
0.594
0.550
1.000
0.250
0.250
0.094
0.094
0.406
0.188
0.406
0.375
0.750
0.188
0.093
2.000
2 X ø 0.070 X 0.4 DEEP
2-56 UNC X 0.3
All dimensions are in inches unless otherwise specified.
TOLERANCES UNLESS OTHERWISE SPECIFIED:
FRACTIONAL ± 1/64
.X ± .015
.XX ± .010
.XXX ± .005
.XXXX ± .0005
ANGULAR ± 1/2°
UNITED STATES DEPARTMENT OF COMMERCE
NATIONAL INSTITUTE OF STANDARDS AND TECHNOLOGY
MOVING GRIP -- PART 8
Drawn by: DTR
Scientist or Eng.: David T. Read
File Name: part8.dwg
Scale: 1:1
Quantity: 1
Date: 10/6/97
Material: Al

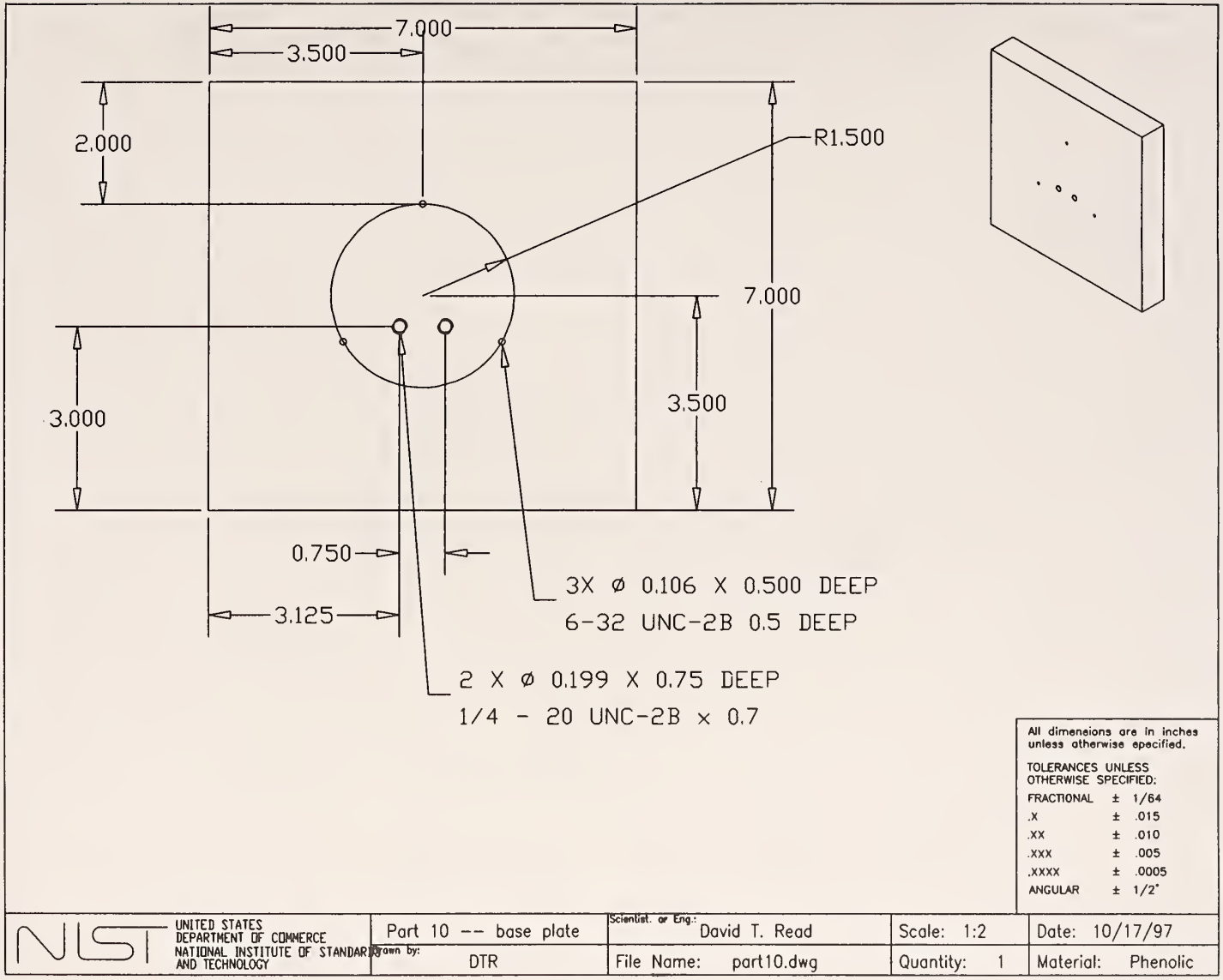
7.000
3.500
2.000
R1.500
7.000
3.500
3.000
0.750
3.125
3X ø 0.106 X 0.500 DEEP
6-32 UNC-2B 0.5 DEEP
2 X ø 0.199 X 0.75 DEEP
1/4 - 20 UNC-2B x 0.7
All dimensions are in inches unless otherwise specified.
TOLERANCES UNLESS OTHERWISE SPECIFIED:
FRACTIONAL ± 1/64
.X ± .015
.XX ± .010
.XXX ± .005
.XXXX ± .0005
ANGULAR ± 1/2°
UNITED STATES DEPARTMENT OF COMMERCE NATIONAL INSTITUTE OF STANDARDS AND TECHNOLOGY
Part 10 -- base plate
Drawn by: DTR
Scientist or Eng.: David T. Read
File Name: part10.dwg
Scale: 1:2
Quantity: 1
Date: 10/17/97
Material: Phenolic

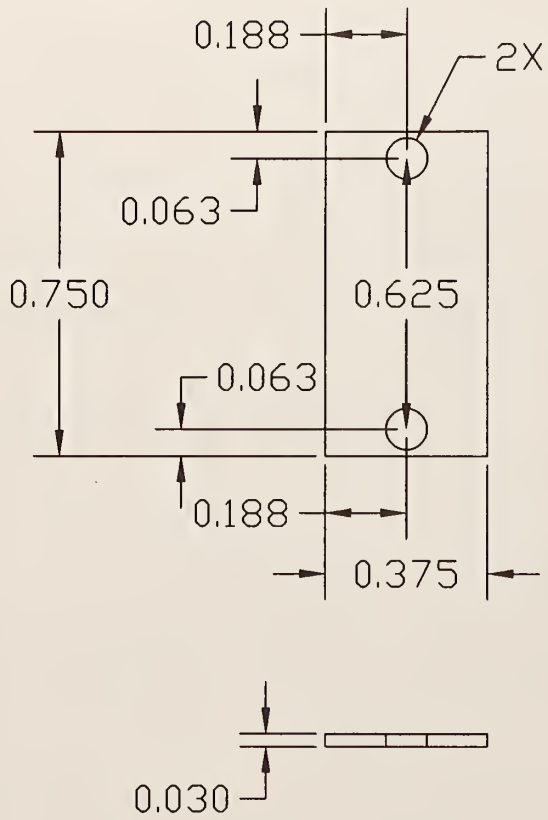

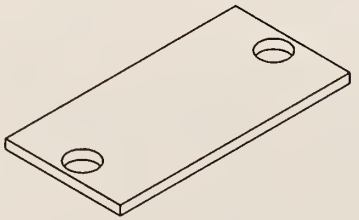

All dimensions are in inches unless otherwise specified.

TOLERANCES UNLESS OTHERWISE SPECIFIED:

FRACTIONAL	± 1/64
.X	± .015
.XX	± .010
.XXX	± .005
.XXXX	± .0005
ANGULAR	± 1/2°

NIST UNITED STATES DEPARTMENT OF COMMERCE NATIONAL INSTITUTE OF STANDARDS AND TECHNOLOGY	Grip Plates Part 11	Scientist. or Eng.: David T. Read	Scale: 3:1	Date: 10/03/97
	Drawn by: DTR	File Name: part 11.dwg	Quantity: 6	Material: Al

Appendix G. Computer Programs

These programs operate satisfactorily with the present tester and its data. However, they have not been tested on other computers or by other users. Therefore, caution is in order regarding the use of these programs and any calculated results.

NIST Technical Publications

Periodical

Journal of Research of the National Institute of Standards and Technology—Reports NIST research and development in those disciplines of the physical and engineering sciences in which the Institute is active. These include physics, chemistry, engineering, mathematics, and computer sciences. Papers cover a broad range of subjects, with major emphasis on measurement methodology and the basic technology underlying standardization. Also included from time to time are survey articles on topics closely related to the Institute's technical and scientific programs. Issued six times a year.

Nonperiodicals

Monographs—Major contributions to the technical literature on various subjects related to the Institute's scientific and technical activities.

Handbooks—Recommended codes of engineering and industrial practice (including safety codes) developed in cooperation with interested industries, professional organizations, and regulatory bodies.

Special Publications—Include proceedings of conferences sponsored by NIST, NIST annual reports, and other special publications appropriate to this grouping such as wall charts, pocket cards, and bibliographies.

Applied Mathematics Series—Mathematical tables, manuals, and studies of special interest to physicists, engineers, chemists, biologists, mathematicians, computer programmers, and others engaged in scientific and technical work.

National Standard Reference Data Series—Provides quantitative data on the physical and chemical properties of materials, compiled from the world's literature and critically evaluated. Developed under a worldwide program coordinated by NIST under the authority of the National Standard Data Act (Public Law 90-396). NOTE: The Journal of Physical and Chemical Reference Data (JPCRD) is published bimonthly for NIST by the American Chemical Society (ACS) and the American Institute of Physics (AIP). Subscriptions, reprints, and supplements are available from ACS, 1155 Sixteenth St., NW, Washington, DC 20056.

Building Science Series—Disseminates technical information developed at the Institute on building materials, components, systems, and whole structures. The series presents research results, test methods, and performance criteria related to the structural and environmental functions and the durability and safety characteristics of building elements and systems.

Technical Notes—Studies or reports which are complete in themselves but restrictive in their treatment of a subject. Analogous to monographs but not so comprehensive in scope or definitive in treatment of the subject area. Often serve as a vehicle for final reports of work performed at NIST under the sponsorship of other government agencies.

Voluntary Product Standards—Developed under procedures published by the Department of Commerce in Part 10, Title 15, of the Code of Federal Regulations. The standards establish nationally recognized requirements for products, and provide all concerned interests with a basis for common understanding of the characteristics of the products. NIST administers this program in support of the efforts of private-sector standardizing organizations.

Consumer Information Series—Practical information, based on NIST research and experience, covering areas of interest to the consumer. Easily understandable language and illustrations provide useful background knowledge for shopping in today's technological marketplace.
Order the **above** *NIST publications from: Superintendent of Documents, Government Printing Office. Washington, DC 20402.*
Order the **following** *NIST publications—FIPS and NISTIRs—from the National Technical Information Service, Springfield, VA 22161.*

Federal Information Processing Standards Publications (FIPS PUB)—Publications in this series collectively constitute the Federal Information Processing Standards Register. The Register serves as the official source of information in the Federal Government regarding standards issued by NIST pursuant to the Federal Property and Administrative Services Act of 1949 as amended, Public Law 89-306 (79 Stat. 1127), and as implemented by Executive Order 11717 (38 FR 12315, dated May 11, 1973) and Part 6 of Title 15 CFR (Code of Federal Regulations).

NIST Interagency Reports (NISTIR)—A special series of interim or final reports on work performed by NIST for outside sponsors (both government and non-government). In general, initial distribution is handled by the sponsor; public distribution is by the National Technical Information Service, Springfield, VA 22161, in paper copy or microfiche form.

U.S. Department of Commerce
National Institute of Standards and Technology
325 Broadway
Boulder, Colorado 80303-3328

Official Business
Penalty for Private Use, $300